Investigation of Reactivity Ratios for the AMPS/AAm/AAc Terpolymer and Associated Copolymers

by

Alison J. Scott

A thesis
presented to the University of Waterloo
in fulfillment of the
thesis requirement for the degree of
Master of Applied Science
in
Chemical Engineering

Waterloo, Ontario, Canada, 2015

Author's Declaration

I hereby declare that I am the sole author of this thesis. This is a true copy of the thesis, including any required final revisions, as accepted by my examiners.

I understand that my thesis may be made electronically available to the public.

Abstract

Water-soluble polymers of acrylamide (AAm) and acrylic acid (AAc) have significant potential in enhanced oil recovery, as well as in other specialty applications. However, to improve the shear strength of the polymer, it may be beneficial to add a third comonomer to the pre-polymerization mixture. Homopolymerization kinetics of acrylamide and acrylic acid have been studied previously, as have the copolymerization kinetics of these two comonomers. Therefore, in the current study, the kinetics of three additional systems are investigated: copolymerization of AMPS/AAm and AMPS/AAc and terpolymerization of AMPS/AAm/AAc.

Copolymerization experiments for both AMPS/AAm and AMPS/AAc were designed using two optimal techniques (Tidwell-Mortimer and the error-in-variables-model (EVM)) and terpolymerization experiments for AMPS/AAm/AAc were optimally designed using EVM. From these optimally designed experiments, accurate reactivity ratio estimates were determined for AMPS/AAm, AMPS/AAc and AMPS/AAm/AAc.

To better understand the error associated with each system, reactivity ratio point estimates for both the binary and ternary systems were presented using joint confidence regions (JCRs). The estimates were evaluated by comparing model predictions to experimental data, and the effect of experimental error was studied using sensitivity analyses. Finally, a direct comparison of binary and ternary reactivity ratios (for similar systems under the same experimental conditions) was possible for the first time.

Acknowledgements

"I can do all things through Christ who strengthens me." This has been true throughout my time at the University of Waterloo, and has particular significance with regards to my MASc work. I am so thankful to God for the many wonderful opportunities that He has given me, and I have been blessed by His constancy throughout my degree.

I would also like to thank Professor Alex Penlidis for his tireless efforts in encouraging my "well-roundedness" and ultimately making me a better student. I appreciate the wide variety of projects that he has encouraged me to pursue, and I have learned so much under his guidance. His patience, both in terms of my technical progress and my various extra-curricular responsibilities, has not gone unnoticed. Thank you!

Next, I would like to thank the many people within the Chemical Engineering Department at UW who have supported me throughout my undergraduate and MASc degree. I have enjoyed getting to know so many faculty and staff within the department, and have appreciated the day-to-day assistance that so many have graciously provided. I would especially like to thank Professor Neil McManus for his help with overcoming problems in the lab. The experimental portion of my thesis was made possible with the assistance of many friends and coworkers, including Niousha Kazemi, Marzieh Riahinezhad, Kate Stewart and Yasaman Amintowlieh.

This thesis would not have been possible without the unwavering support I've received from family and friends. My parents, Dave and Janet, have always encouraged me to pursue my

passions; I appreciate their love and support more than I can express! I am also extremely grateful for my hard-working brother, Brian, who has always been a motivating influence in my life. Finally, I wish to thank my loyal friends, both local and otherwise, who have always been available to lend a listening ear or to offer a word of encouragement.

Table of Contents

List of Figures

List of Tables

CHAPTER 1. THESIS OBJECTIVES AND OUTLINE

1.1 Motivation

Water-soluble polymers have been used for a wide variety of applications due to their versatility [1]. Both natural and synthetic water-soluble polymers are often found in medical applications including antiviral and antibacterial treatments, pharmaceuticals, and hydrogels (used in soft contact lenses, artificial organs, tissue prostheses, dental cements, and more). Pharmaceutical applications are plentiful, as water-soluble polymers are used in everything from creating binding agents and tablet coatings to controlling sustained drug delivery and degradation [2]. In addition to medical applications, water-soluble polymers are often used as thickeners, emollients and lubricants in cleaning products and cosmetics [3].

Beyond these personal-care and medical applications, water-soluble polymers are also used in many different industries including agriculture, food, plastics, pulp and paper, mining, petroleum, textiles, and waste water treatment [1]. Often, they are used as both processing aids and components of final products. Addition of water-soluble polymers to industrial processes tends to improve control of fluid motion, which may involve drag reduction, fluid thickening, or flocculation [3].

One of the major applications of water-soluble polymers is as processing aids in enhanced oil recovery (EOR) [4]. Specifically, water-soluble polymers have the ability to increase the

viscosity of the aqueous phase during oil recovery, which increases the efficiency of the overall process.

Many polymers are available for use in EOR. Several of these formulations are copolymers with polyacrylamide backbones, but xanthan gum (a biopolymer) is also widely used [5]. Each water-soluble polymer presents unique advantages and disadvantages in EOR, so the material selection ultimately depends on the requirements of the specific oil recovery process.

Some of the most common acrylamide copolymer systems used in EOR are acrylamide (AAm) and acrylic acid (AAc) copolymers. However, these AAm/AAc copolymers, like many other water-soluble polymers with high molecular weights, are very shear sensitive. That is, when the copolymer is subjected to high temperatures and stresses, there is potential for the polymer backbone to break [6]. This directly affects the polymer's efficiency in enhanced oil recovery, as the polymer in this case will not be able to increase the aqueous phase viscosity as much as was originally desired. The shear degradation of AAm/AAc copolymers in EOR is common, as the polymer is subjected to stirring and pumping, as well as high temperatures, flow rates and pressures. Once the backbone of the polymer is broken, the damage is irreversible. Thus, it is essential to minimize degradation in EOR applications.

One solution that has been proposed to limit shear degradation of AAm/AAc copolymers is the addition to the polymerization recipe of a third (co)monomer, such as N-vinylpyrrolidone (NVP) or 2-acrylamido-2-methylpropane sulfonic acid (AMPS). NVP has been used previously as a comonomer in water-soluble polymers, as it can improve polymer hydrophilicity [7]. Also,

perhaps more importantly in this application, its presence has been known to improve shear stability [8]. The addition of bulky monomer groups increases the rigidity of the polymer structure (and hence the glass transition temperature), and ultimately provides greater stability, which is beneficial for the application [6]. However, previous studies indicating low reactivity ratios for the related comonomer pairs suggest that it is inherently difficult to increase the rates of incorporation of NVP units in the AAm/AAc/NVP terpolymer (unless special semi-continuous reactor technology is used), which makes the terpolymer synthesis impractical for the types of benefits gained (for more details on NVP copolymerization characteristics, see Appendix A).

2-acrylamido-2-methylpropane sulfonic acid (AMPS) has also been considered as a comonomer in water-soluble polymers. As with NVP, addition of AMPS has the potential to improve main chain stability in harsh environments; the steric hindrance provided by the sulfonic group in AMPS is expected to control potential degradation of the polymer backbone [9]. In addition, AMPS has an advantage over NVP with regards to favourable reactivity ratios and rates of incorporation of AMPS monomer units in copolymers and terpolymers with AAm and AAc. A survey of existing (yet unreliable) reactivity ratios in the literature for the related copolymers (AMPS/AAm and AMPS/AAc) confirms that synthesis of the AMPS/AAm/AAc terpolymer is more promising than that of the AAm/AAc/NVP terpolymer. More details on the reactivity ratio (and hence rate of incorporation) issues will be given in Chapter 2.

A water-soluble terpolymer based on 2-acrylamido-2-methylpropane sulfonic acid, acrylamide, and acrylic acid will be the topic of the thesis. Polymerization kinetics for the terpolymer system

and its binary components will be examined, since these particular combinations of monomers are largely unstudied. AAm/AAc copolymerization kinetics have recently been clarified [10], so this research will focus on the addition of the third monomer (AMPS) to the system. Thus, the copolymerization kinetics for the synthesis of AMPS/AAm and AMPS/AAc with desirable property targets will also be investigated.

1.2 Objectives

Water-soluble polymers used in enhanced oil recovery (EOR) must meet several basic requirements, including suitable viscosity modification, long-term stability in hostile conditions, brine compatibility, and cost effectiveness [9, 11]. Based on an extensive review of the literature, it is believed that terpolymers containing 2-acrylamido-2-methylpropane sulfonic acid (AMPS), acrylamide (AAm) and acrylic acid (AAc) will meet these requirements and provide improved performance over existing EOR polymers.

The main objective for this research is to investigate polymerization kinetics for the AMPS/AAm/AAc terpolymer system. However, two of the associated copolymer systems, AMPS/AAm and AMPS/AAc are largely unstudied, especially in terms of kinetics. Therefore, as a first step, reliable kinetic data should be collected in order to estimate reliable reactivity ratios for the binary systems. It has been suggested that binary reactivity ratios are not to be used when ternary data are available, as simplifying assumptions tend to affect the error structure and hence the final estimated parameter values for the reactivity ratios. Essentially, using binary reactivity

ratios ignores the presence of the third comonomer [12]. However, obtaining accurate reactivity ratios for AMPS/AAm and AMPS/AAc can provide additional insight into the ternary system and can be used to determine optimal feed compositions for estimating improved ternary reactivity ratios. This comprehensive study will also allow for direct comparison of binary and ternary reactivity ratios based on experimental data. Ultimately, the information gathered and presented herein will make it possible to synthesize tailor-made copolymers and terpolymers with desirable properties for specific applications including, but not limited to, enhanced oil recovery.

1.3 Outline

This thesis is divided into seven chapters. A brief description of each chapter is presented below:

Chapter 2 provides background information for the topics discussed in this work. The introduction starts with an overview of free radical polymerization kinetics, and includes details specific to homopolymerization, copolymerization and terpolymerization reactions. Next, the concept of reactivity ratio estimation is discussed. The primary estimation technique used in this work is the error-in-variables-model (EVM); both the motivation in choosing this technique and the details regarding its implementation are discussed herein. Finally, existing literature related to the comonomers used in the current study (2-acrylamido-2-methylpropane sulfonic acid (AMPS), acrylamide (AAm) and acrylic acid (AAc)) is explored. This literature review focuses on the AMPS/AAm and AMPS/AAc copolymers as well as the AMPS/AAm/AAc terpolymer.

Chapter 3 describes the experimental work that has been performed as part of this thesis. The materials acquisition and purification, pre-polymerization preparation, copolymer and terpolymer synthesis, and polymer characterization are discussed in this chapter.

Chapters 4 through 6 outline the experimental design, preliminary and optimal experimental results, and reactivity ratio estimation for three polymerization systems. **Chapter 4** examines the AMPS/AAm copolymer, **Chapter 5** focuses on the AMPS/AAc copolymer, and **Chapter 6** presents work done with the AMPS/AAm/AAc terpolymer. In each of these chapters, preliminary recipes are selected based on existing literature values. Reactivity ratio estimates from these preliminary experiments are then used to design optimal experiments (via both Tidwell-Mortimer and error-in-variables-model approaches) for reactivity ratio estimation.

In **Chapter 7**, the conclusions drawn from this work are presented, and the main contributions of the study are enumerated. In light of these contributions, short-term and long-term recommendations for future work are also included.

Appendix A, entitled "Investigation of N-vinylpyrrolidone (NVP) as a Potential Comonomer" gives a literature review outlining the advantages and disadvantages of using NVP as the third monomer in the terpolymer system. Ultimately, AMPS/AAm/AAc was deemed more promising than AAm/AAc/NVP, and the reasoning is presented in this appendix.

A substantial amount of the research presented herein was experimental, and lab safety was a priority throughout the project. Safety considerations are briefly presented in **Appendix B**.

Some preliminary data collected for Chapters 4 and 5 are listed in **Appendix C** for the interested reader, and **Appendix D** contains sample calculations and additional data sets relevant to this investigation. These include experimental design, conversion/composition calculations and other sensitivity analysis considerations.

CHAPTER 2. BACKGROUND INFORMATION

2.1 Free Radical Polymerization

2.1.1 Free Radical Homopolymerization

Many water-soluble polymers are produced via free radical polymerization (FRP). FRP is a type of chain polymerization which involves four main steps: initiation, propagation, chain transfer (to either small or large molecules) and termination. A very basic overview of the free radical polymerization mechanism is presented in Table 2.1. Note that *r* and *s* denote chain length, while *i* and *j* represent monomer species.

The kinetics of free radical polymerization are well understood, and standard equations are available to provide information about both polymerization rate and molecular weight development [13]. The initiation rate, R_i, is proportional to the concentration of initiator in the system, according to Equation 2.1.

$$R_i = 2 f k_d [I] \tag{2.1}$$

where R_i = rate of initiation, f = initiator efficiency, k_d = initiator decomposition rate constant (very sensitive to temperature), and $[I]$ = initiator concentration. Using the stationary state hypothesis for radicals, one can set the termination rate, R_t, equal to the initiation rate, R_i.

Table 2.1: FRP Mechanism Overview

Description	Mechanism
Initiation	$\boldsymbol{I \xrightarrow{k_d} 2\, R^{\bullet}_{in}}$ $\boldsymbol{R^{\bullet}_{in} + M_i \xrightarrow{k_{p,0i}} R^{\bullet}_{1,i}}$
Propagation	$\boldsymbol{R^{\bullet}_{1,i} + M_j \xrightarrow{k_{pij}} R^{\bullet}_{2,j}}$ $\vdots$ $\boldsymbol{R^{\bullet}_{r,i} + M_j \xrightarrow{k_{pij}} R^{\bullet}_{r+1,j}}$
Chain transfer to monomer	$\boldsymbol{R^{\bullet}_{r,i} + M_j \xrightarrow{k_{fMij}} P_r + R^{\bullet}_{1,j}}$
Chain transfer to solvent	$\boldsymbol{R^{\bullet}_{r,i} + S \xrightarrow{k_{fSi}} P_r + R^{\bullet}_{1}}$
Chain transfer to chain transfer agent (CTA)	$\boldsymbol{R^{\bullet}_{r,i} + CTA \xrightarrow{k_{fCTAi}} P_r + R^{\bullet}_{1}}$
Chain transfer to impurity (retarder/inhibitor)	$\boldsymbol{R^{\bullet}_{r,i} + Z \xrightarrow{k_{fZi}} P_r - Z^{\bullet}}$ (unreactive)
Chain transfer to polymer (long chain branching)	$\boldsymbol{R^{\bullet}_{r,i} + P_{s,j} \xrightarrow{k_{fPij}} P_{r,i} + R^{\bullet}_{s,j}}$
Chain transfer reaction (general)	$\boldsymbol{R^{\bullet}_{r,i} + X - A \xrightarrow{k_{fXi}} P_r - X + A^{\bullet}}$
Terminal double-bond polymerization (long chain branching)	$\boldsymbol{R^{\bullet}_{r,i} + P_{s,j} \xrightarrow{k^{*}_{pij}} R^{\bullet}_{r+s}}$
Internal double-bond polymerization (crosslinking)	$\boldsymbol{R^{\bullet}_{r,i} + P_{s,j} \xrightarrow{k^{**}_{pij}} R^{\bullet}_{r+s}}$
Termination by combination	$\boldsymbol{R^{\bullet}_{r,i} + R^{\bullet}_{s,j} \xrightarrow{k_{tc}} P_{r+s}}$
Termination by disproportionation	$\boldsymbol{R^{\bullet}_{r,i} + R^{\bullet}_{s,j} \xrightarrow{k_{td}} P_r + P_s}$

Therefore, the relationship presented in Equation 2.2 can be used to define $[R^{\bullet}]$ in terms of more easily measurable values.

$$R_i = R_t = k_t[R^{\bullet}]^2 \tag{2.2}$$

where $[R^{\bullet}]$ = total free radical concentration and k_t = overall termination rate constant. After some algebraic manipulation, one can obtain the important equation for the rate of polymerization (Equation 2.3), which shows that the rate of polymerization, R_p, is proportional to $[M]$ and to $[I]^{1/2}$.

$$R_p = k_p[M][R^\bullet] = k_p[M]\left(\frac{R_i}{k_t}\right)^{1/2} = k_p[M]\left(\frac{2fk_d[I]}{k_t}\right)^{1/2} \quad (2.3)$$

In Equation 2.3, R_p = rate of polymerization, k_p = propagation rate constant (again, sensitive to temperature) and [*M*] = monomer concentration. The overall rate of polymerization, R_p, describes the rate of consumption of monomer (-*d*[*M*]/*dt*), with the majority of the monomer molecules consumed in the propagation step (long chain approximation).

Chain transfer reactions are an important aspect of free radical polymerization kinetics, especially for molecular weight development. As presented in Table 2.1, chain transfer may be to any small molecule, such as monomer, solvent, chain transfer agent (modifier for molecular weight), impurity, or any other substance, as long as the small molecule has a labile hydrogen. The rate of chain transfer (for the general case, to *X*–*A*) is given by Equation 2.4. *X* is the (labile) species being transferred (usually a hydrogen atom).

$$R_{tr} = k_{fX}[R^\bullet][X - A] \quad (2.4)$$

Since chain transfer essentially interrupts the propagation of polymer chains by transferring radical activity to the small transfer molecule, all transfer reactions to small molecules decrease the average chain length of polymer molecules (especially when a specific chain transfer agent (CTA) is present). This ultimately affects the molecular weight averages.

The chain transfer reaction described above produces a new transfer radical, $A^\bullet$, which can re-initiate. Hence, an ideal transfer agent does not affect the rate of an ideal polymerization, but reduces the product's molecular weight. If the transfer radical is stable and has trouble re-initiating, then the small molecule acts as a retarder or inhibitor (impurity effects).

Thus, propagation may be interrupted in the presence of an inhibitor or retarder, Z. The inhibitor attracts the radical from the propagating chain, forming $P_r - Z^{\bullet}$. These radicals do not re-initiate or re-initiate very slowly. The relationship between $[Z]$ and the other polymerization variables described previously is presented in Equation 2.5.

$$\frac{2R_p^2 k_t}{k_p^2[M]^2} + \frac{R_p[Z]k_{fZ}}{k_p[M]} - R_i = 0 \qquad (2.5)$$

These very basic expressions for free radical polymerization will be instrumental in investigating the kinetics of copolymerizations and terpolymerizations.

2.1.2 Free Radical Copolymerization

The addition of a second comonomer in the system complicates the kinetics further. Since more components are present during the reaction, more information is required to describe copolymerization kinetics [14].

The most widely used model in copolymerization is the terminal model. This model was originally presented for the copolymerization of styrene and methyl methacrylate in 1944, by Mayo and Lewis [15]. The terminal model assumes that the reactivity of the propagating radical only depends on the reactivity of the monomer unit at the end of the radical (the terminal monomer unit). With this assumption, there are four possible propagation reactions:

$$R^{\bullet}_{r,1} + M_1 \xrightarrow{k_{p11}} R^{\bullet}_{r+1,1}$$
$$R^{\bullet}_{r,1} + M_2 \xrightarrow{k_{p12}} R^{\bullet}_{r+1,2}$$
$$R^{\bullet}_{r,2} + M_1 \xrightarrow{k_{p21}} R^{\bullet}_{r+1,1}$$
$$R^{\bullet}_{r,2} + M_2 \xrightarrow{k_{p22}} R^{\bullet}_{r+1,2}$$

In this series of reactions, $R_{r,j}$ represents a radical species of length r with monomer j at the chain end (j = 1, 2). Similarly, M_k represents monomer k that is being added to the chain end (k = 1, 2). Each of the four reactions has a rate constant, k_{pjk} (radical j adding monomer k). Just as in free radical homopolymerization, the overall rate of polymerization can be determined by measuring the rate of overall monomer consumption in the system.

2.1.2.1 Copolymerization Models

The Mayo-Lewis model is the most widely used one for copolymerization systems. This classical equation, also called the instantaneous copolymer composition equation, is based on the terminal model described previously. With two distinct monomers, two rate equations can be written for the consumption rate of the two monomers (Equations 2.6 and 2.7).

$$\frac{-d[M_1]}{dt} = k_{p11}[R_1^{\bullet}][M_1] + k_{p21}[R_2^{\bullet}][M_1] \quad (2.6)$$

$$\frac{-d[M_2]}{dt} = k_{p12}[R_1^{\bullet}][M_2] + k_{p22}[R_2^{\bullet}][M_2] \quad (2.7)$$

In order to eliminate the radical concentrations from Equations 2.6 and 2.7, the quasi-steady state approximation for radicals can be used. After some mathematical manipulation, the resulting equation is the Mayo-Lewis equation, or the instantaneous copolymer composition equation (Equation 2.8).

$$\frac{d[M_1]}{d[M_2]} = \left(\frac{[M_1]}{[M_2]}\right)\left(\frac{r_1[M_1]+[M_2]}{[M_1]+r_2[M_2]}\right) \quad (2.8)$$

where $[M_1]$ and $[M_2]$ are the concentrations of monomer 1 and 2 in the polymerizing mixture, and

$$r_1 = \frac{k_{p11}}{k_{p12}} \quad and \quad r_2 = \frac{k_{p22}}{k_{p21}} \quad (2.9)$$

The monomer reactivity ratios, r_1 and r_2, describe the potential for homopropagation (that is, having the same monomer type added that is already in the terminal monomer position) relative to the potential for cross-propagation (having the monomer type being added that is different from that in the terminal monomer position on the radical). These parameters are specific to each copolymer system, and many summary tables are available citing reactivity ratios of common copolymer systems [16]. Reactivity ratios can be estimated using experimental data, if the free (unreacted) monomer composition in the polymerizing mixture and the bound (incorporated) monomer composition in the polymer chains (i.e., copolymer composition) are known. Techniques for reactivity ratio estimation are discussed further in Section 2.2.

Another popular form of the copolymerization equation (Equation 2.8) is given by Equation 2.10, which provides information directly about the instantaneous composition of the copolymer, F_1, given the comonomer composition in the polymerizing mixture. An advantage of Equation 2.10 is that monomer mole fractions are used rather than monomer concentrations. This eliminates the need to assume that volume is constant throughout the polymerization, which may not always be a valid assumption.

$$F_1 = \frac{r_1 f_1^2 + f_1 f_2}{r_1 f_1^2 + 2 f_1 f_2 + r_2 f_2^2} \quad (2.10)$$

where f_1 and f_2 represent the unreacted mole fractions of monomer 1 and monomer 2 in the mixture, respectively. F_1 is the instantaneous mole fraction of monomer 1 units bound in the copolymer chains, corresponding to f_1. Equations 2.11 and 2.12 give additional definitions and show relations between monomer mole fractions and concentrations.

$$f_1 = 1 - f_2 = \frac{[M_1]}{[M_1]+[M_2]} \tag{2.11}$$

$$F_1 = 1 - F_2 = \frac{d[M_1]}{d[M_1]+d[M_2]} \tag{2.12}$$

An additional point of interest in copolymerization kinetics is establishing the azeotropic composition (if it exists) for the system. At the azeotropic point, the feed composition (f_1) and the instantaneous copolymer composition (F_1) are equivalent. If the reactivity ratios are known, we can use the instantaneous copolymerization equation (Equation 2.10) to examine F_1 as a function of f_1 and to establish the azeotropic point. By setting $F_1 = f_1$, Equation 2.10 is simplified to the binary azeotropic composition, shown in Equation 2.13.

$$F_1 = f_1 = \frac{1-r_2}{2-r_1-r_2} \tag{2.13}$$

2.1.3 Free Radical Terpolymerization

Free radical terpolymerization involves three comonomers. As expected, the addition of a third monomer further complicates the polymerization kinetics. Terpolymerization systems have not been studied as widely as copolymerizations, as there are almost endless combinations of monomers to be discovered and characterized [17]. The kinetics of terpolymerization systems were first described by Alfrey and Goldfinger in 1944 [18]. Given that there are three different

possibilities for the terminal monomer (on the growing radical), and three options for the added monomer, nine different propagation steps are possible:

$$R^{\bullet}_{r,1} + M_1 \xrightarrow{k_{p11}} R^{\bullet}_{r+1,1}$$
$$R^{\bullet}_{r,1} + M_2 \xrightarrow{k_{p12}} R^{\bullet}_{r+1,2}$$
$$R^{\bullet}_{r,1} + M_3 \xrightarrow{k_{p13}} R^{\bullet}_{r+1,3}$$
$$R^{\bullet}_{r,2} + M_1 \xrightarrow{k_{p21}} R^{\bullet}_{r+1,1}$$
$$R^{\bullet}_{r,2} + M_2 \xrightarrow{k_{p22}} R^{\bullet}_{r+1,2}$$
$$R^{\bullet}_{r,2} + M_3 \xrightarrow{k_{p23}} R^{\bullet}_{r+1,3}$$
$$R^{\bullet}_{r,3} + M_1 \xrightarrow{k_{p31}} R^{\bullet}_{r+1,1}$$
$$R^{\bullet}_{r,3} + M_2 \xrightarrow{k_{p32}} R^{\bullet}_{r+1,2}$$
$$R^{\bullet}_{r,3} + M_3 \xrightarrow{k_{p33}} R^{\bullet}_{r+1,3}$$

In this case, the overall polymerization rate can be expressed by the addition of the individual rates of monomer consumption for each of the three monomer types. For the sake of brevity, only the final equations (not containing radical concentrations) are presented here. Equations 2.14, 2.15 and 2.16 may be seen as equivalent to the Mayo-Lewis equation (Equation 2.8), modified for three-component systems [19].

$$\frac{d[M_1]}{d[M_2]} = \left(\frac{[M_1]}{[M_2]}\right)\left(\frac{[M_1]/r_{31}r_{21}+[M_2]/r_{21}r_{32}+[M_3]/r_{31}r_{23}}{[M_1]/r_{12}r_{31}+[M_2]/r_{12}r_{32}+[M_3]/r_{32}r_{13}}\right)\left(\frac{[M_1]+[M_2]/r_{12}+[M_3]/r_{13}}{[M_2]+[M_1]/r_{21}+[M_3]/r_{23}}\right) \quad (2.14)$$

$$\frac{d[M_1]}{d[M_3]} = \left(\frac{[M_1]}{[M_3]}\right)\left(\frac{[M_1]/r_{31}r_{21}+[M_2]/r_{21}r_{32}+[M_3]/r_{31}r_{23}}{[M_1]/r_{13}r_{21}+[M_2]/r_{23}r_{12}+[M_3]/r_{13}r_{23}}\right)\left(\frac{[M_1]+[M_2]/r_{12}+[M_3]/r_{13}}{[M_3]+[M_1]/r_{31}+[M_2]/r_{32}}\right) \quad (2.15)$$

$$\frac{d[M_2]}{d[M_3]} = \left(\frac{[M_2]}{[M_3]}\right)\left(\frac{[M_1]/r_{12}r_{31}+[M_2]/r_{12}r_{32}+[M_3]/r_{32}r_{13}}{[M_1]/r_{13}r_{21}+[M_2]/r_{23}r_{12}+[M_3]/r_{13}r_{23}}\right)\left(\frac{[M_2]+[M_1]/r_{21}+[M_3]/r_{23}}{[M_3]+[M_1]/r_{31}+[M_2]/r_{32}}\right) \quad (2.16)$$

As before, $[M_i]$ represents the concentration of monomer i (i = 1, 2, 3) in the system, and the r_{ij} values represent (binary) monomer reactivity ratios.

Similarly, the instantaneous terpolymer compositions (F_i) can be calculated (in slightly different but equivalent expressions) as a function of unreacted monomer mole fractions (f_i) (in a way analogous to Equation 2.10 for copolymerization).

$$\frac{F_1}{F_2} = \left(\frac{f_1}{f_2}\right)\left(\frac{f_1/r_{31}r_{21}+f_2/r_{21}r_{32}+f_3/r_{31}r_{23}}{f_1/r_{12}r_{31}+f_2/r_{12}r_{32}+f_3/r_{32}r_{13}}\right)\left(\frac{f_1+f_2/r_{12}+f_3/r_{13}}{f_2+f_1/r_{21}+f_3/r_{23}}\right) \tag{2.17}$$

$$\frac{F_1}{F_3} = \left(\frac{f_1}{f_3}\right)\left(\frac{f_1/r_{31}r_{21}+f_2/r_{21}r_{32}+f_3/r_{31}r_{23}}{f_1/r_{13}r_{21}+f_2/r_{23}r_{12}+f_3/r_{13}r_{23}}\right)\left(\frac{f_1+f_2/r_{12}+f_3/r_{13}}{f_3+f_1/r_{31}+f_2/r_{32}}\right) \tag{2.18}$$

$$\frac{F_2}{F_3} = \left(\frac{f_2}{f_3}\right)\left(\frac{f_1/r_{12}r_{31}+f_2/r_{12}r_{32}+f_3/r_{32}r_{13}}{f_1/r_{13}r_{21}+f_2/r_{23}r_{12}+f_3/r_{13}r_{23}}\right)\left(\frac{f_2+f_1/r_{21}+f_3/r_{23}}{f_3+f_1/r_{31}+f_2/r_{32}}\right) \tag{2.19}$$

Numerous studies have been completed over the years to gain a better understanding of three-component (ternary) systems [17]. However, conventional analysis is based on the combination of multiple (binary) copolymer systems; a ternary system is therefore treated as a combination of three binary systems. While this may present a good starting point, using binary data to estimate ternary reactivity ratios can lead to severe estimation problems [12]. Concerns surrounding this technique include the inaccuracy of the binary reactivity ratios in the literature, the unfounded assumption that no composition drift will occur at low conversion, and induced correlations (linear dependencies) between mole fractions. Ultimately, using binary data for terpolymerization studies is a gross oversimplification, and should be avoided as much as possible [12].

As shown in Equations 2.17 through 2.19, the Alfrey & Goldfinger (A-G) model uses ratios of mole fractions as responses. However, the measurements taken from experimental work are typically single mole fractions (not ratios). Therefore, in evaluating (F_i/F_j), information is lost and the error structure is distorted. This can have a severe impact on parameter estimates. In a

recent study, Kazemi et al. [12] presented an alternative technique for estimating individual ternary reactivity ratios using the error-in-variables-model (EVM). The A-G model was recast so that each terpolymer mole fraction was presented as a single response (see Equations 2.20 to 2.22). While these expressions may seem more complex than the conventional A-G expressions, this formulation is still symmetrical and error structures are not distorted [12].

$$F_1 - \frac{f_1\left(\frac{f_1}{r_{21}r_{31}}+\frac{f_2}{r_{21}r_{32}}+\frac{f_3}{r_{31}r_{23}}\right)\left(f_1+\frac{f_2}{r_{12}}+\frac{f_3}{r_{13}}\right)}{f_1\left(\frac{f_1}{r_{21}r_{31}}+\frac{f_2}{r_{21}r_{32}}+\frac{f_3}{r_{31}r_{23}}\right)\left(f_1+\frac{f_2}{r_{12}}+\frac{f_3}{r_{13}}\right)+f_2\left(\frac{f_1}{r_{12}r_{31}}+\frac{f_2}{r_{12}r_{32}}+\frac{f_3}{r_{13}r_{32}}\right)\left(f_2+\frac{f_1}{r_{21}}+\frac{f_3}{r_{23}}\right)+f_3\left(\frac{f_1}{r_{13}r_{21}}+\frac{f_2}{r_{23}r_{12}}+\frac{f_3}{r_{13}r_{23}}\right)\left(f_3+\frac{f_1}{r_{31}}+\frac{f_2}{r_{32}}\right)} = 0 \qquad (2.20)$$

$$F_2 - \frac{f_2\left(\frac{f_1}{r_{12}r_{31}}+\frac{f_2}{r_{12}r_{32}}+\frac{f_3}{r_{13}r_{32}}\right)\left(f_2+\frac{f_1}{r_{21}}+\frac{f_3}{r_{23}}\right)}{f_1\left(\frac{f_1}{r_{21}r_{31}}+\frac{f_2}{r_{21}r_{32}}+\frac{f_3}{r_{31}r_{23}}\right)\left(f_1+\frac{f_2}{r_{12}}+\frac{f_3}{r_{13}}\right)+f_2\left(\frac{f_1}{r_{12}r_{31}}+\frac{f_2}{r_{12}r_{32}}+\frac{f_3}{r_{13}r_{32}}\right)\left(f_2+\frac{f_1}{r_{21}}+\frac{f_3}{r_{23}}\right)+f_3\left(\frac{f_1}{r_{13}r_{21}}+\frac{f_2}{r_{23}r_{12}}+\frac{f_3}{r_{13}r_{23}}\right)\left(f_3+\frac{f_1}{r_{31}}+\frac{f_2}{r_{32}}\right)} = 0 \qquad (2.21)$$

$$F_3 - \frac{f_3\left(\frac{f_1}{r_{13}r_{21}}+\frac{f_2}{r_{23}r_{12}}+\frac{f_3}{r_{13}r_{23}}\right)\left(f_3+\frac{f_1}{r_{31}}+\frac{f_2}{r_{32}}\right)}{f_1\left(\frac{f_1}{r_{21}r_{31}}+\frac{f_2}{r_{21}r_{32}}+\frac{f_3}{r_{31}r_{23}}\right)\left(f_1+\frac{f_2}{r_{12}}+\frac{f_3}{r_{13}}\right)+f_2\left(\frac{f_1}{r_{12}r_{31}}+\frac{f_2}{r_{12}r_{32}}+\frac{f_3}{r_{13}r_{32}}\right)\left(f_2+\frac{f_1}{r_{21}}+\frac{f_3}{r_{23}}\right)+f_3\left(\frac{f_1}{r_{13}r_{21}}+\frac{f_2}{r_{23}r_{12}}+\frac{f_3}{r_{13}r_{23}}\right)\left(f_3+\frac{f_1}{r_{31}}+\frac{f_2}{r_{32}}\right)} = 0 \qquad (2.22)$$

Given these new equations, the error-in-variables-model (EVM) is used to obtain estimates of the parameters (reactivity ratios). This parameter estimation technique is appropriate, since it takes into account the error present in all variables. The details of implementing EVM are discussed in Section 2.2.1. Finally, Kazemi et al. [12] investigated the potential to use the cumulative composition model for medium-high conversion data in terpolymer systems. This alternative presents several advantages over the standard instantaneous model (for low conversion data). Namely, we can eliminate the assumption that composition drift is negligible (a requirement for implementing the instantaneous model) and we are able to retain more information content (that is, more data points over the conversion trajectory) from a single experiment. Advantages and implementation of the cumulative composition model are presented in more detail in Section 2.2.2.

Studies have shown that binary and ternary reactivity ratios can be different (often, drastically) within a single system [12]. Addition of the third monomer to the system essentially changes the reaction medium (compared to binary studies), which can significantly affect reactivity ratios. Therefore, wherever possible, terpolymer reactivity ratios should be estimated directly from terpolymerization data. Regardless, a good understanding of homopolymerization and copolymerization behaviour is essential prior to the evaluation of terpolymerization kinetics.

2.2 Reactivity Ratio Estimation

Reactivity ratios are extremely important parameters in copolymerization kinetics. Many researchers have attempted to find the most accurate parameter estimation technique; as a result, many different methods have been implemented for reactivity ratio estimation. This has created a serious problem in the literature, as it calls into question the accuracy of reported reactivity ratios. Sources of error may include poorly designed experiments (i.e. too few data points, usually unreplicated, and chosen at random), inherent experimental difficulties, inappropriate kinetic models, and incorrect estimation procedures. Therefore, to obtain reliable reactivity ratio estimates, it is important to ensure that sufficient data are carefully collected, and that limiting assumptions are avoided in modeling and estimation.

In general, reactivity ratios are obtained from experimental data by analyzing the copolymer composition at several different feed compositions. Traditionally, linear regression techniques have incorrectly been used for reactivity ratio estimation. These techniques include the Mayo-Lewis method (method of intersections), the Fineman-Ross method, and the Kelen-Tudos method [13]. These techniques were originally chosen for their simplicity, as technology was not

readily available for intense computation. However, linearizing the kinetic models (which are inherently non-linear in the parameters) requires making imprecise, subjective and invalid assumptions. An additional consideration is the use of the instantaneous copolymerization model in these linear techniques; the reaction must be kept at low conversion so that the assumption of "constant composition" in the feed is somewhat valid [20]. However, polymerizations at low conversions are extremely error-prone, and it is impossible to guarantee that the feed composition will remain constant (especially when dealing with an unstudied system). The problems associated with linear methods for parameter estimation have been thoroughly discussed in the literature [20–22], and will not be repeated again in the current study.

The current work uses the statistically correct error-in-variables-model (EVM), as it is a non-linear estimation technique which considers the error present in all variables. Through EVM and direct numerical integration, we are also able to estimate reactivity ratios using cumulative composition data (as opposed to standard analysis of low-conversion data) [20]. This provides additional advantages, including eliminating unnecessary assumptions and avoiding the experimental challenges associated with collecting low-conversion data.

The error-in-variables-model is also employed as part of the experimental design for binary reactivity ratio estimation. The EVM design criterion considers error present in all variables to select optimal feed compositions for reactivity ratio estimation experiments [23]. Reactivity ratios (and associated joint confidence regions) obtained through EVM design are contrasted with those obtained through the traditional Tidwell-Mortimer design [24, 25], which is based on D-optimality.

2.2.1 Error-in-Variables-Model (EVM)

Fortunately, we no longer face limitations with numerical computations that require model simplification. It is straightforward to use statistically sound non-linear methods for parameter estimation. One of the most powerful non-linear regression approaches is the error-in-variables-model (EVM) technique, which considers all sources of experimental error (both in the independent and dependent variables) [21]. EVM not only forces the experimenter to consider all sources of error, but it also provides estimates of the true values of other variables involved in the model along with the parameter estimates. Therefore, it is by far the most statistically correct and comprehensive approach for reactivity ratio estimation [22, 26].

The nested-iterative EVM implementation has been described in detail by Reilly and Patino-Leal [27], therefore only a brief overview will be presented herein. Implementation of EVM is based on the following two equations (Equations 2.23 and 2.24). The first, Equation 2.23, relates the vector of known measurements ($\underline{x}_i$) to the vector of their unknown true values ($\underline{\xi}_i$) and an error term, $k\underline{\varepsilon}_i$ (where k is a constant that reflects the magnitude of measurement uncertainty, usually estimated from process information). The second, Equation 2.24, is the model for the system, which shows the relationship between the true values of the variables ($\underline{\xi}_i$) and the true (but unknown) parameter values to be estimated ($\underline{\theta}$).

$$\underline{x}_i = \underline{\xi}_i + k\underline{\varepsilon}_i \qquad \text{where i = 1, 2, ..., n} \qquad (2.23)$$

$$\underline{g}\left(\underline{\xi}_i, \underline{\theta}\right) = 0 \qquad \text{where i = 1, 2, ..., n} \qquad (2.24)$$

In both Equations 2.23 and 2.24, i represents the trial number (out of n trials), and underlined terms are either vectors or matrices. The goal of EVM is to minimize the sum of squares between the observed and predicted values, both in terms of the parameter estimates and in terms of error in the independent variables [28]. The nested-iterative EVM algorithm accomplishes this by using two nested loops; the outer loop searches for parameter estimates while the inner loop identifies estimates of the true values of the variables involved. Mathematically, the following objective function (Equation 2.25) should be minimized:

$$\phi = \frac{1}{2}\sum_{i=1}^{n} r_i(\underline{\bar{x}}_i - \underline{\hat{\xi}}_i)'\underline{V}^{-1}(\underline{\bar{x}}_i - \underline{\hat{\xi}}_i) \tag{2.25}$$

where r_i represents the number of replicates for the i^{th} trial, $\underline{\bar{x}}_i$ is the average of r_i measurements ($\underline{x}_i$), $\underline{\hat{\xi}}_i$ is an estimate of the true values of the variables ($\underline{\xi}_i$), and $\underline{V}$ is the variance-covariance matrix. To gain a better understanding of the magnitude of the error, the error distribution, the relationship between variables and errors (additive or multiplicative), and potential correlation, independent replication becomes necessary [28].

In terms of the nested-iterative scheme used to minimize the objective function, the EVM technique used herein is based on work published by Reilly et al. [29]. The algorithm begins with the inner loop searching for estimates of the true values of the variables ($\underline{\xi}_i$), while keeping the parameter estimates ($\underline{\hat{\theta}}$) constant. The inner loop uses Equation 2.26 to update the estimates of $\underline{\xi}_i^{(k)}$, where k represents the iteration step.

$$\underline{\xi}_{\mathrm{i}}^{(k+1)} = \underline{\bar{x}}_i - \underline{V B_i'}\left(\underline{B_i V}\,\underline{B_i'}\right)^{-1}[\underline{g}\left(\underline{\xi}_{\mathrm{i}}^{(k)}, \underline{\theta}\right) + \underline{B_i}\left(\underline{\bar{x}}_i - \underline{\xi}_{\mathrm{i}}^{(k)}\right)] \tag{2.26}$$

$\underline{B_i}$ is the vector of partial derivatives of the function $\underline{g}\left(\underline{\xi}_i, \underline{\theta}\right)$ with respect to the variables for the t^{th} element, as demonstrated below in Equation 2.27.

$$\underline{B_j} = \left[\frac{\partial \underline{g}\left(\underline{\xi_i}, \underline{\theta}\right)}{\partial\left(\underline{\xi_i}\right)_t}\right]_{\underline{\xi}_i = \underline{\xi}_i^{(k)}} \tag{2.27}$$

Next, the outer iteration searches for the values of the parameter estimates that will minimize the objective function. In this case, Equations 2.28 through 2.31 are used to update the estimates of $\underline{\theta}^{(u)}$, where *u* represents the iteration step.

$$\underline{\theta}^{(u+1)} = \underline{\theta}^{(u)} - \underline{G}^{-1}\underline{q} \tag{2.28}$$

$\underline{G}$ is the expected information matrix for the *i*,*j* elements (see Equation 2.29) and $\underline{q}$ is the gradient vector (see Equation 2.30).

$$\underline{G} = E\left[\frac{d^2\phi}{d\theta_i d\theta_j}\right] = \sum_{i=1}^{n} r_i \underline{Z_i'}\left(\underline{B_j}\underline{V}\underline{B_i'}\right)^{-1}\underline{Z_j} \tag{2.29}$$

$$\underline{q} = \left[\frac{d\phi}{d\theta_j}\right] = \sum_{i=1}^{n} r_i \underline{Z_i'}\left(\underline{B_j}\underline{V}\underline{B_i'}\right)^{-1}\underline{B_j}\left(\underline{\bar{x}_i} - \underline{\hat{\xi}_i}\right) \tag{2.30}$$

Finally, $\underline{Z_i}$ is the vector of partial derivatives of the function $\underline{g}\left(\underline{\xi_i}, \underline{\theta}\right)$ with respect to the parameters for the m^{th} element.

$$\underline{Z_j} = \left[\frac{\partial \underline{g}\left(\underline{\xi_i}, \underline{\theta}\right)}{\partial \theta_m}\right] \tag{2.31}$$

After estimates are obtained by EVM for both model parameters and model variables, it is important to evaluate the estimation results. This is primarily done by determining the precision of the parameter estimates. In the case of reactivity ratio estimation, several parameters are being estimated simultaneously. Thus, joint confidence regions (JCRs) are invaluable. JCRs are typically elliptical contours that quantify the level of uncertainty in the parameter estimates;

smaller JCRs indicate higher precision and therefore more confidence in the estimation results [28].

The joint confidence region for parameter estimates can be visualized using one of two expressions. The expression used in the current study, for elliptical JCRs (Equation 2.32), requires that the error be normally distributed and that the variance be known. Here, it is important to note that $\underline{\hat{\theta}}^{(u)}$ represents the vector of parameter estimates that minimize the objective function (Equation 2.25).

$$\left(\underline{\theta} - \underline{\hat{\theta}}\right)' \underline{G} \left(\underline{\theta} - \underline{\hat{\theta}}\right) \leq {\chi^2}_{p,1-\alpha} \tag{2.32}$$

where ${\chi^2}_{p,1-\alpha}$ represents the chi-squared distribution for p parameters and a confidence level of (1-α).

2.2.2 Cumulative Composition Data

As mentioned previously, one of the many problems associated with linear estimation techniques is the necessity to use experimental data from low conversion levels. The instantaneous copolymer composition model (Equation 2.10) is only valid if we assume that composition drift is negligible in the feed [20]. However, this is rarely a valid assumption, as feed composition almost inevitably changes with conversion. From a more practical perspective, collecting low-conversion data presents some experimental challenges, and is extremely prone to error.

The cumulative copolymerization model (that is, the integrated form of the instantaneous copolymer composition model) can be used as an alternative to the instantaneous copolymer

composition model [20]. This makes it possible to avoid restrictive assumptions, eliminates experimental challenges of collecting low-conversion data, and provides additional data points (additional information content) for analysis (otherwise ignored by the instantaneous model, despite the fact that it represents the major portion of the conversion trajectory).

Two forms of the cumulative copolymer composition model, analytical integration and direct numerical integration (DNI), have been studied in detail by Kazemi et al. [20, 30]. Analytical integration of the Mayo-Lewis model (Equation 2.8) results in the Meyer-Lowry model (Equation 2.33), which is applicable for low to moderate levels of conversion (up to 20-40%) [31].

$$X_n = 1 - \left(\frac{f_1}{f_{10}}\right)^{\alpha} \left(\frac{f_2}{f_{20}}\right)^{\beta} \left(\frac{f_{10}-\delta}{f_1-\delta}\right)^{\gamma} \tag{2.33}$$

where $\alpha = \frac{r_2}{1-r_2}$; $\beta = \frac{r_1}{1-r_1}$; $\gamma = \frac{1-r_1 r_2}{(1-r_1)(1-r_2)}$; $\delta = \frac{1-r_2}{2-r_1-r_2}$

X_n represents molar conversion, f_1 and f_2 are the mole fractions of unreacted monomer at time t, and f_{10} and f_{20} are initial feed compositions. Since X_n cannot be measured directly during experimentation, we use the following equation (Equation 2.34) to express conversion as a function of feed composition (f_1) and cumulative copolymer composition ($\bar{F}_1$).

$$X_n = \frac{f_1 - f_{10}}{f_1 - \bar{F}_1} \tag{2.34}$$

Based on the above information, the analytical integration expression can also be modified to be in terms of initial feed composition (f_{10}), cumulative copolymer composition ($\bar{F}_1$) and mass conversion (X_w). This is the most useful form of the model, since all variables involved can be tracked experimentally, and is presented in Equation 2.35:

$$X_n = X_w \frac{Mw_1 f_{10} + (1 - f_{10}) Mw_2}{Mw_1 \bar{F}_1 + (1 - \bar{F}_1) Mw_2} \tag{2.35}$$

where Mw_1 and Mw_2 are the molecular weights of monomer 1 and monomer 2, respectively. In earlier approximations, Mw_1 and Mw_2 were considered the same.

While the Meyer-Lowry model does allow for consideration of higher conversion data, it still has several limitations [20]. First, it only allows for analysis of moderate conversion data. While this is an improvement over the instantaneous model, it is still not ideal. Second, the model assumes that propagation rate constants remain constant over the course of polymerization, which is unlikely as the reaction reaches higher levels of conversion (diffusional limitations). Third, previous studies have indicated that the model has some convergence issues for certain conditions [32]. While transformations do exist to avoid instability, they may inadvertently affect the error structure.

The other alternative available for analysis of cumulative copolymer composition data is the direct numerical integration (DNI) method [20]. DNI is a powerful alternative to the analytical integration method, as it employs a direct approach and does not rely on model transformations or other potentially restrictive assumptions. The technique directly relates the cumulative copolymer composition to the mole fraction of unreacted monomer using the Skeist equation (Equation 2.36):

$$\bar{F}_1 = \frac{f_{10} - f_1 (1 - X_n)}{X_n} \tag{2.36}$$

As before, f_1 represents the fraction of unreacted monomer in the feed at a given time (t) and conversion (X_n). The value of f_1 can be obtained by solving the following differential copolymer composition equation (Equation 2.37), with initial conditions $f_1 = f_{10}$ at $X_n = 0$.

$$\frac{df_1}{dX_n} = \frac{(f_1 - F_1)}{1 - X_n} \tag{2.37}$$

In a series of case studies, the analytical integration method was compared to DNI to establish the level of precision possible with each technique [20]. In general, there was good agreement between the instantaneous (low conversion) model and the cumulative (moderate to high conversion) model. However, the cumulative data provided more precise estimates than the instantaneous model (due to the enhanced information content). It was also found that direct numerical integration is almost always superior to the Meyer-Lowry model, as the former gave more precise reactivity ratio estimates and the latter often failed to converge. Ultimately, the work by Kazemi et al. [20] has shown that reactivity ratios can be more accurately estimated using EVM and cumulative copolymer composition models.

2.2.3 Experimental Design for Reactivity Ratio Estimation

An important part of reactivity ratio estimation is the experimental design. A series of experiments should be designed in an optimal way; this leads to increased information content while minimizing the number of experiments and obtaining more precise parameter estimates. Optimally designed experiments typically have much smaller joint confidence regions (JCRs), which is indicative of higher precision estimates [28]. Needless to say, design of experiments is hardly ever used in the literature in parameter estimation schemes.

One of the earliest (mechanistic model-based) techniques used to design reactivity ratio estimation experiments was presented by Tidwell and Mortimer [24]. Tidwell and Mortimer applied an (approximate) D-optimality criterion to the Mayo-Lewis copolymerization equation to determine the best feed compositions at which to run reactivity ratio estimation experiments. The Tidwell-Mortimer design gives the following experimental conditions as optimal suggestions:

$$f_{2,1} = \frac{r_1}{2+r_1} \qquad \text{and} \qquad f_{2,2} = \frac{2}{2+r_2} \tag{2.38}$$

where $f_{2,1}$ and $f_{2,2}$ denote the feed composition of monomer 2 for the 1st and 2nd experiments, respectively. Preliminary reactivity ratio estimates (r_1 and r_2) can be obtained from the literature or from some type of preliminary experimentation.

The Tidwell-Mortimer (T-M) equations are recognized as practical tools for the design of optimal experiments in reactivity ratio estimation. However, the method does have some limitations. The T-M design cannot take composition constraints into account, nor can it be used to design penultimate reactivity ratio estimation experiments [33]. When composition constraints are being considered, it is important to note that reactivity ratios estimated over a limited range may differ from those estimated for the overall polymerization. In this case, it becomes necessary to maximize the D-optimal criterion within the constraints [33]. General (heuristic) rules have been developed for this special case, and are presented below:

$$f_{2,1} = \frac{r_1}{2}\left[1 - \exp\left(-\frac{f_{2,2}}{r_1}\right)\right] \qquad \text{for } 0 < r_1 < 1.5 \qquad (2.39\text{ (a)})$$

$$= \frac{f^*_{2,1}}{f^*_{2,2}} f_{2,2} \qquad \text{for } r_1 \geq 1.5 \qquad (2.39\text{ (b)})$$

$$f_{2,2} = 1 - \frac{r_2}{2}\left[1 - \exp\left(-\frac{(1-f_{2,1})}{r_2}\right)\right] \qquad \text{for } 0 < r_2 < 1.5 \qquad (2.40\text{ (a)})$$

$$= 1 - \frac{(1-f^*_{2,2})}{(1-f^*_{2,1})}(1 - f_{2,1}) \qquad \text{for } r_2 \geq 1.5 \qquad (2.40\text{ (b)})$$

where $f_{2,1}^{*}$ and $f_{2,2}^{*}$ represent the feed compositions at which the D-optimality criterion is maximized, without considering any constraints. For feed composition restricted by an upper bound, *a*, $f_{2,2} = a$ and $f_{2,1}$ is calculated by one of the above equations (Equation 2.39 (a) or (b)). Similarly, for feed composition restricted by a lower bound, *b*, $f_{2,1} = b$ and $f_{2,2}$ is calculated by Equation 2.40 (a) or (b). In general, the optimal feed compositions ($f_{2,1}$ and $f_{2,2}$) that will be chosen under composition constraints should be as close to the unconstrained optimal feed compositions ($f_{2,1}^{*}$ and $f_{2,2}^{*}$) as possible [33].

D-optimality is an extremely powerful criterion, and through its "ease-of-use" can act as a good starting point for experimental design. A more complex, yet equally valid technique for designing optimal reactivity ratio estimation experiments is the error-in-variables-model, EVM. As discussed previously (with regards to reactivity ratio estimation in Section 2.2.1), EVM considers error terms in all variables. Therefore, when error is likely to exist in both the independent and dependent variables, it may be beneficial to use a design of experiments technique within the EVM context [23].

The information matrix ($\underline{I}$) to be optimized within EVM is more complex than that of the standard T-M D-optimal design. For typical D-optimal designs (in the regular non-linear regression context),

$$I_{D-opt} = \sum_{i=1}^{n} \frac{1}{{\sigma^2}_{1i}} \underline{Z}_i' \underline{Z}_i \tag{2.41}$$

Alternatively, for EVM designs,

$$I_{EVM} = \sum_{i=1}^{n} \frac{1}{{\sigma^2}_{1i} + {\sigma^2}_{2i}\left(\beta_i\left(\underline{\xi}_i, \underline{\theta}\right)\right)^2} \underline{Z}_i(\underline{\xi}_i, \underline{\theta}) \underline{Z}_i'(\underline{\xi}_i, \underline{\theta}) \tag{2.42}$$

where σ_1^2 = variance of dependent variables, σ_2^2 = variance of independent variables, $\underline{\beta}$ = vector of partial derivatives of the model ($\underline{g}(\underline{\xi}_i, \underline{\theta})$) with regard to the variables ($\underline{\xi}_i$) (see Equation 2.27), and $\underline{Z}$ = vectors of partial derivatives of the model with regard to the parameters ($\underline{\theta}$) (see Equation 2.31).

During experimentation, there are both initial and sequential design schemes. The initial design is used when no prior information is known about the system; the design is based solely on a certain number of trials (usually chosen arbitrarily or at random, so they may or may not be optimal), and is a function of the number of parameters in the model. Alternatively, a sequential design is employed when some prior information is available for the system, but the parameters have not yet been estimated with sufficient precision. As the name suggests, the sequential design is an iterative process, and is repeated until the desired level of precision is obtained for the parameter estimates being studied [23]. Typically, sequential design schemes provide smaller JCRs, thus indicating that the results are more reliable than initial designs.

2.3 Literature Background: Comonomers for Case Study

The terpolymerization of 2-acrylamido-2-methylpropane sulfonic acid (AMPS), acrylamide (AAm), and acrylic acid (AAc) is largely unstudied. Therefore, to gain a better understanding of the system, copolymer combinations of the three monomers are investigated. Since the copolymerization kinetics of AAm/AAc are well studied [10], the two other comonomer combinations (AMPS/AAm and AMPS/AAc) are examined first.

2.3.1 Copolymerization of AMPS and Acrylamide

The majority of the work in the copolymerization of 2-acrylamido-2-methylpropane sulfonic acid (AMPS) with acrylamide (AAm) has focused on crosslinking systems, as crosslinked copolymers of AMPS and AAm have applications as superabsorbent hydrogels [34–40]. As with many other copolymer systems, such studies look at the final polymer (synthesis and characterization without considering the full conversion trajectory) and its performance properties, while they rarely investigate polymerization kinetics or reactivity ratio estimation.

There has also been some work done in examining the effectiveness of AMPS/AAm copolymers in enhanced oil recovery (EOR) [9, 41–43]. The focus of these articles is intended to be the synthesis and testing of polymers for EOR use. In enhanced oil recovery, copolymers must withstand hostile conditions and undergo minimal degradation. Therefore, the AMPS/AAm copolymer should exhibit good stability. Characterization techniques that are specific to EOR applications include determination of stability limits (thermal hydrolysis and salinity effects), shear resistance, molecular compositions (through infrared spectroscopy and proton or ^{1}H-NMR), apparent viscosities, crystallinities (through X-ray diffraction and thermogravimetric analysis), and performance in porous media.

It has been suggested that the steric hindrance from the sulfonic group in AMPS will increase main-chain stability and control potential degradation of AAm [9, 42]. However, Moradi-Araghi et al. [41] reported that the NaAMPS/AAm copolymer did not withstand thermal hydrolysis any better than the AAm homopolymer, and concluded that NaAMPS does not protect AAm against

thermal hydrolysis. While the addition of AMPS (or NaAMPS) has been shown to improve the copolymer stability slightly, it has a much more noticeable effect on brine compatibility [42]. According to Sabhapondit et al. [42, 43], the best copolymer performance with respect to brine compatibility, shear resistance and thermal stability was obtained when acrylamide was replaced with N,N-dimethylacrylamide (NNDAM) and copolymerized with NaAMPS.

In the current work, one of our objectives is to obtain accurate and reliable reactivity ratios for the AMPS/AAm copolymer, which is eventually extended to the AMPS/AAm/AAc terpolymer. Therefore, we have assembled a collection of reactivity ratios reported in the literature for the copolymerization of AMPS and AAm. As outlined in Section 2.2, there tend to be significant discrepancies between reported values. This may be due, in part, to poorly designed experiments, inconsistent experimental methodologies, and incorrect reactivity ratio estimation techniques. A summary of reactivity ratios for the AMPS/AAm copolymer, along with the associated experimental techniques and reactivity ratio estimation methods, is presented in Table 2.2.

Table 2.2: Reactivity Ratio Summary for AMPS/AAm

Ref.	Experimental	Estimation Technique	r_{AMPS}	r_{AAm}
[44]	--Type: Aqueous solution copolymerization --Initiator: KPS --Temperature: 50°C --Composition: EA	Billmeyer 1 [45] Billmeyer 2 [45] Kelen-Tudos Average	0.76 0.70 0.62 0.70 ± 0.08	1.00 1.06 1.21 1.10 ± 0.10
[46]	--Type: Aqueous solution copolymerization --Initiator: KPS --Temperature: 35°C & 55°C --Composition: ^{1}H-NMR & vibrational Raman spectroscopy	Fineman-Ross	1.00	1.00
[34]	--Type: Aqueous solution crosslinking copolymerization --Initiator: KPS --Temperature: 40°C --pH = 7 --Composition: IR & EA	Comparison of feed & copolymer compositions (no statistical estimation)	1.00	1.00
[47]	--Type: Aqueous solution copolymerization --Initiator: KPS --Temperature: 30°C --pH = 9 --Composition: IR & EA	Fineman-Ross Kelen-Tudos Integrated Mayo-Lewis	0.49 ± 0.02 0.52 ± 0.07 0.50 ± 0.01	0.98 ± 0.09 1.00 ± 0.08 1.02 ± 0.01
[48]	--Type: Aqueous solution copolymerization --Initiator: APS --Temperature: 60°C --Composition: EA & ^{13}C-NMR	Fineman-Ross Kelen-Tudos	0.37 ± 0.04 0.42 ± 0.03	1.01 ± 0.01 1.05 ± 0.06
[48]	--Type: Aqueous solution redox copolymerization --Initiator: APS/$NaHSO_3$ --Temperature: 25°C --Composition: ^{13}C-NMR	Fineman-Ross Kelen-Tudos	0.54 ± 0.03 0.51 ± 0.03	1.07 ± 0.01 1.05 ± 0.06

Nomenclature: AAm, acrylamide; AMPS, 2-acrylamido-2-methylpropane sulfonic acid; APS, ammonium persulfate; EA, elemental analysis; IR, infrared spectroscopy; KPS, potassium persulfate; NMR, nuclear magnetic resonance

Although some of the estimates are similar (especially for r_{AAm}), there are notable inconsistencies between experimental techniques and reactivity ratio estimation methods. It is also important to note that all of the estimation techniques used to date have been linear. Given the numerous sources of error associated with linear estimation methods and the advantages of

non-linear techniques (described in Section 2.2), it seems only reasonable that future reactivity ratios be estimated using EVM.

2.3.2 Copolymerization of AMPS and Acrylic Acid

Very few studies have been found with regards to the copolymerization of 2-acrylamido-2-methylpropane sulfonic acid (AMPS) and acrylic acid (AAc). Even fewer have investigated the polymerization kinetics and, specifically, copolymer reactivity ratios. In previous studies, AMPS and acrylic acid have been copolymerized in the presence of crosslinking agents such as N,N'-methylenebisacrylamide (MBA) [49–52], and the crosslinked products have been grafted onto backbones via free radical graft polymerization [53–55]. Crosslinked AMPS/AAc polymers typically act as hydrogels, therefore most studies to date have examined the swelling behaviour and thermal stability of the hydrogels. Characterization techniques have included Fourier Transform Infrared Spectroscopy (FTIR), Soxhlet extraction, thermogravimetric analysis (TGA) and scanning electron microscopy (SEM).

Only two studies [49, 56] have been identified that provided reactivity ratio estimates for the AMPS/AAc copolymer along with a description of synthesis and characterization methods. In the work by Abdel-Azim et al. [49], crosslinking for hydrogel formation was still the primary objective, but the system was also studied at low conversions and in the absence of crosslinker for comparison purposes. However, reactivity ratios for the AMPS/AAc copolymer were estimated using both the Fineman-Ross and Kelen-Tudos (linear!) methods. The techniques showed relatively good agreement, and the authors chose to average the two values obtained (see Table 2.3), which is a gross approximation for r_{AMPS}.

Table 2.3: Reactivity Ratio Estimates for AMPS/AAc Copolymer [49]

Estimation Technique	r_{AMPS}	r_{AAc}
Fineman-Ross	0.304	0.915
Kelen-Tudos	0.15	0.98
Average	0.27	0.95

Experimentally, the AMPS/AAc copolymer was synthesized in aqueous solution (under nitrogen) at 328 K, with 0.02 wt% benzoyl peroxide (BPO) as the initiator [49]. After polymerization, the copolymer samples were precipitated in methyl ethyl ketone, filtered, washed, and dried under vacuum at 308 K. To estimate the reactivity ratios, 5 different feed compositions were used ($f_{AMPS,0}$ ranged from 0.4 to 0.8, as a mass fraction) and conversion was kept below 10%.

Based on this previous study [49], synthesis of the AMPS/AAc copolymer for the current work seems very promising. Despite the inaccurate reactivity ratio estimation techniques described above, it is still possible to conclude that reactivity ratios for r_{AMPS} and r_{AAc} are of similar orders of magnitude. Therefore, the copolymer of AMPS/AAc should be easily synthesized at a variety of feed compositions.

2.3.3 Terpolymerization of AMPS, Acrylamide, and Acrylic Acid

In recent years, several studies have investigated the AMPS/AAm/AAc terpolymer. Many of these works have focused on synthesis, characterization, and potential applications for this terpolymer; none of the studies have included terpolymerization kinetics.

For example, Bao et al. [57] grafted the AMPS/AAm/AAc terpolymer onto sodium carboxymethyl cellulose (CMC) and motmorillonite (MMT) to create a superabsorbent hydrogel. In this case, physical properties of the synthesized terpolymer (such as degree of swelling, water retention, and morphology) were the focus of the analysis, and reaction kinetics were not discussed.

Similarly, Ma et al. [58] synthesized the AMPS/AAm/AAc terpolymer via UV irradiation for use as a flocculant. While this group did provide more information about their synthesis process, the overall focus of the paper was applications. Polymer characteristics including intrinsic viscosity, dissolving time and flocculation performance were presented [58].

This particular terpolymer has also been used in drug-delivery applications [59]. The drug-delivery system uses tailor-made superabsorbent polymer composites, so characteristics such as swelling capacity and drug encapsulation efficiency were studied. While the investigation included release kinetics for drug-delivery, it did not discuss details surrounding the polymerization kinetics [59].

In perhaps the most relevant papers to the current work, Peng et al. [60] and Zaitoun et al. [6] have studied the AMPS/AAm/AAc terpolymer for petrochemical applications. The work by Peng et al. describes the free-radical terpolymerization of AMPS/AAm/AAc and its application as a high-temperature resistant filtration control agent [60]. Zaitoun et al. have investigated the potential to use AMPS/AAm/AAc in enhanced oil recovery (EOR) applications, as the AMPS comonomer is expected to improve shear stability and limit thermal degradation (compared to

standard AAm/AAc copolymers) [6]. However, in both of these cases, the authors make no mention of polymerization kinetics.

The characteristics of the terpolymer being synthesized in this work are directly related to its microstructure. Therefore, it is important to have a clear understanding of the terpolymerization kinetics. Since this information is not available in the literature, reliable reactivity ratios for this AMPS/AAm/AAc system will be determined experimentally in what follows.

CHAPTER 3. EXPERIMENTAL

3.1 Experimental Approach

Ultimately, polymerization kinetics for the AMPS/AAm/AAc terpolymer system are investigated. However, as a first step, reliable kinetic data are collected for two of the associated copolymer systems, AMPS/AAm and AMPS/AAc (since the third one, AAm/AAc, has been well-studied in a parallel investigation [10]). For all of the experimental work, statistical design of experiments was used to select pre-polymerization recipes; more design information will be presented in system-specific chapters.

Obtaining accurate reactivity ratios for the binary systems can provide additional insight into the ternary system and can be used to determine optimal feed compositions for estimating ternary reactivity ratios. The latter part is very important, as experimenting with optimal feed compositions (at the design stage) can reduce considerably the overall experimental effort and lead to greatly improved information content.

3.2 Materials

Monomers 2-acrylamido-2-methylpropane sulfonic acid (AMPS; 99%), acrylamide (AAm; electrophoresis grade, 99%), and acrylic acid (AAc; 99%) were purchased from Sigma-Aldrich. AAc was purified via vacuum distillation at 30°C, while AAm and AMPS were used as received. Initiator (4,4'-azo-bis-(4-cyanovaleric acid), ACVA), inhibitor (hydroquinone) and sodium

hydroxide were also purchased from Sigma-Aldrich. Sodium chloride from EMD Millipore was used as received. In terms of solvents, water was Millipore quality (18 MΩ cm^{-1}); acetone and methanol were used as received from suppliers. Nitrogen gas (4.8 grade) used for degassing solutions was purchased from Praxair.

3.3 Polymer Synthesis

Monomer stock solutions with a total monomer concentration of 2 M were prepared. The comonomer ratios in each system (AMPS/AAm, AMPS/AAc and AMPS/AAm/AAc) are not cited here, but are described in detail later as part of the experimental design for each individual system. For each polymerization, 50 ml of the stock solution was used in a 100 ml pre-polymerization solution (that is, the total monomer concentration was diluted to 1 M). This pre-polymerization solution was prepared as follows: first, 50 ml of the stock solution was pipetted into a small beaker, at which point the initial solution pH was measured. The stock solution was then titrated with sodium hydroxide (1.5 M or 3 M) to adjust the pH to approximately 7 (±0.5), for direct comparison with the AAm/AAc copolymer studied previously [10]. Early in the titration, ~0.1121 g ACVA (initiator) was dissolved in a small amount of NaOH and added to the stock solution, such that the initiator concentration in the pre-polymerization recipe would be 0.004 M. Additionally, sodium chloride was added to each recipe to ensure constant ionic strength among the experiments (with different comonomer ratios). Both constant pH and ionic strength are extremely important in copolymer and terpolymer synthesis, as has been demonstrated previously [61], so the experimental procedures of Riahinezhad et al. [61] were

adopted throughout this thesis. Finally, the solution was diluted with high purity water to achieve a total solution volume of 100 ml and a total monomer concentration of 1 M.

Once each pre-polymerization solution was prepared, it was transferred to a round bottom flask and purged with 200 ml/min nitrogen for 2 hours. After degassing, aliquots of ~20 ml of solution were transferred to sealed vials using the cannula transfer method [10].

To initiate the polymerization reaction, vials were placed in a temperature controlled shaker-bath (Grant, OLS200) at 40°C and 100 rpm. Vials were removed at selected time intervals to ensure a well-defined conversion versus time plot. Once removed from the bath, the vials were placed in ice and further injected with approximately 1 ml of 0.2 M hydroquinone solution to stop the polymerization. Polymer samples were then isolated by precipitating the products in a 10-fold excess of acetone, or in a 50/50 mixture of acetone and methanol. In general, the AMPS/AAm copolymer was precipitated in excess acetone for high f_{AMPS}, while a 50/50 mixture of acetone and methanol was used for AMPS/AAm copolymers with low f_{AMPS} and all AMPS/AAc copolymers. Finally, the polymer samples were filtered (paper filter grade number 41, Whatman) and vacuum dried for 1 week at 50°C.

3.4 Polymer Characterization

Conversion of the polymer samples was determined using gravimetry. That is, the weight of each isolated, dried polymer (in a sample) was compared to the weight of the monomer that was initially within the vial. Mathematically, conversion can be calculated according to Equation 3.1:

$$X_w = \frac{\text{mass of polymer}}{\text{initial mass of monomer (in vial)}} \tag{3.1}$$

The mass of the sodium ions was also considered in conversion calculations, as per the recommendation of Riahinezhad et al. [61]. Not doing so would introduce error and may bias results; sample calculations are presented in Appendix D (Section D.1).

Polymer composition was measured using elemental analysis (CHNS, Vario Micro Cube, Elementar). The content of elemental C, H, N and S in the samples was determined. However, calculation of the copolymer or terpolymer composition did not include H content, as residual water has been known to affect the determined H content [10]. Appendix D (Section D.2) shows sample calculations for the determination of cumulative composition.

CHAPTER 4. AMPS/AAm COPOLYMER

4.1 Preliminary Experiments

4.1.1 Selection of Preliminary Feed Compositions

The preliminary design for the copolymer of 2-acrylamido-2-methylpropane sulfonic acid (AMPS) and acrylamide (AAm) was based on information from several different sources. Initial estimates of monomer reactivity ratios for the AMPS/AAm copolymer from the literature were first scrutinized, and the classical work by McCormick and Chen [47] was chosen as the most suitable reference (see Table 4.1). These preliminary reactivity ratios were incorporated into both Tidwell-Mortimer and EVM design techniques (see Section 2.2.3), and the following results were obtained.

Table 4.1: Preliminary Design for AMPS/AAm

Reactivity Ratios:	r_1 (r_{AMPS})	r_2 (r_{AAm})
From Literature [47]	0.50	1.02
Feed Composition:	$f_{11,0}$	$f_{12,0}$
Tidwell-Mortimer	0.34	0.80
EVM	0.10	0.69
Selected Design	0.15	0.80

Ultimately, the selected design (presented in the final row of Table 4.1) was chosen according to a combination of Tidwell-Mortimer and EVM designs, based on process understanding. The lower feed composition, $f_{AMPS,0}$ = 0.15 was selected as a compromise between the Tidwell-Mortimer and EVM designs. The higher feed composition, $f_{AMPS,0}$ = 0.80, was selected to ensure

that one of the copolymers would be rich in AMPS. It was anticipated that this combination of pre-polymerization recipes would provide a substantial amount of kinetic information.

4.1.2 Preliminary Reactivity Ratio Estimation

For the preliminary experiments, copolymerizations were independently replicated at least once at each feed composition. Some variability was observed between replicates, as evidenced by Figure 4.1 (the full data set is also available in Appendix C, Table C.1). This is to be expected for preliminary runs, mainly due to the learning curve of the operator and also establishment of appropriate experimental procedures and steps. However, process and data repeatability tends to improve in subsequent steps, as the replication error becomes increasingly smaller with more experience in both experimental and analytical techniques.

At both $f_{AMPS,0} = 0.15$ and $f_{AMPS,0} = 0.80$, the polymerization took place fairly quickly. As exhibited by the conversion vs. time plots in Figure 4.1, both polymerizations had reached about 20% conversion after 10 minutes. Therefore, instantaneous reactivity ratio estimation techniques requiring low conversion levels (and negligible composition drift) would not be appropriate for this particular data set.

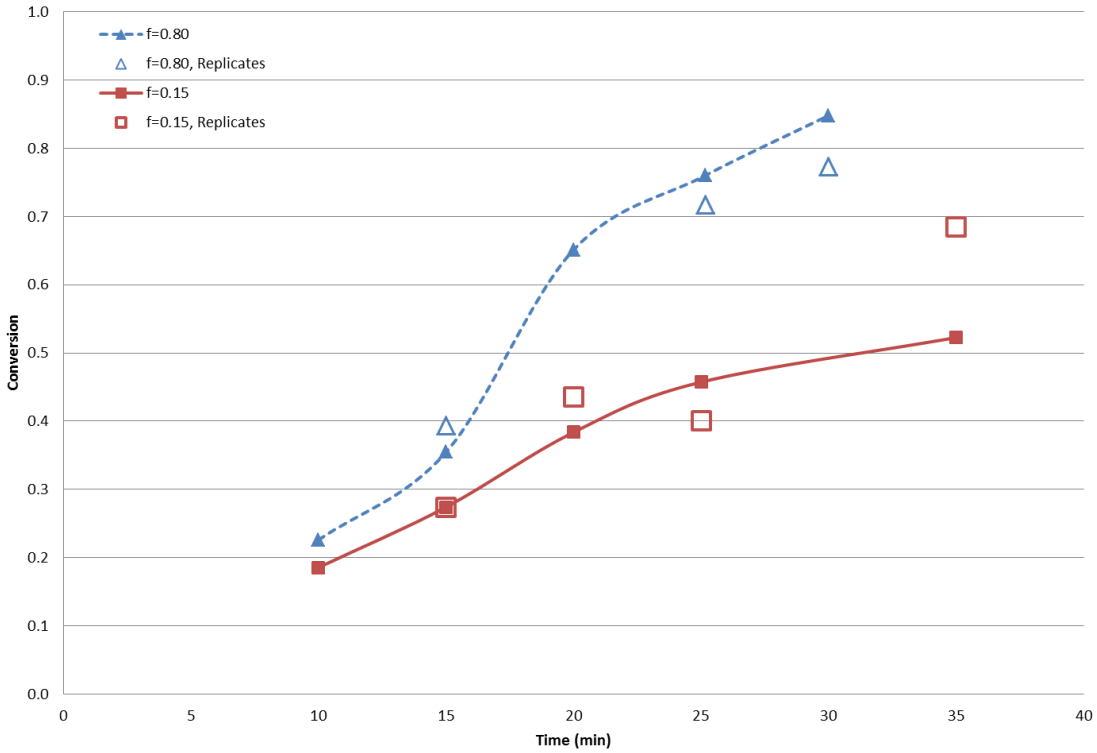

Figure 4.1: Conversion vs. Time Plot for Preliminary AMPS/AAm Copolymerization Experiments

Thus, preliminary reactivity ratio estimates (both r_{AMPS} and r_{AAm}) were calculated by applying the cumulative composition model (using direct numerical integration, DNI, as described in Kazemi et al. [20]) to the data through EVM. As mentioned in Table 4.1, the initial point estimates (r_{AMPS} = 0.50, r_{AAm} = 1.02) were taken from McCormick and Chen [47]. Because there seemed to be considerable error in the conversion vs. time data, the variance estimate for X (where X is the conversion at time t) was determined as follows [30]:

$$V(X) = \frac{k^2}{3} = \frac{(0.1)^2}{3} = 0.00\overline{3} \qquad (4.1)$$

where k represents the best estimate of measurement error, as described previously for Equation 2.23 (see Section 2.2.1).

The joint confidence region (JCR) for the preliminary reactivity ratios is presented in Figure 4.2. The point estimate from literature is included in the figure for reference, and the current updated estimate is $r_{AMPS} = 0.13$ and $r_{AAm} = 0.84$.

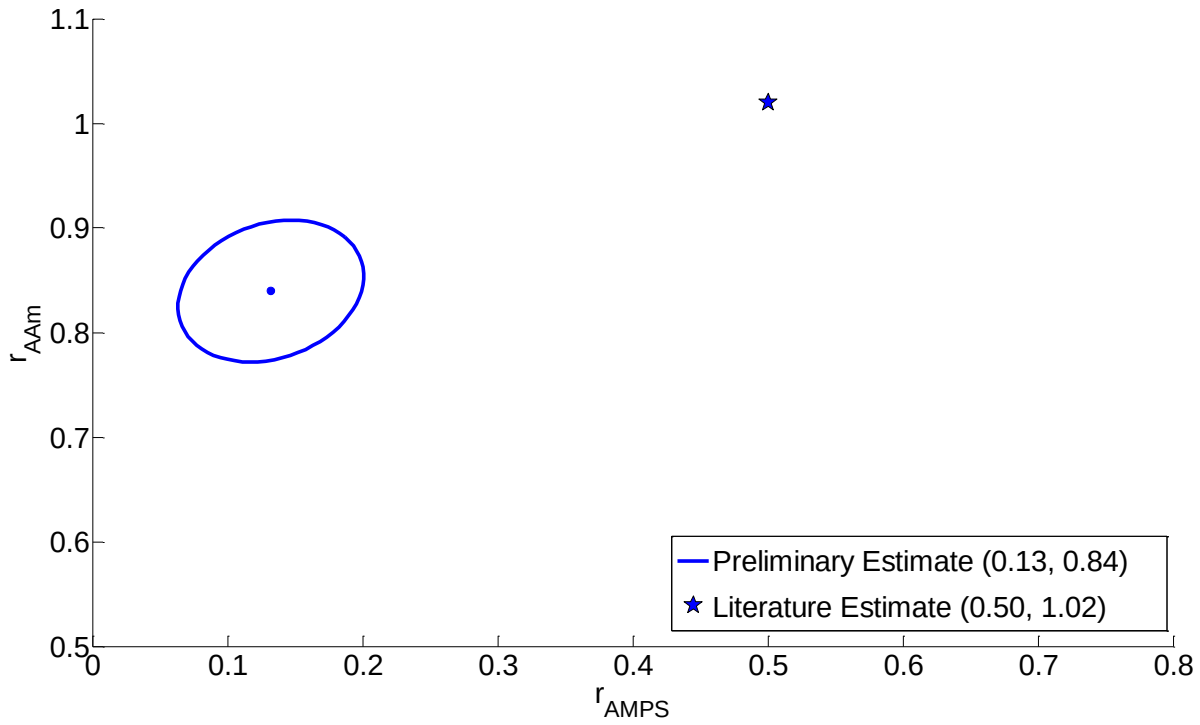

Figure 4.2: Preliminary Reactivity Ratio Estimates for AMPS/AAm

In Figure 4.2, it is clear that the reactivity ratio estimates made by McCormick and Chen [47] are different from our newly determined reactivity ratios; the estimates from the literature study are not contained within the JCR for the initial stage. However, as indicated in Table 2.2, the work by McCormick and Chen [47] was at pH = 9, 30°C and used potassium persulfate (KPS) as the initiator. This is in contrast to the current experimental work, which is at pH = 7, 40°C and uses ACVA as the initiator (see Section 3.3 for more information). Because the polymerization conditions are different in both cases, especially in terms of pH, a difference in results is somewhat expected. These preliminary results can now be used to design optimal experiments

for reactivity ratio estimation for the next stage; the sequential investigation is continued in what follows.

4.2 Optimal Experiments

4.2.1 Selection of Optimal Feed Compositions

Next, analysis of the binary system involved design of optimal experiments for reactivity ratio determination. For comparison purposes, both the Tidwell-Mortimer design and the EVM design were employed to determine optimal feed compositions. New estimates of the reactivity ratios (based on the preliminary experiments of Section 4.1) were used in finding optimal feed compositions (mole fractions) for the AMPS/AAm copolymerization, which are presented in Table 4.2.

Table 4.2: Optimal Design for AMPS/AAm

Reactivity Ratios	r_1 (r_{AMPS})	r_2 (r_{AAm})
Experimentally Determined (from preliminary experiments)	0.13	0.84
Feed Composition	f_{11}	f_{12}
Tidwell-Mortimer (T-M)	0.30	0.94
EVM	0.10	0.89

It is anticipated that the EVM design will provide more precise parameter estimates (that is, smaller joint confidence regions), but both techniques are investigated to confirm this hypothesis and also provide a comparison between the T-M vs EVM design approaches (not readily available in the literature).

4.2.2 Tidwell-Mortimer Design

As shown in Table 4.2, the Tidwell-Mortimer design dictates two levels for the feed composition: a "low" and a "high" fraction of AMPS. Despite the Tidwell-Mortimer design dictating a "high" f_{AMPS} level of 0.94, the feed composition for the second experiment was chosen as $f_{AMPS} = 0.91$. Because the kinetics for this system are still largely unknown, a slightly lower fraction was chosen to ensure that there would still be sufficient AAm in the recipe to produce a copolymer of AMPS/AAm. The experimental results are shown in Table 4.3.

Table 4.3: Experimental Data for AMPS/AAm Copolymerization; Tidwell-Mortimer Design

Run #	X	$f_{AMPS,0}$	$f_{AAm,0}$	$\overline{F}_{AMPS}$	$\overline{F}_{AAm}$
1	0.0061	0.30	0.70	0.3243	0.6757
	0.1078	0.30	0.70	0.2592	0.7408
	0.2614	0.30	0.70	0.2683	0.7317
	0.3335	0.30	0.70	0.2701	0.7299
	0.4717	0.30	0.70	0.2841	0.7159
2	0.0583	0.91	0.09	0.6772	0.3228
	0.1483	0.91	0.09	0.6779	0.3221
	0.2829	0.91	0.09	0.7043	0.2957
	0.5207	0.91	0.09	0.7223	0.2777
	0.7076	0.91	0.09	0.7374	0.2626
3	0.0671	0.30	0.70	0.2794	0.7206
	0.1035	0.30	0.70	0.2626	0.7374
	0.1830	0.30	0.70	0.2735	0.7265
	0.2604	0.30	0.70	0.2797	0.7203
	0.3910	0.30	0.70	0.2858	0.7142
4	0.0519	0.91	0.09	0.8335	0.1665
	0.1441	0.91	0.09	0.7955	0.2045
	0.2710	0.91	0.09	0.7648	0.2352
	0.4626	0.91	0.09	0.7715	0.2285
	0.6151	0.91	0.09	0.7762	0.2238

As before, both runs were independently replicated and the data points collected were reproducible. However, it is important to note that an additional source of error may exist due to residual monomer in the product (especially for low conversion samples), which is very difficult to remove due to the nature of the monomer.

As for the preliminary experiments of Section 4.1, the cumulative composition model (using direct numerical integration) was applied to the conversion and cumulative composition data through the error-in-variables-model. The resulting reactivity ratio estimates (r_{AMPS} = 0.16 & r_{AAm} = 0.77) and the associated JCR are presented in Figure 4.3, with the literature estimate [47] and the preliminary experiments from Section 4.1 included for reference.

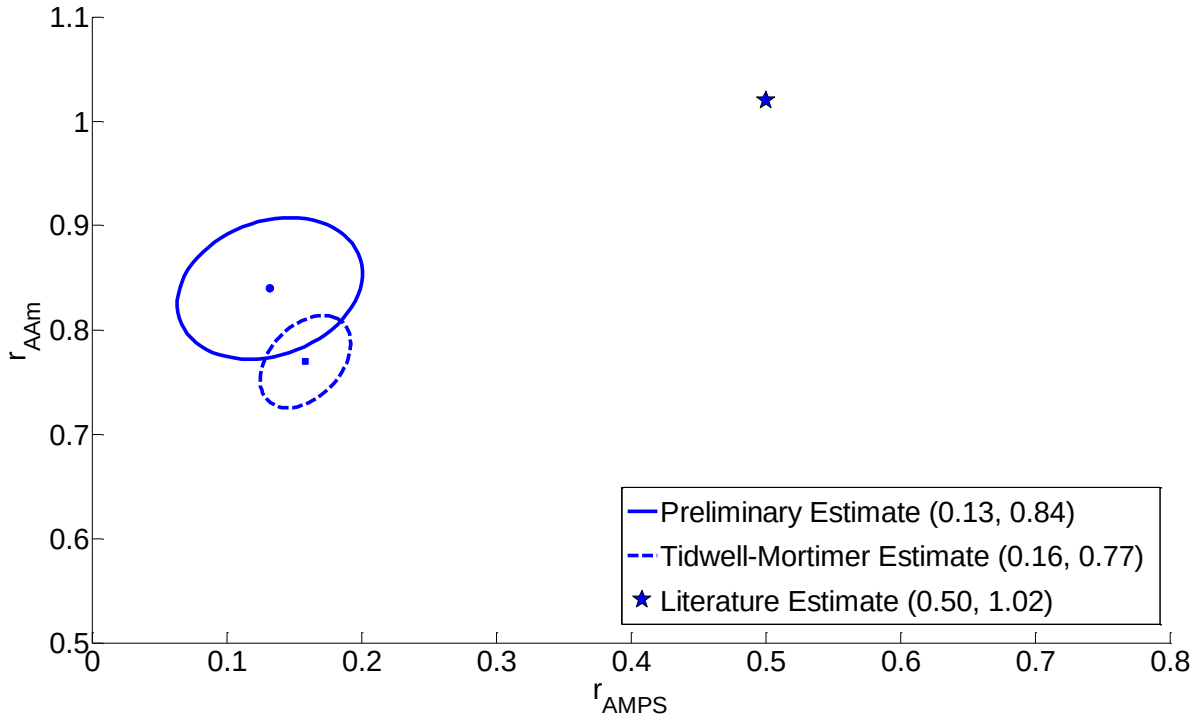

Figure 4.3: Tidwell-Mortimer-Designed Reactivity Ratio Estimates for AMPS/AAm

Now, we begin to see the advantages of using optimally designed experiments for reactivity ratio estimation. The JCR obtained using the Tidwell-Mortimer design is much smaller than the preliminary design, which indicates that we have a much smaller degree of uncertainty (therefore greater confidence in our estimates) with the same amount of experimental data. Overall, the T-M-designed results show good agreement with the preliminary results. While the r_{AAm} estimate is slightly lower than the preliminary one, the new r_{AMPS} estimate is well within the preliminary range. In addition, the two JCRs are overlapping. This not only allows for a high degree of confidence in the T-M-designed results, but also prompts the continuation of optimal sequential design of experiments towards the EVM design.

4.2.3 Error-In-Variables-Model Design

As for the Tidwell-Mortimer design, the EVM design was established using the preliminary estimates of Section 4.1. Again, a slightly lower value was used for the "high" feed composition level, based on process constraints and understanding. Therefore, the EVM design used f_{AMPS} = 0.10 and f_{AMPS} = 0.84 (with independent replicates) to estimate reactivity ratios. The experimental results are shown in Table 4.4.

The reactivity ratio estimates obtained from this data set (r_{AMPS} = 0.20 & r_{AAm} = 0.57), as well as the corresponding JCR, are shown in Figure 4.4. Again, prior estimates for the AMPS/AAm system are shown for comparison purposes.

Table 4.4: Experimental Data for AMPS/AAm Copolymerization; EVM Design

Run #	X	$f_{AMPS,0}$	$f_{AAm,0}$	$\overline{F}_{AMPS}$	$\overline{F}_{AAm}$
1	0.2065	0.10	0.90	0.1878	0.8122
	0.2202	0.10	0.90	0.2336	0.7664
	0.3408	0.10	0.90	0.1141	0.8859
	0.3425	0.10	0.90	0.0937	0.9063
	0.7073	0.10	0.90	0.0801	0.9199
2	0.0267	0.84	0.16	0.7033	0.2967
	0.0731	0.84	0.16	0.5977	0.4023
	0.1412	0.84	0.16	0.6332	0.3668
	0.1923	0.84	0.16	0.7141	0.2859
	0.3348	0.84	0.16	0.6555	0.3445
3	0.1064	0.10	0.90	0.1681	0.8319
	0.1473	0.10	0.90	0.0911	0.9089
	0.2373	0.10	0.90	0.2431	0.7569
	0.3556	0.10	0.90	0.0898	0.9102
	0.6174	0.10	0.90	0.0922	0.9078
4	0.0261	0.84	0.16	0.6741	0.3259
	0.2862	0.84	0.16	0.7030	0.2970
	0.3589	0.84	0.16	0.6938	0.3062

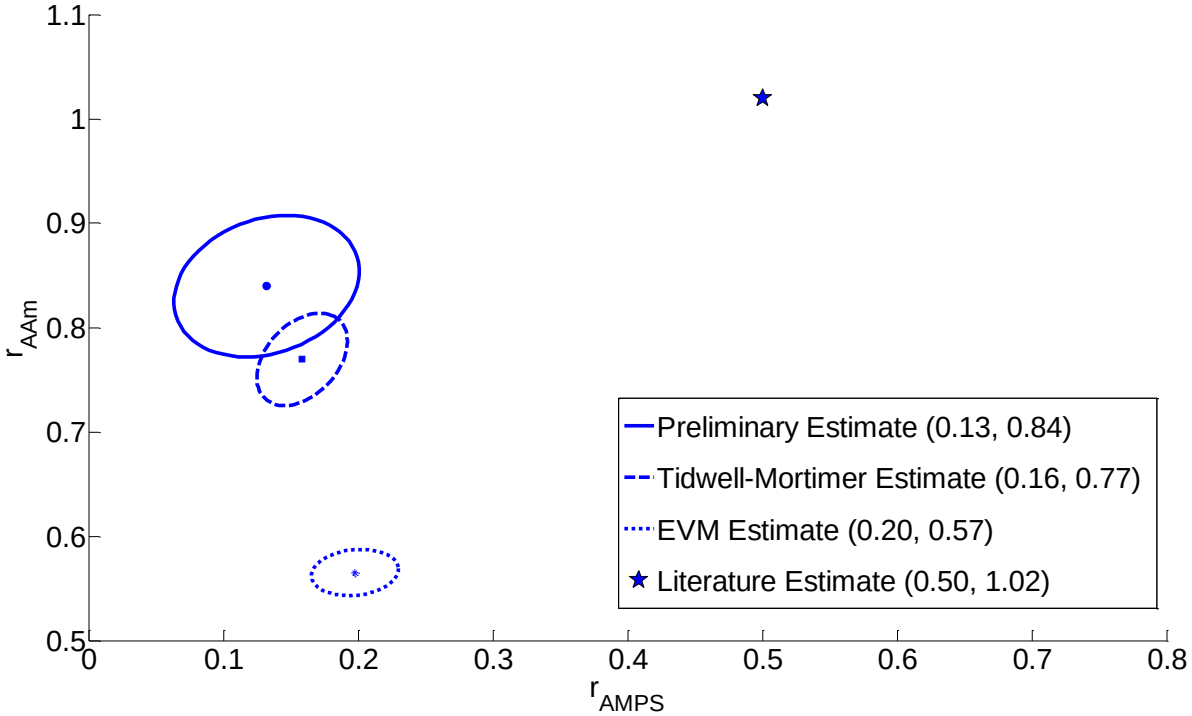

Figure 4.4: EVM-Designed Reactivity Ratio Estimates for AMPS/AAm

Here, we see good agreement in terms of r_{AMPS} estimates. However, the estimate for r_{AAm} changes significantly with the EVM design (compared to the preliminary and T-M designs). One possible reason for the drift in r_{AAm} is the fact that experimental data was collected in terms of AMPS (this is true of both feed composition and cumulative copolymer composition). Similarly, elemental analysis calculations were performed on a sulfur basis (see Appendix D), which may increase the accuracy of AMPS composition measurements at the expense of AAm composition measurements. Further analysis of the data and the effects of data perturbation will be presented in Section 4.4.

In general, though, the trends are satisfactory. Despite the discrepancy in the r_{AAm} estimates, r_{AAm} is consistently less than 1.0 (with the exception of the literature value [47]), and $r_{AAm} > r_{AMPS}$ in all cases.

4.3 Discussion of Results for AMPS/AAm

As mentioned previously, reactivity ratios are extremely important parameters in copolymerization kinetics. We can compare the results from literature, T-M design, and EVM design, and use the best estimates to characterize the copolymer.

To summarize the results of the experimental work, reactivity ratios for each data set are presented in Table 4.5. As the parameter estimates become more precise (that is, as the JCR area decreases), r_{AMPS} increases slightly whereas r_{AAm} decreases more significantly.

Table 4.5: Summary of Reactivity Ratio Estimates for AMPS/AAm

Step 1: Preliminary Design	r_{AMPS}	r_{AAm}
Literature Values [47]	0.50	1.02
Preliminary Estimates	0.13	0.84
Step 2: Optimal Designs		
Tidwell-Mortimer Estimates	0.16	0.77
Error-in-Variables-Model Estimates	0.20	0.57

It is important to establish whether these differences in reactivity ratio estimates for the same system will affect subsequent calculations. Reactivity ratios can be used to predict polymer properties such as copolymer composition. Eventually, this information could be used for custom polymer production for specific applications [62], so it extremely important that all estimates be as accurate as possible. Therefore, in this section, predictions from reactivity ratio estimates by McCormick and Chen [47], T-M design and EVM design are compared.

4.3.1 Cumulative Composition Analysis

First, the initial feed compositions selected using Tidwell-Mortimer designs are examined in Figure 4.5. Given the reactivity ratios from the two optimal designs and from literature (see Table 4.5) and the initial feed compositions ($f_{AMPS,0} = 0.30$ and $f_{AMPS,0} = 0.91$), we can predict the cumulative copolymer composition using the Skeist equation (Equation 2.36 in Section 2.2.2).

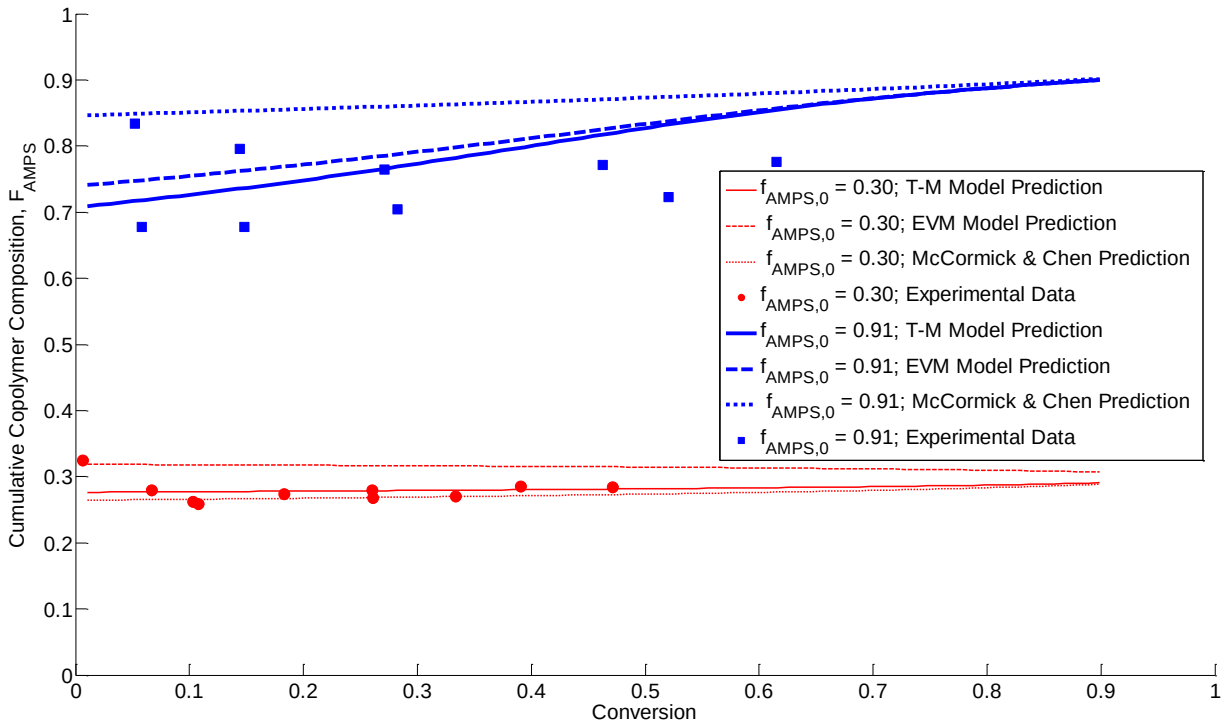

Figure 4.5: Cumulative Copolymer Composition for T-M-Designed Experiments ($f_{AMPS,0}$ = 0.30 & $f_{AMPS,0}$ = 0.91)

It is clear that slight differences in reactivity ratio estimates can have a significant effect on the prediction of $\overline{F}_{AMPS}$. For example, at $f_{AMPS,0}$ = 0.30, there is almost a 5% difference in composition predictions at low conversion. However, at this lower feed composition, the experimental data shows fairly good agreement with both the T-M-designed results and the literature data. It is reasonable that the results here are in better agreement with the T-M prediction than with the EVM prediction, as this feed composition was initially selected using the Tidwell-Mortimer procedure.

On the other hand, the model predictions at $f_{AMPS,0}$ = 0.91 show poor agreement with the experimental data. The discrepancies are likely due to experimental error, but the dissimilar trends necessitate further investigation (which will be discussed in Section 4.4). An additional point of interest here is the significant difference between the literature estimate predictions and

the optimally designed estimate predictions. At $f_{AMPS,0}$ = 0.30, the model predictions with the literature estimates were lower than the model predictions with optimally designed estimates (T-M and EVM). Conversely, at $f_{AMPS,0}$ = 0.91, the model predictions with the literature estimates were higher than the model predictions with optimally designed estimates. This is likely due to the fact that r_{AAm} > 1.0 in the literature, but the current analysis indicates that r_{AAm} < 1.0. Again, these results highlight the importance of obtaining accurate reactivity ratios in order to calculate other copolymer property trajectories properly.

Similarly, the initial feed compositions selected using EVM designs are shown in Figure 4.6. Again, cumulative copolymer composition was predicted using T-M-designed reactivity ratios, EVM-designed reactivity ratios, and literature values from McCormick and Chen [47].

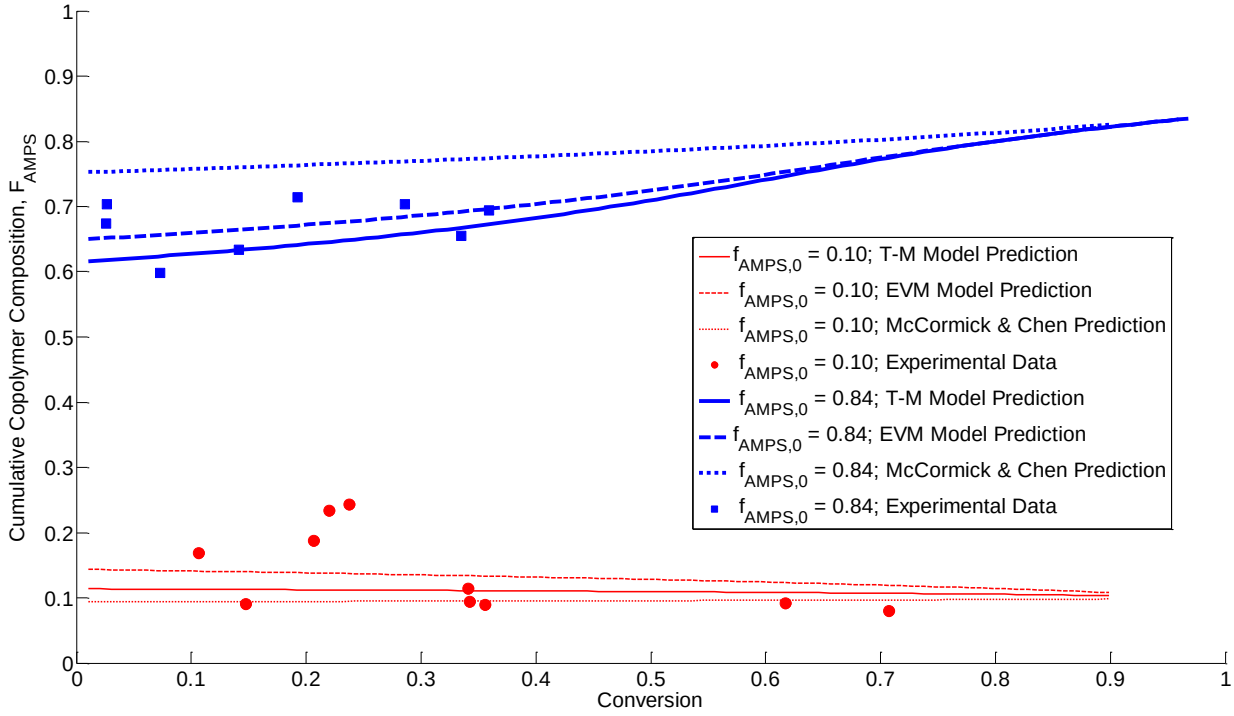

Figure 4.6: Cumulative Copolymer Composition for EVM-Designed Experiments ($f_{AMPS,0}$ = 0.10 & $f_{AMPS,0}$ = 0.84)

In this case, the experimental data points are highly variable. Specifically, the low conversion data (<5%) at $f_{AMPS,0}$ = 0.84 and the cumulative composition data between 20% and 25% conversion at $f_{AMPS,0}$ = 0.10 seem to stand out as outliers. Again, the validity of the experimental characterization technique is called into question, and the effect of these outliers (and other troubleshooting perturbations) will be investigated further in Section 4.4. However, these results confirm once more the fact that slight differences in reactivity ratio estimates will, in theory, significantly affect the cumulative copolymer composition. Therefore, accurate reactivity ratios are necessary for the production of custom-made polymers for specific applications.

4.3.2 Instantaneous Composition Analysis

The instantaneous copolymer composition can also be predicted in the same way that the cumulative copolymer composition was established using feed compositions and reactivity ratio estimates. As an example, the cumulative and instantaneous composition predictions for $f_{AMPS,0}$ = 0.84 are presented in Figure 4.7.

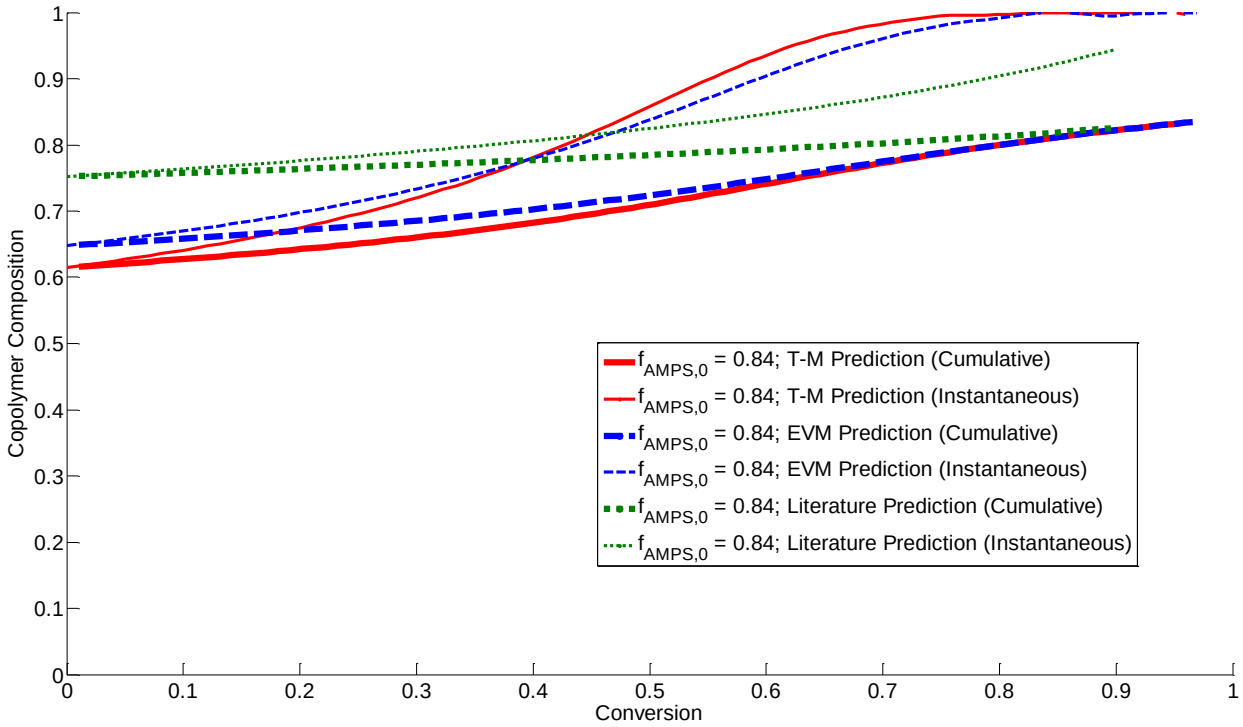

Figure 4.7: Instantaneous and Cumulative Copolymer Composition Predictions for $f_{AMPS,0}$ = 0.84

The above plot shows clear similarities between the T-M-designed prediction and the EVM-designed prediction, with slight discrepancies at low conversion. However, the trends are consistent, and the models seem to converge at higher levels of conversion (> 50%). Conversely, the instantaneous and cumulative copolymer composition models using the reactivity ratios from McCormick and Chen [47] give very different results. The initial copolymer composition is at least 10% higher than that predicted by the current investigation, and the trends differ significantly. This is another indication that the accuracy of reactivity ratios is extremely important, which confirms previous observations made in this thesis (and in other literature).

4.3.3 Azeotropic Investigation

An additional point of interest in this study is establishing whether an azeotropic composition exists for the AMPS/AAm copolymer system. At the azeotropic point, the feed composition (f_{AMPS}) and the instantaneous copolymer composition (F_{AMPS}) are equivalent. Since the reactivity ratios are known, we can use the Mayo-Lewis copolymerization equation (Equation 2.10) to examine F_{AMPS} as a function of f_{AMPS} and to establish the azeotropic point.

Figure 4.8 demonstrates how F_{AMPS} varies with f_{AMPS}, given three sets of reactivity ratio estimates ((a) literature data, (b) T-M-designed data, and (c) EVM-designed data). The point at which the curve passes through the 45° line ($F_{AMPS} = f_{AMPS}$) represents the azeotropic composition.

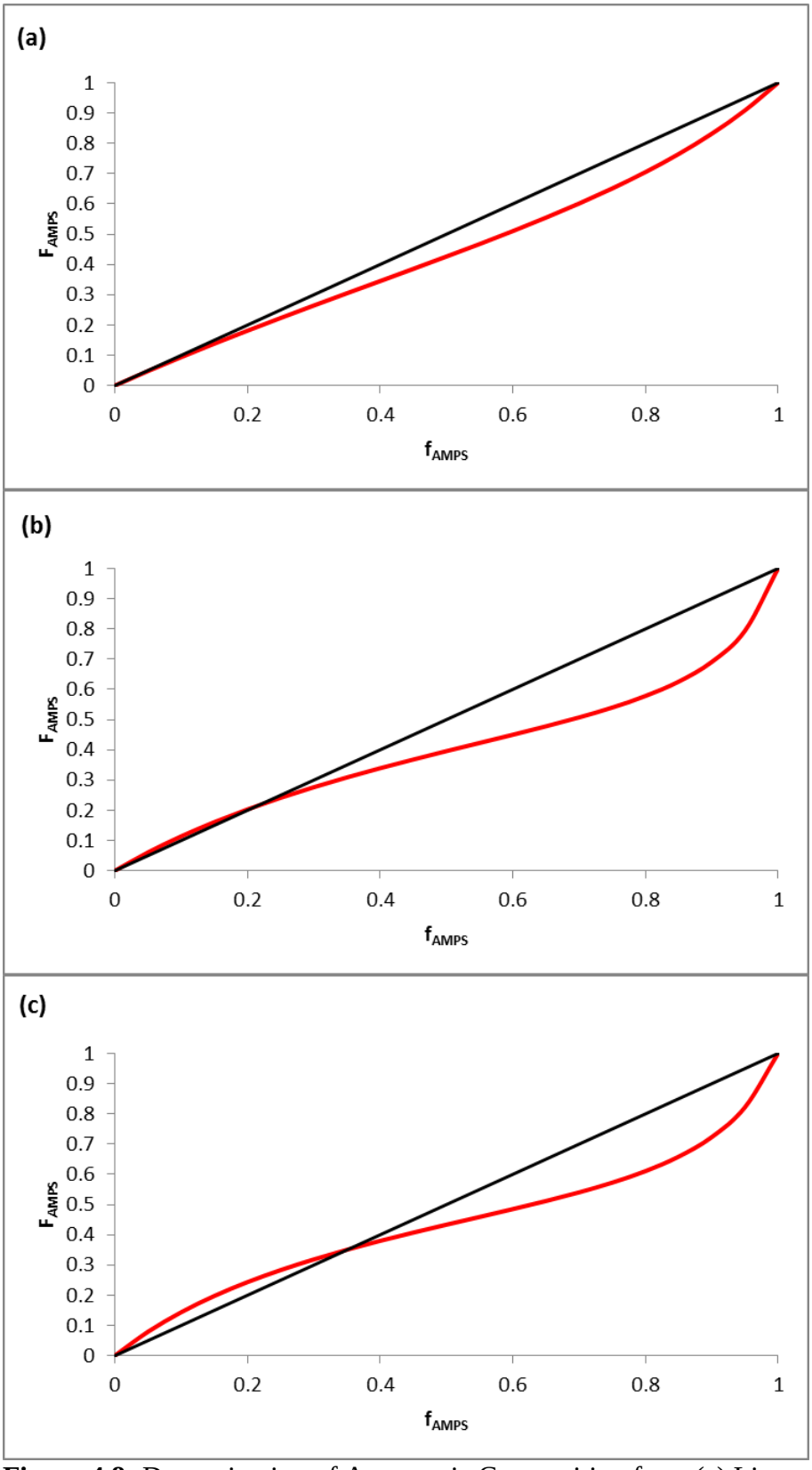

Figure 4.8: Determination of Azeotropic Composition from (a) Literature Data [47], (b) T-M-Designed Data, (c) EVM-Designed Data

As expected, the curve does not pass through the 45° line in case (a). From a mathematical perspective, it is only feasible to observe a non-negative azeotropic point in the binary system when both reactivity ratios are less than or greater than unity; according to McCormick and Chen, $r_{AMPS} = 0.50$ and $r_{AAm} = 1.02$. Therefore, their reactivity ratio estimates suggest that an azeotrope does not occur in this system.

However, in cases (b) and (c), both reactivity ratios are less than unity. Therefore, we expect to observe an azeotrope in the model, and the plots confirm these expectations. Using the reactivity ratios found with T-M-designed data ($r_{AMPS} = 0.16$ and $r_{AAm} = 0.77$), the azeotrope occurs at $f_{AMPS} = F_{AMPS} = 0.22$. On the other hand, reactivity ratios from the EVM-designed data ($r_{AMPS} = 0.20$ and $r_{AAm} = 0.57$) predict an azeotrope at $f_{AMPS} = F_{AMPS} = 0.35$.

The azeotropic point for the AMPS/AAm copolymer is likely somewhere between these two compositions. In fact, the experimental results from $f_{AMPS,0} = 0.30$ had very consistent cumulative composition measurements that did not vary with conversion (within experimental error), and model predictions stayed approximately constant using all three pairs of reactivity ratio estimates (see again Figure 4.5). Therefore, it seems that the azeotropic composition for the system is approximately $f_{AMPS} = F_{AMPS} = 0.30$.

4.4 Effect of Experimental Error

For the AMPS/AAm copolymer, the reactivity ratio estimates and associated JCR were most dissimilar for the EVM-designed estimates, compared to the preliminary and T-M-designed

estimates. Even though the general trends remained consistent, and the JCR was very small, further investigation of the EVM results is necessary. Therefore, a brief case study analyzing the effect of perturbations on experimental data from the EVM design will be discussed in what follows. For reference, the original data was presented in Table 4.4.

This troubleshooting case study will be completed in two stages. The first stage (Section 4.4.1) will examine the existing data in light of the cumulative composition analysis of Section 4.3.1 and remove any obvious outlying data points for subsequent analyses. The second stage (Section 4.4.2) will use previous (and incorrect) elemental analysis results to estimate the error associated with the composition measurements, and identify the effect of the data's variability on the resulting reactivity ratio estimates.

4.4.1 Troubleshooting with Outliers

The experimental data of Table 4.4 were plotted against a series of cumulative copolymer composition models in Figure 4.6, and several outlying data points were detected. In order to identify the effects of these outliers on the reactivity ratio estimates, they were removed from the data set sequentially. For clarification, all of the modified data sets are presented in Appendix D (Section D.4). First, two low conversion data points for $f_{AMPS,0} = 0.84$ were removed from the data set and the reactivity ratio estimates were recalculated. The results are shown in Figure 4.9.

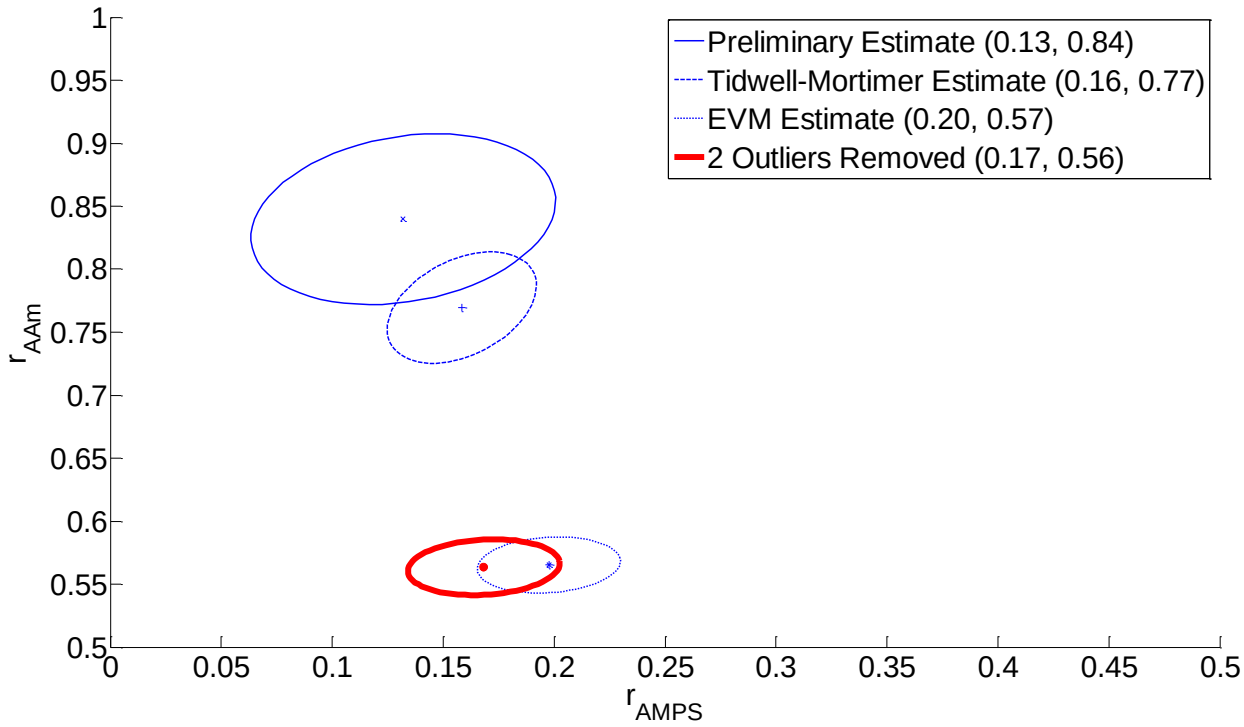

Figure 4.9: EVM-Designed Reactivity Ratio Estimates for AMPS/AAm; Low-Conversion Outliers ($f_{AMPS,0}$ = 0.84) Removed

By removing the two low conversion values for $f_{AMPS,0}$ = 0.84, the estimate for r_{AMPS} is shifted from 0.20 to 0.17. While this change confirms the influence of these two data points, the shift is fairly minor; the new point estimate is within the original JCR, and r_{AAm} is unaffected.

The next step in the sequential troubleshooting analysis was to reinstate the two low conversion data points for $f_{AMPS,0}$ = 0.84 but to remove three data points between 20% and 25% conversion from the $f_{AMPS,0}$ = 0.10. These outliers were initially identified in Figure 4.6, and the effect of these data points on the reactivity ratio estimates is shown in Figure 4.10.

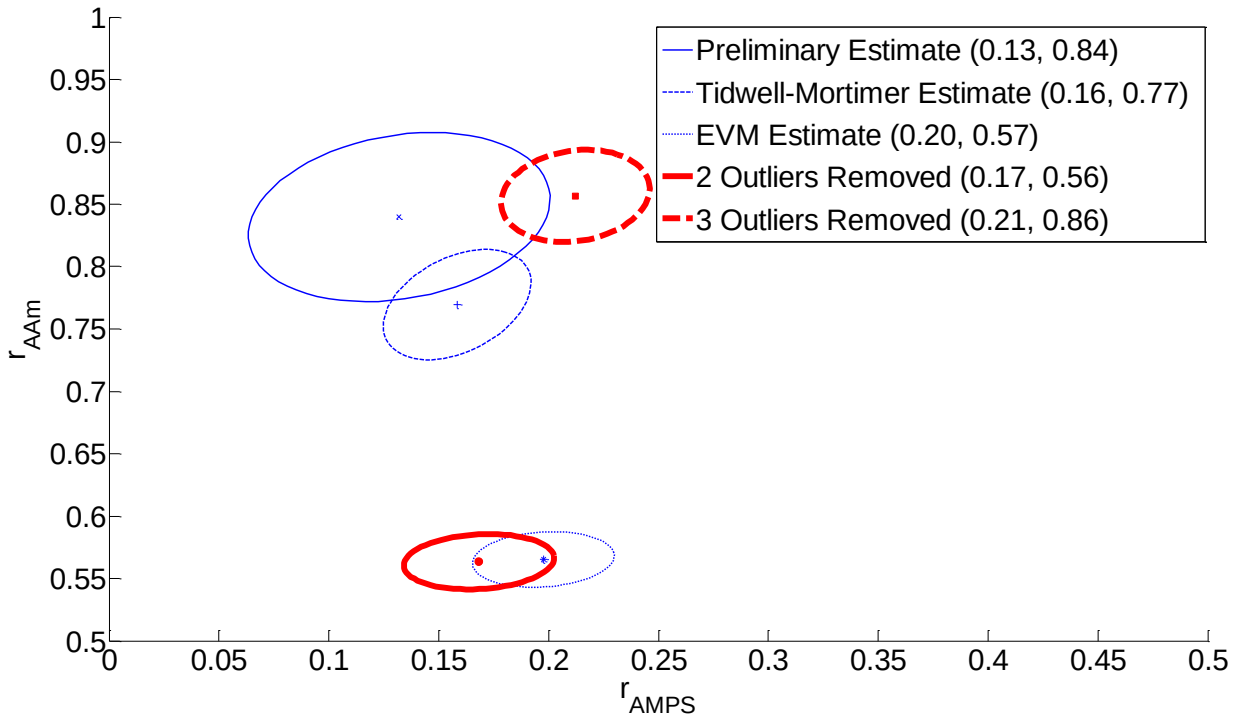

Figure 4.10: EVM-Designed Reactivity Ratio Estimates for AMPS/AAm; Mid-Conversion Outliers ($f_{AMPS,0}$ = 0.10) Removed

Here, we see a drastic shift in the value of r_{AAm}, whereas r_{AMPS} remains approximately constant. It is interesting to note that the new JCR (with 3 outliers removed) is much closer to the preliminary and Tidwell-Mortimer-designed JCRs. These results seem more reasonable, as all three analyses are describing the same copolymer system. One disadvantage with the new data set is the increased area of the JCR. However, since fewer data points are being used in the analysis, a slight increase in variability is to be expected.

As a final step, all 5 outliers described previously (2 at low conversion for $f_{AMPS,0}$ = 0.84 and 3 at mid-conversion for $f_{AMPS,0}$ = 0.10) were removed from the data set. The results, presented in Figure 4.11, are as expected given previous observations.

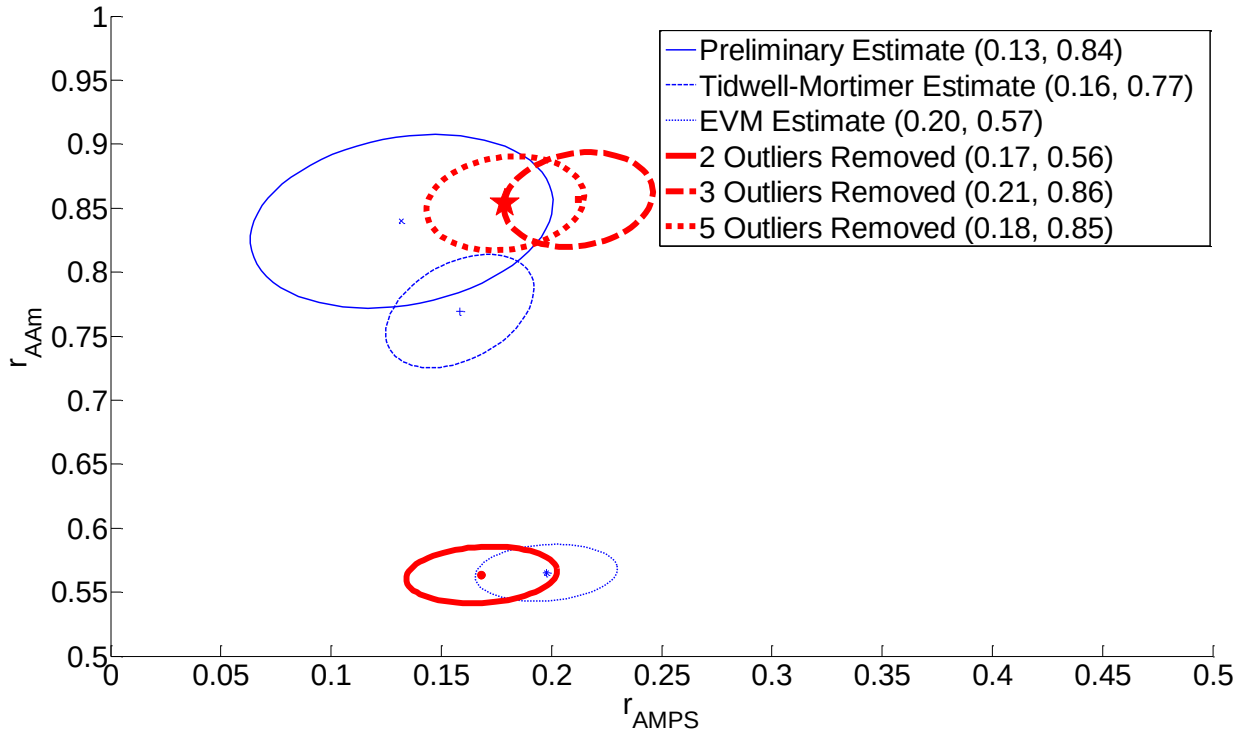

Figure 4.11: EVM-Designed Reactivity Ratio Estimates for AMPS/AAm; All Outliers Removed

When all five outlying data points are removed, both r_{AMPS} and r_{AAm} shift toward the preliminary point estimate. Now, good agreement between all three experimental designs is evident. While the new JCR (with 5 outliers removed) is larger than the initial EVM estimate from Section 4.2.3, it is still smaller than the Tidwell-Mortimer-designed estimate. This is impressive, considering fewer data points are being used in the analysis.

From this analysis, we have learned that a few select cumulative composition measurements can have a significant effect on reactivity ratio estimates. Therefore, identification and removal of outliers is a crucial part of the reactivity ratio estimation process. Given this modified data set, we can be confident in the new reactivity ratio estimates for this copolymer system: $r_{AMPS} = 0.18$ and $r_{AAm} = 0.85$. There is no doubt that both reactivity ratios are less than 1.0, so the analysis has already improved the previously accepted values from the literature. In addition, the justification

for removing the five outlying composition points is based on the fact that the elemental analysis equipment (for composition measurements) was very unreliable; this is discussed in detail in Section 4.4.2 that follows.

4.4.2 Effect of Additional Variability

Elemental analysis (EA) measurements for the determination of cumulative composition (as described in Section 3.4) were independently replicated. The replicates, both within a single (24 hour) run and over a period of 6 months, revealed that the instrument drifted and measurements were largely unrepeatable. During some early EA runs, the equipment was poorly calibrated and the resulting composition measurements were clearly unreliable and incorrect. Therefore, the instrument was recalibrated and all samples were analyzed a second (and sometimes a third) time, which made the analysis unnecessarily tedious and costly.

While this setback was unexpected and somewhat inconvenient, it did provide an estimate of the error associated with the elemental analysis equipment when it was not properly maintained. Therefore, the initial (incorrect) composition estimates and the more accurate data were combined to calculate the pooled variance for both feed compositions associated with the EVM-designed analysis ($f_{AMPS,0}$ = 0.10 and $f_{AMPS,0}$ = 0.84). For $f_{AMPS,0}$ = 0.10, s_p^2 = 0.0053 and for $f_{AMPS,0}$ = 0.84, s_p^2 = 0.0105; full calculations are presented in Appendix D (Section D.4).

To fully understand how the variability in composition measurements can affect the final reactivity ratio estimates, we can modify the data set by introducing the pooled variance to the composition values. The data set was modified in four different ways:

1. The pooled standard deviation was added to each cumulative composition value (+0.0728 for $f_{AMPS,0}$ = 0.10 and +0.1024 for $f_{AMPS,0}$ = 0.84) to demonstrate the effect of over-estimated composition measurements on reactivity ratio estimates.
2. The pooled standard deviation was subtracted from each cumulative composition value to demonstrate the effect of under-estimated composition measurements on reactivity ratio estimates.
3. An alternating pattern of adding and subtracting the pooled standard deviation from the cumulative composition measurements was employed to determine the effect of a wide spread of error on the reactivity ratio estimates.
4. The data set was doubled; first, the pooled standard deviation was added to each composition value. Then, the pooled standard deviation was subtracted from each composition value. It is anticipated that the increased size of the data set will result in a smaller JCR, in spite of the increased spread of the data.

The results of all four modifications are shown in Figure 4.12, and the original EVM estimate is included for comparison. It is also important to note that all experimental data were used in this analysis, and the outlying data discussed in Section 4.4.1 were not removed.

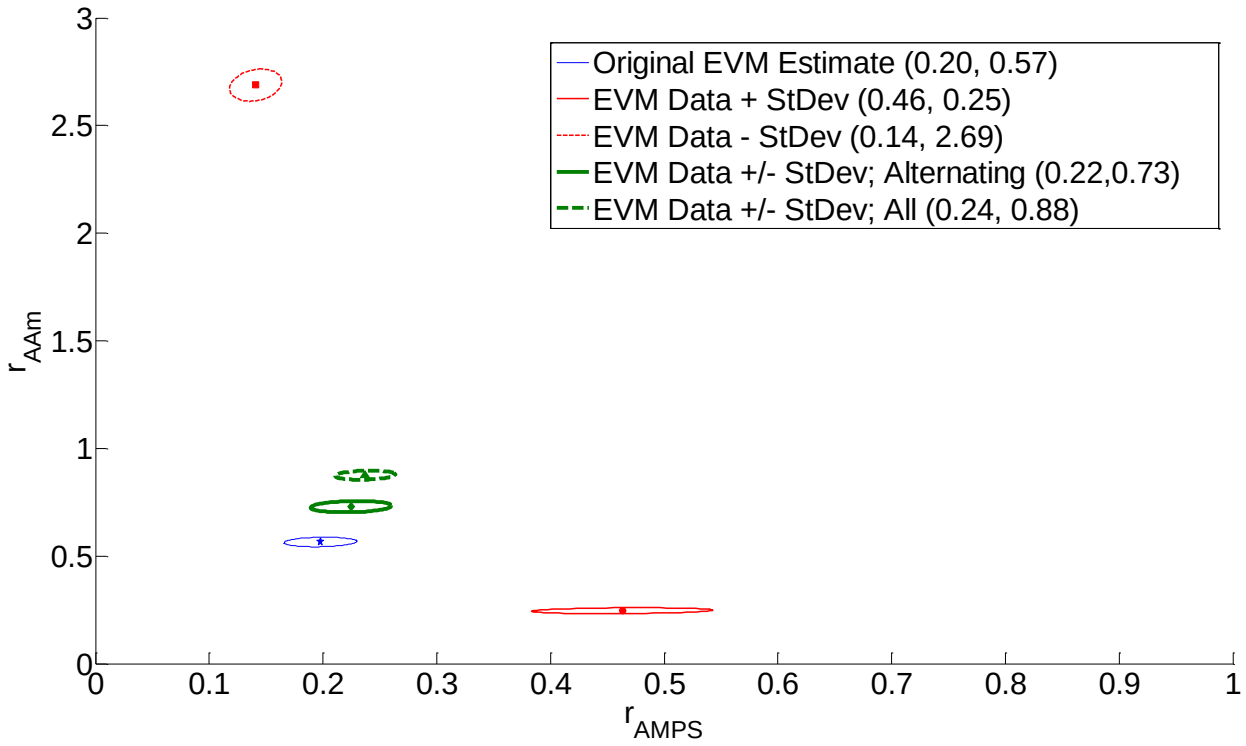

Figure 4.12: Controlled Sensitivity Analysis for Reactivity Ratio Estimates of AMPS/AAm

As expected, adding or subtracting the standard deviation to all data points results in drastic shifts in the point estimates (as well as the JCRs). In Case 1, when the pooled standard deviation is added to the composition data, $\overline{F}_{AMPS}$ increases and $\overline{F}_{AAm}$ decreases. Given this information, it makes sense that r_{AMPS} will increase and r_{AAm} will decrease with this adjustment to the data. Similarly, in Case 2, $\overline{F}_{AMPS}$ decreases and $\overline{F}_{AAm}$ increases; as a result, we see that r_{AMPS} is lowered slightly and r_{AAm} is increased significantly. By adding more variability to the data sets, an increase in the JCR area is also observed. This decreased confidence in the reactivity ratio estimates is to be expected, given the circumstances.

Conversely, combining addition and subtraction of the standard deviation (Cases 3 and 4) resulted in reactivity ratio estimates that were fairly close to the unperturbed data. Doubling the size of the data set (by both adding and subtracting the standard deviation) decreased the error

associated with the estimate, but not to any significant extent. Ultimately, the conclusion that can be reached from this exercise is that some random error in the data is reasonable, but a positive or negative bias in the cumulative composition data could have a significant impact on the reactivity ratio estimates.

Next, the data were modified by adding random error to the original data set. As before, s_p values specific to $f_{AMPS,0}$ = 0.10 and $f_{AMPS,0}$ = 0.84 were used, but the decision to add or subtract the standard deviation was made with a random coin toss. The data set was modified three times using this technique, and the resulting reactivity ratio estimates and JCRs are presented in Figure 4.13.

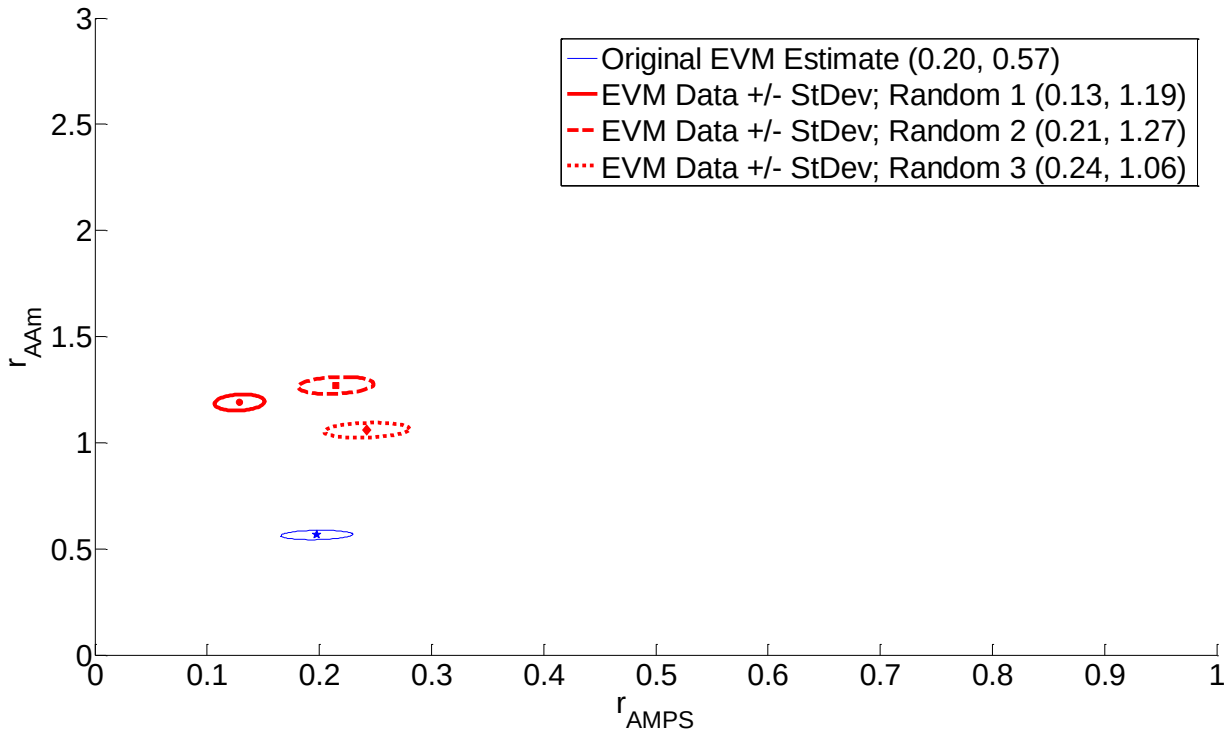

Figure 4.13: Randomized Sensitivity Analysis for Reactivity Ratio Estimates of AMPS/AAm

When random error is added to the data set, r_{AAm} seems much more susceptible to change. This confirms the reliability of the r_{AMPS} estimate compared to the r_{AAm} estimate, which was also observed previously (see, for example, Figure 4.4 and Figure 4.11). From this, we can conclude that obtaining accurate cumulative composition data is extremely important, and the need for a more reliable analytical method (with independent replicates) becomes increasingly obvious.

Despite the drastic change in reactivity ratio estimates that is observed when random error is added to the data set, we can be confident in our results. All experimental work required for the AMPS/AAm copolymerization was fully replicated (in terms of both synthesis and characterization), and all three designs agree when outliers are removed (see again Figure 4.11).

CHAPTER 5. AMPS/AAc COPOLYMER

5.1 Preliminary Experiments

5.1.1 Selection of Preliminary Feed Compositions

As for the AMPS/AAm system, the preliminary design for the AMPS and acrylic acid (AAc) copolymer was based on both background literature [49] and process understanding. Ultimately, the same initial feed compositions were chosen for both the AMPS/AAc and the AMPS/AAm systems. Details regarding the preliminary design for AMPS/AAc are presented in Table 5.1.

Table 5.1: Preliminary Design for AMPS/AAc

Reactivity Ratios	r_1 (r_{AMPS})	r_2 (r_{AAc})
From Literature [49]	0.27	0.95
Feed Composition	$f_{11,0}$	$f_{12,0}$
Tidwell-Mortimer (T-M)	0.32	0.88
EVM	0.10	0.81
Conditions chosen for preliminary experiments	0.15	0.80

5.1.2 Preliminary Reactivity Ratio Estimation

Again, preliminary experiments for the AMPS/AAc were independently replicated at least once at each feed composition. Figure 5.1 shows that the preliminary experiments were not very repeatable, and were subject to significant error, again for the same reasons as discussed in Section 4.1. As before, the full data set is available in Appendix C (Table C.2).

Both feed compositions presented unique concerns. At the lower AMPS feed composition ($f_{AMPS,0}$ = 0.15), we found that the polymerization was extremely slow and that minimal precipitate formed during the product isolation stage of the experiment. Acetic acid was added to the non-solvent mixture (50/50 acetone/methanol, as described in Section 3.3) to lower the solution pH. It was thought that this may stabilize the solution, therefore allowing the copolymer to precipitate properly. However, this attempt to improve the quality of the precipitate was unsuccessful; the product was still very sticky and low conversion was observed.

The high AMPS run ($f_{AMPS,0}$ = 0.80) was better in terms of conversion and copolymer precipitation, but presented other difficulties. As shown in Figure 5.1, the reaction took place very quickly, which increased variability in the system. The conversion data were not very repeatable, but trends were consistent. This is, to some extent, characteristic of preliminary experiments. It will be shown in Section 5.2 that the error observed in the replicates decreased substantially for the optimally designed experiments.

Again, preliminary reactivity ratio estimates (both r_{AMPS} and r_{AAc}) were calculated by applying the cumulative composition model and direct numerical integration to the data using the error-in-variables-model. As mentioned in Table 5.1, the initial point estimate in this case (r_{AMPS} = 0.27, r_{AAc} = 0.95) was taken from Abdel-Azim et al. [49].

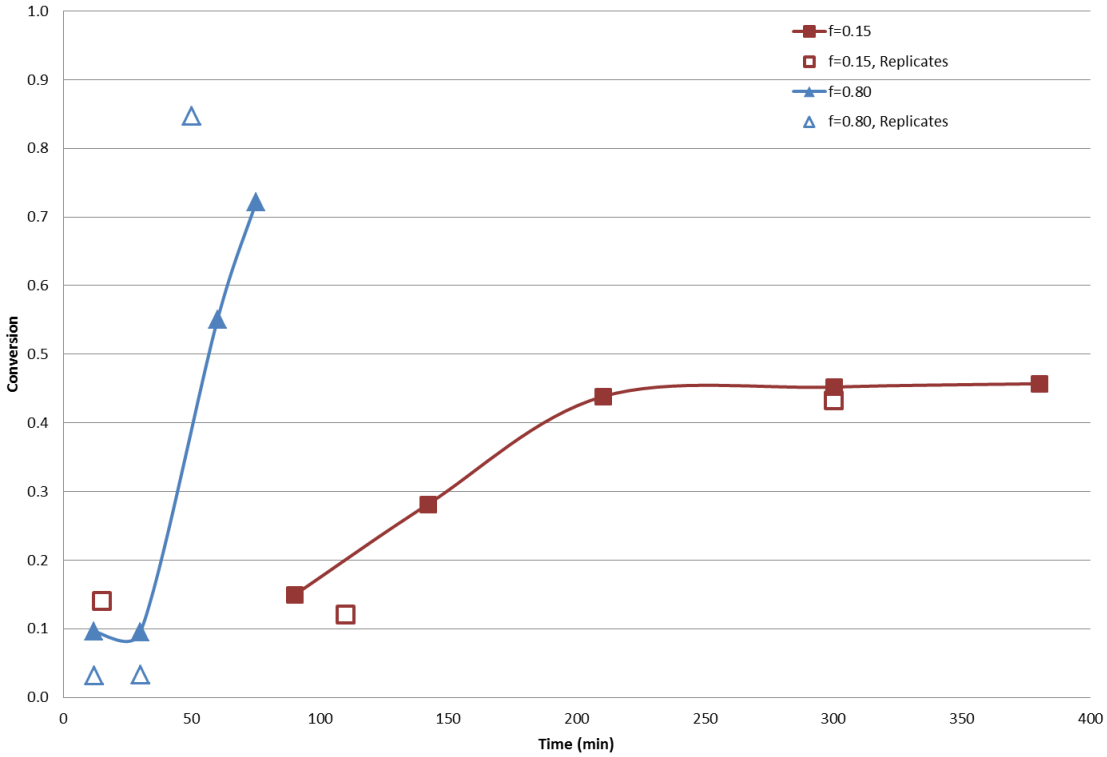

Figure 5.1: Conversion vs. Time Plot for Preliminary AMPS/AAc Copolymerization Experiments

The preliminary JCR for the AMPS/AAc system is shown in Figure 5.2. The point estimate from literature is included in the figure for reference, and the current reactivity ratio estimates are $r_{AMPS} = 0.48$ and $r_{AAc} = 0.95$.

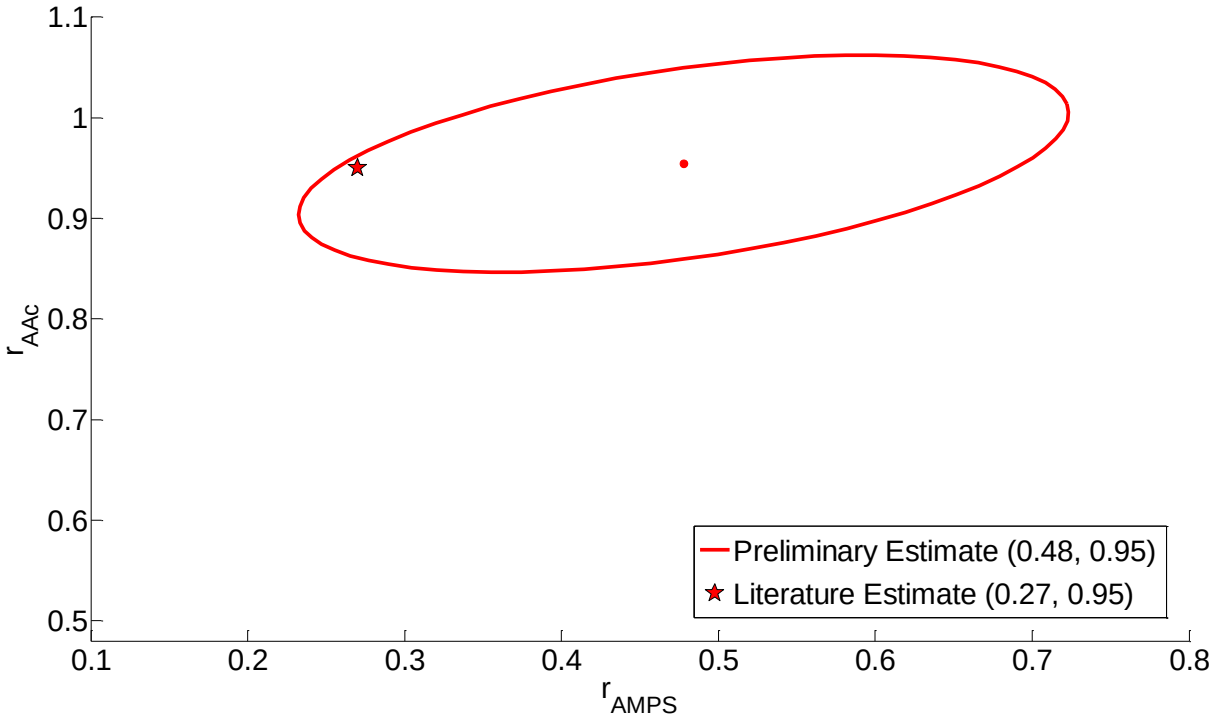

Figure 5.2: Preliminary Reactivity Ratio Estimates for AMPS/AAc

The point estimate from Abdel-Azim et al. [49] is very close to the edge of the preliminary JCR. While it is reassuring to see that the literature data are contained within the JCR for the current study, the preliminary JCR is quite large (as expected for preliminary experimental work). As mentioned in Section 2.3.2, the study by Abdel-Azim et al. [49] provided limited insight as to the polymerization conditions for the synthesis of the AMPS/AAc copolymer. However, it is clear that the initiator (benzoyl peroxide), reaction temperature (55°C) and precipitant selection (methyl ethyl ketone) differed from the currently used conditions. Arguably one of the most important reaction conditions, pH, is not mentioned at all in the work by Abdel-Azim et al. [49], so a direct comparison is difficult. However, in general, the estimates made in the previous literature study seem to agree with our newly determined reactivity ratios.

5.2 Optimal Experiments

5.2.1 Selection of Optimal Feed Compositions

Optimal experiments for reactivity ratio determination are designed according to both Tidwell-Mortimer and EVM techniques, and are shown in Table 5.2. As before, updated reactivity ratio estimates (based on preliminary experiments of Section 5.1) are used in finding optimal feed conditions for the AMPS/AAc copolymerization. To avoid the low conversion and poor precipitation that was observed for $f_{AMPS,0} = 0.15$, a constraint ($0.2 < f_{AMPS,0} < 1.0$) was included when designing optimal experiments through EVM. The ability to introduce limits on feed compositions is yet another advantage of EVM for optimal design of experiments.

Table 5.2: Optimal Design for AMPS/AAc

Reactivity Ratios:	r_1 (r_{AMPS})	r_2 (r_{AAc})
Experimentally Determined (based on the preliminary experiments of Table 5.1)	0.48	0.95
Feed Composition:	$f_{11,0}$	$f_{12,0}$
Tidwell-Mortimer	0.32	0.81
Error-in-Variables-Model (constraint: $0.2 < f_{AMPS,0} < 1.0$)	0.20	0.73

5.2.2 Tidwell-Mortimer Design

Both runs designed using the Tidwell-Mortimer technique were independently replicated. The experimental data for all four runs (two feed compositions and two replicates) are presented in Table 5.3.

Table 5.3: Experimental Data for AMPS/AAc Copolymerization; Tidwell-Mortimer Design

Run #	X	$f_{AMPS,0}$	$f_{AAc,0}$	$\overline{F}_{AMPS}$	$\overline{F}_{AAc}$
1	0.0617	0.32	0.68	0.2259	0.7741
	0.1461	0.32	0.68	0.2397	0.7603
	0.2613	0.32	0.68	0.2333	0.7667
	0.4426	0.32	0.68	0.2386	0.7614
	0.4426	0.32	0.68	0.3182	0.6818
2	0.0462	0.81	0.19	0.6014	0.3986
	0.0462	0.81	0.19	0.5642	0.4358
	0.0874	0.81	0.19	0.6032	0.3968
	0.1574	0.81	0.19	0.5378	0.4623
3	0.0528	0.32	0.68	0.3701	0.6299
	0.0804	0.32	0.68	0.3298	0.6702
	0.1177	0.32	0.68	0.3253	0.6747
	0.2395	0.32	0.68	0.3120	0.6880
4	0.0223	0.81	0.19	0.8097	0.1903
	0.0524	0.81	0.19	0.6802	0.3198
	0.1038	0.81	0.19	0.6849	0.3151
	0.2576	0.81	0.19	0.6182	0.3818
	0.2576	0.81	0.19	0.5992	0.4008

As before, reactivity ratios were calculated using conversion and cumulative composition data. The resulting reactivity ratio estimates (r_{AMPS} = 0.22 and r_{AAc} = 0.85) and corresponding JCR are shown in Figure 5.3.

As expected, using experiments that were optimally designed using the Tidwell-Mortimer technique has significantly decreased the error associated with the reactivity ratio estimates. The new estimates are in relatively good agreement with both the preliminary estimates and the literature values, which allows for a high degree of confidence in the results.

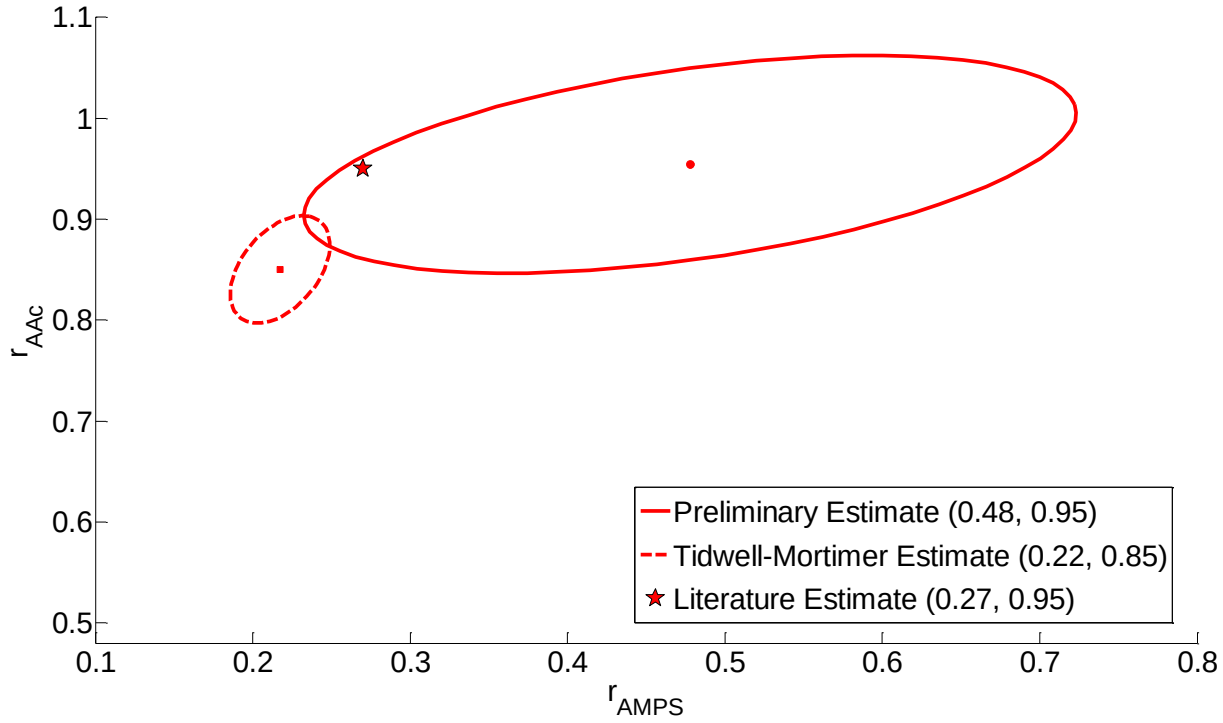

Figure 5.3: Tidwell-Mortimer-Designed Reactivity Ratio Estimates for AMPS/AAc

5.2.3 Error-in-Variables-Model Design

Similarly, the runs designed using EVM (at two feed compositions with two independently replicated runs) are presented in Table 5.4.

As shown in Figure 5.4, the reactivity ratio estimates obtained from the EVM-designed data are $r_{AMPS} = 0.24$ and $r_{AAm} = 0.87$. The JCR associated with this data set is small (as it was for the T-M-designed estimates), which is indicative of a well-designed experiment and accurate estimates. The overlap between JCRs from the preliminary, T-M-designed and EVM-designed experiments is also a very good sign, and provides additional confidence in these results.

Table 5.4: Experimental Data for AMPS/AAc Copolymerization; EVM Design

Run #	X	$f_{AMPS,0}$	$f_{AAc,0}$	$\overline{F}_{AMPS}$	$\overline{F}_{AAc}$
1	0.0269	0.20	0.80	0.2652	0.7348
	0.1369	0.20	0.80	0.2119	0.7881
	0.4156	0.20	0.80	0.2075	0.7925
	0.4950	0.20	0.80	0.1860	0.8140
	0.4950	0.20	0.80	0.1723	0.8277
	0.5813	0.20	0.80	0.1649	0.8351
2	0.0127	0.73	0.27	0.7942	0.2058
	0.0895	0.73	0.27	0.5939	0.4061
	0.0895	0.73	0.27	0.4449	0.5551
	0.1250	0.73	0.27	0.5115	0.4885
	0.1642	0.73	0.27	0.5131	0.4869
	0.5256	0.73	0.27	0.4303	0.5697
3	0.1458	0.20	0.80	0.2474	0.7526
	0.1458	0.20	0.80	0.1418	0.8582
	0.2951	0.20	0.80	0.1439	0.8561
4	0.0162	0.73	0.27	0.6919	0.3081
	0.0798	0.73	0.27	0.6063	0.3937
	0.4756	0.73	0.27	0.5455	0.4545
	0.5664	0.73	0.27	0.6069	0.3931

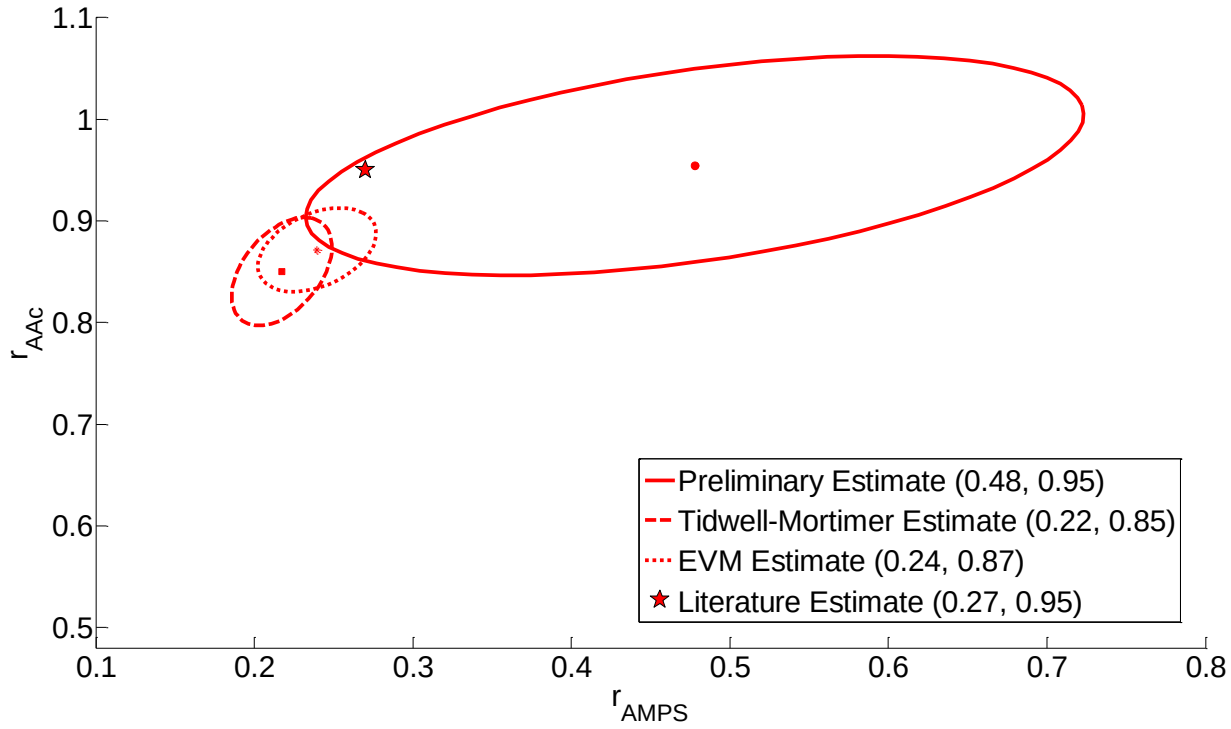

Figure 5.4: EVM-Designed Reactivity Ratio Estimates for AMPS/AAc

5.3 Discussion of Results for AMPS/AAc

In the AMPS/AAc case, the reactivity ratios are much closer together, and do not seem to vary with different designs. For a quick visual comparison, the results are summarized in Table 5.5.

Table 5.5: Summary of Reactivity Ratio Estimates for AMPS/AAc

Step 1: Preliminary Design	r_{AMPS}	r_{AAc}
Literature Values [49]	0.27	0.95
Preliminary Estimates	0.48	0.95
Step 2: Optimal Designs		
Tidwell-Mortimer Estimates	0.22	0.85
Error-in-Variables-Model Estimates	0.24	0.87

Because the reactivity ratio estimates from literature, T-M design and EVM design are all similar, it is unlikely that the differences in values will affect composition predictions or other calculations related to the copolymer microstructure. Therefore, an in-depth comparison of results (as was completed in Section 4.3 for the AMPS/AAm copolymer system) is unnecessary for the AMPS/AAc copolymer.

5.3.1 Cumulative Composition Analysis

It is still useful to compare model predictions to experimental results. Therefore, assuming the EVM-designed results are the most accurate (as they produce the smallest JCR), the reactivity ratios $r_{AMPS} = 0.24$ and $r_{AAm} = 0.87$ can be used to calculate cumulative copolymer composition profiles. Results are shown in Figure 5.5.

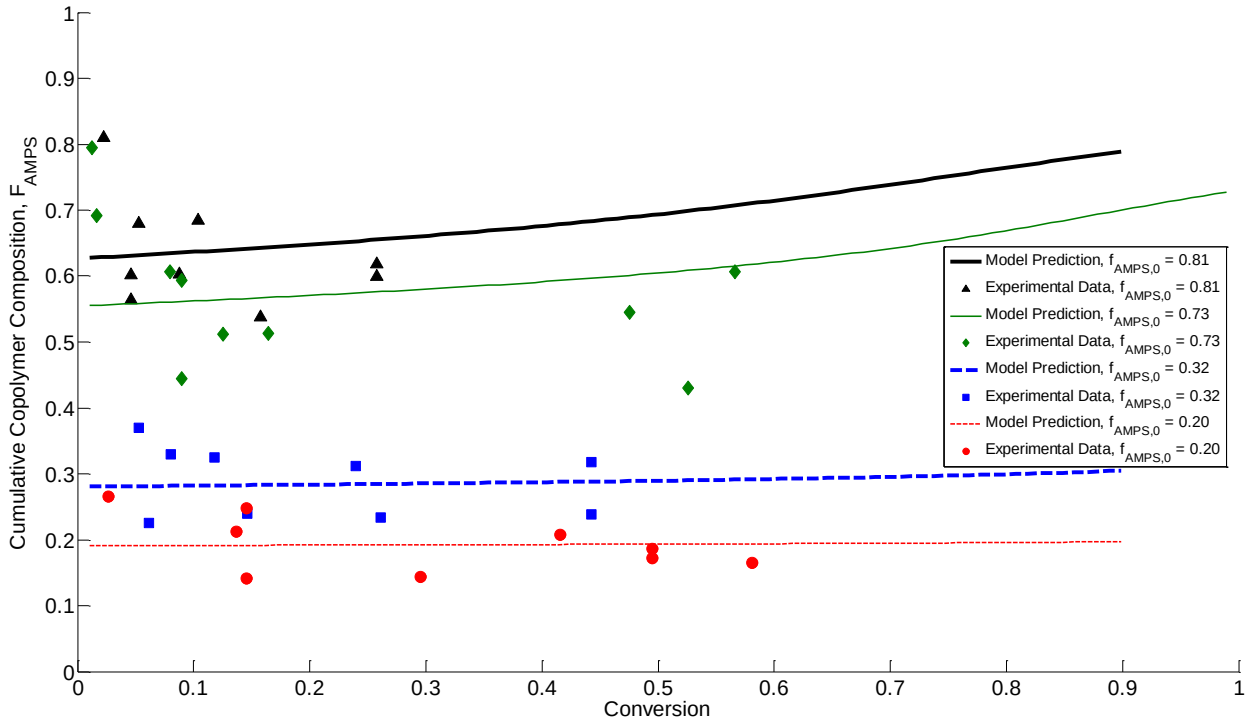

Figure 5.5: Cumulative Copolymer Composition for AMPS/AAc

Here, we see good agreement between the model predictions and the experimental results at low feed compositions ($f_{AMPS,0}$ = 0.20 and $f_{AMPS,0}$ = 0.32). On the other hand, at higher levels of AMPS in the feed, there are substantial discrepancies visible. There is significantly more variability in the experimental data, and the model seems especially inadequate at very low conversion (< 5%). This is largely due to the nature of the system being studied, as there is typically more variability at low conversions. However, due to the high confidence in reactivity ratio estimates (based on the size of the JCRs) and the good agreement at low feed compositions, the discrepancies are (again) more likely due to inaccurate experimental measurements from elemental analysis.

CHAPTER 6. AMPS/AAm/AAc TERPOLYMER

The AMPS/AAm/AAc terpolymer was studied in collaboration with PhD student Niousha Kazemi (January – June 2014), and some of these results have already been presented in the PhD thesis [32]. However, they are an important aspect of the current study, and hence only the key results from the optimally designed experiments will be presented herein.

6.1 Preliminary and Optimal Experiments

6.1.1 Selection of Feed Compositions

For the AMPS/AAm/AAc terpolymer, six different feed compositions were selected as part of the preliminary experimentation. These feed compositions were selected in such a way that three runs represent extreme ranges (that is, each is rich in one of the three comonomers), whereas the other three runs represent mid-range mole fractions (where the feed composition is well distributed among the three comonomers). Observations from existing literature and knowledge of the process (such as feed composition constraints discovered in the binary systems) were taken into account when choosing the feed compositions. A graphical representation of the preliminary feed compositions is shown in Figure 6.1 and the associated values are presented in Table 6.1.

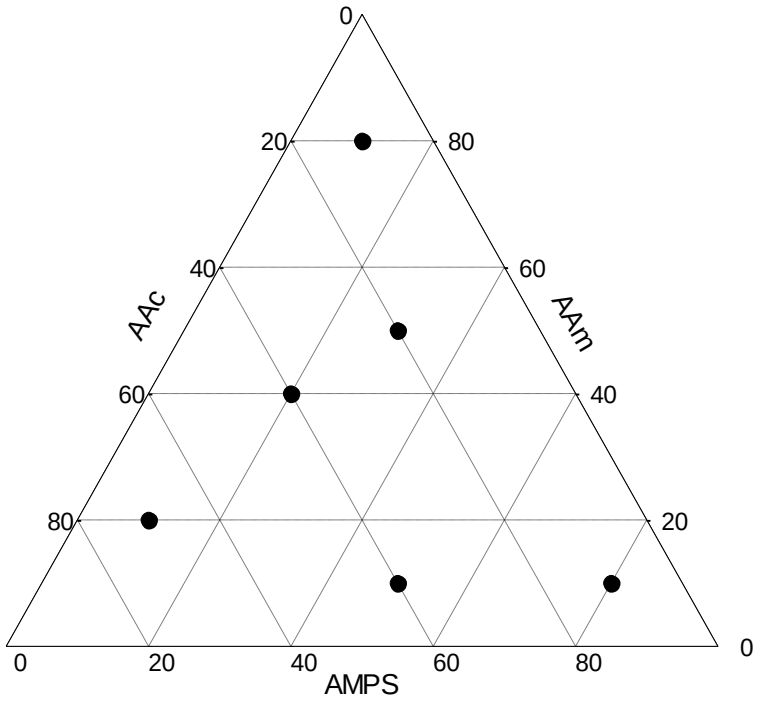

Figure 6.1: Selection of Feed Compositions for AMPS/AAm/AAc Terpolymerization [32]

Table 6.1: Design of Experiments for AMPS[1]/AAm[2]/AAc[3] Terpolymerization [32]

Feed Composition: **Run # (i):**	f_{1i} (AMPS)	f_{2i} (AAm)	f_{3i} (AAc)
1	0.800	0.100	0.100
2	0.100	0.800	0.100
3	0.100	0.200	0.700
4	0.200	0.400	0.400
5	0.300	0.500	0.200
6	0.500	0.100	0.400

It is interesting to note here that while these were initially classified as preliminary experiments, three of the compositions being considered are actually optimal points. According to the EVM design criterion [63], optimal feed compositions for this terpolymer system require 80% of one comonomer and 10% each of the other two comonomers. Runs 1 and 2 in Table 6.1 meet this criterion, and Run 3 is as close as possible given composition constraints described by Ryles and Neff [56].

6.1.2 Terpolymerization Results

The experimental procedure described in Chapter 3 was again used for the terpolymer system, and results from the optimally designed experiments are shown in Table 6.2. As before, the experiments were fully replicated, and the polymerization was not limited to low conversion data.

The experimental data of Table 6.2 were then used to estimate reactivity ratio values for the AMPS/AAm/AAc terpolymer, using the technique described by Kazemi et al. [12]. Because there are now three components being considered, there are additional combinations of reactivity ratios: $r_{AMPS/AAm}$, $r_{AAm/AMPS}$, $r_{AMPS/AAc}$, $r_{AAc/AMPS}$, $r_{AAm/AAc}$ and $r_{AAc/AAm}$. As for the binary systems, each reactivity ratio $r_{i/j}$ represents the ratio of homopropagation ($k_{p,ii}$) to cross-propagation for a particular comonomoner ($k_{p,ij}$); see Sections 2.1.2 and 2.1.3 for additional clarification. The estimation results, along with the corresponding JCRs, are presented in Figure 6.2. Binary estimates, both from literature [10, 47, 49] and from the current work, are also included for comparison purposes. The similarities and differences between the binary and ternary systems will be discussed in more detail in Section 6.2.

Table 6.2: Experimental Data for AMPS/AAm/AAc Terpolymerization [32]

Run #	X	$f_{AMPS,0}$	$f_{AAm,0}$	$f_{AAc,0}$	$\overline{F}_{AMPS}$	$\overline{F}_{AAm}$	$\overline{F}_{AAc}$
1	0.047	0.800	0.100	0.100	0.664	0.161	0.175
	0.057	0.800	0.100	0.100	0.693	0.187	0.120
	0.085	0.800	0.100	0.100	0.775	0.152	0.073
	0.101	0.800	0.100	0.100	0.620	0.205	0.175
	0.232	0.800	0.100	0.100	0.623	0.192	0.185
	0.254	0.800	0.100	0.100	0.667	0.227	0.106
	0.576	0.800	0.100	0.100	0.782	0.079	0.139
	0.628	0.800	0.100	0.100	0.772	0.107	0.121
2	0.025	0.100	0.800	0.100	0.101	0.826	0.073
	0.046	0.100	0.800	0.100	0.099	0.824	0.077
	0.078	0.100	0.800	0.100	0.103	0.827	0.070
	0.085	0.100	0.800	0.100	0.106	0.813	0.081
	0.098	0.100	0.800	0.100	0.081	0.754	0.165
	0.124	0.100	0.800	0.100	0.104	0.839	0.057
	0.151	0.100	0.800	0.100	0.102	0.836	0.062
	0.201	0.100	0.800	0.100	0.081	0.781	0.138
	0.206	0.100	0.800	0.100	0.080	0.779	0.141
	0.247	0.100	0.800	0.100	0.096	0.832	0.072
	0.392	0.100	0.800	0.100	0.104	0.817	0.079
	0.411	0.100	0.800	0.100	0.087	0.782	0.131
	0.542	0.100	0.800	0.100	0.112	0.801	0.087
	0.574	0.100	0.800	0.100	0.097	0.824	0.077
	0.594	0.100	0.800	0.100	0.106	0.809	0.085
3	0.029	0.100	0.200	0.700	0.052	0.400	0.548
	0.035	0.100	0.200	0.700	0.037	0.402	0.561
	0.042	0.100	0.200	0.700	0.066	0.420	0.514
	0.048	0.100	0.200	0.700	0.079	0.363	0.558
	0.055	0.100	0.200	0.700	0.084	0.364	0.552
	0.077	0.100	0.200	0.700	0.180	0.342	0.478
	0.081	0.100	0.200	0.700	0.119	0.380	0.501
	0.089	0.100	0.200	0.700	0.104	0.330	0.566
	0.122	0.100	0.200	0.700	0.060	0.270	0.670
	0.175	0.100	0.200	0.700	0.074	0.335	0.591
	0.194	0.100	0.200	0.700	0.079	0.382	0.539
	0.210	0.100	0.200	0.700	0.098	0.342	0.560
	0.268	0.100	0.200	0.700	0.117	0.334	0.553
	0.363	0.100	0.200	0.700	0.126	0.340	0.534

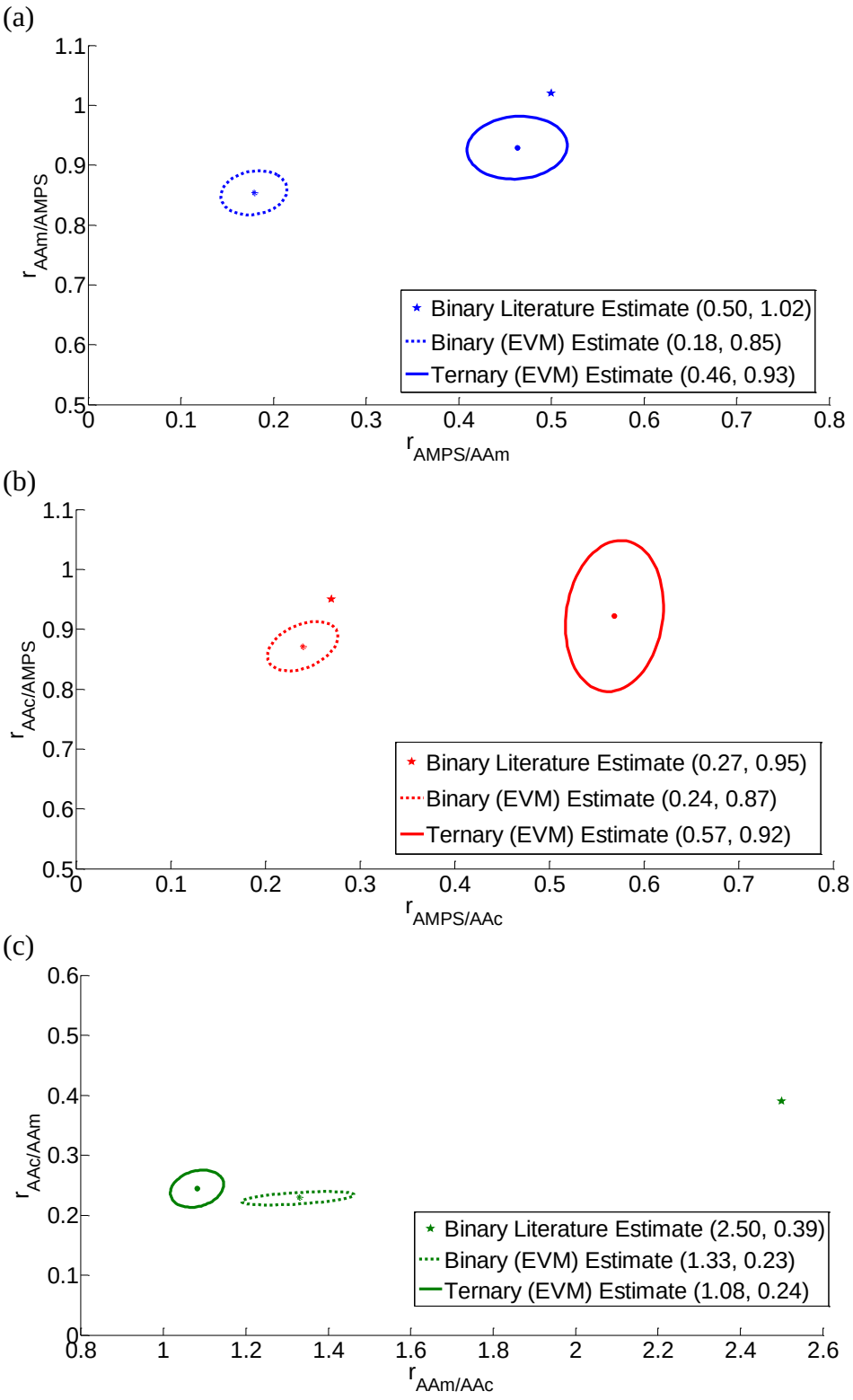

Figure 6.2: AMPS/AAm/AAc Terpolymerization Reactivity Ratio Estimates

6.2 Comparison of Binary and Ternary Reactivity Ratios

It has been suggested previously that binary reactivity ratios cannot be used to describe ternary systems and, at best, can be considered a gross approximation [12, 32]. Binary reactivity ratios are never determined using ternary experimental data, and differences in the system make it imprudent to use binary and ternary reactivity ratios interchangeably. Using inappropriate reactivity ratios may affect the model performance for predicting terpolymer composition (and sequence length characteristics, since these also depend on reactivity ratio values) and the determination of terpolymerization characteristics (such as the azeotropic point). Despite these risks, many studies performed previously employ binary reactivity ratios directly into terpolymer models.

To our knowledge, this is the first time that binary and ternary reactivity ratios have been compared directly, for the same system, with all other variables kept constant. In the current project, variables such as pH, ionic strength, monomer concentration, and other reaction conditions were kept constant; to the extent possible, only the number of comonomers (2 or 3) and the feed composition were varied. Therefore, a direct comparison of binary and ternary reactivity ratios is finally possible.

To simplify the evaluation of binary and ternary reactivity ratios, all of the estimates calculated thus far are summarized in Table 6.3. Since an in-depth analysis of the AAm/AAc copolymerization kinetics has been completed by Riahinezhad et al. [10], only the AMPS/AAm and AMPS/AAc copolymers were studied in more detail.

Table 6.3: Comparison of Reactivity Ratio Estimates for AMPS[1]/AAm[2]/AAc[3]

Experimental Data	Type	r_{12}	r_{21}	r_{13}	r_{31}	r_{23}	r_{32}
Literature Values	Binary	0.50	1.02	0.27	0.95	2.50	0.39
Preliminary	Binary	0.20	0.85	0.48	0.95	--	--
Optimal (T-M)	Binary	0.26	0.68	0.22	0.85	--	--
Optimal (EVM)	Binary	0.18	0.85	0.24	0.87	1.33	0.23
Optimal (EVM)	Ternary	0.46	0.93	0.57	0.92	1.08	0.24

The most useful comparison can be found in the last two rows of Table 6.3 (a graphical representation of these results was displayed previously in Figure 6.2). These last two rows show results from the optimally designed experiments [23], with reactivity ratio estimates calculated using direct numerical integration applied to cumulative composition data through the error-in-variables-model [32]. As mentioned previously, the non-linear estimation method establishes uncertainty using joint confidence regions (see Figure 6.2), which give more detail than typical individual error estimates based on 95% confidence.

For a quantitative comparison of the binary and ternary reactivity ratios, we can use a paired t-test to investigate whether the results are statistically similar (see calculations in Appendix D, Section D.5). Statistical analysis shows that we cannot reject the hypothesis $\mu_D = 0$; there is no significant difference between the binary and ternary arrays of reactivity ratios in this case.

However, the paired t-test only takes the point estimates into account as pure numbers. It is also important to consider how these differences in reactivity ratio estimates will affect model performance and terpolymerization characteristics (i.e., how these point estimates propagate via the related terpolymer model into the final response characteristics). The impact of using binary reactivity ratio estimates for ternary characterization will be discussed in what follows.

6.2.1 Cumulative Composition Analysis

Binary reactivity ratios are often used to predict terpolymer composition using the Alfrey-Goldfinger model [18]. However, for more accurate results, the recast Alfrey-Goldfinger model [12] described in Section 2.1.3 can be used in combination with recently determined reactivity ratios. In what follows, the recast Alfrey-Goldfinger model is used to predict terpolymer composition using both the binary and ternary reactivity ratio estimates of Table 6.3. Experimentally determined composition measurements are also included for evaluation of the model.

The first of three plots, Figure 6.3, exhibits results from the AMPS-rich terpolymer recipe. All three compositions (AMPS, AAm and AAc) are included, and the stark contrast between binary and ternary predictions is clearly visible. In general, the experimental data are in better agreement with the ternary-based model. This is to be expected, and confirms the importance of using ternary reactivity ratios to describe/model terpolymer systems.

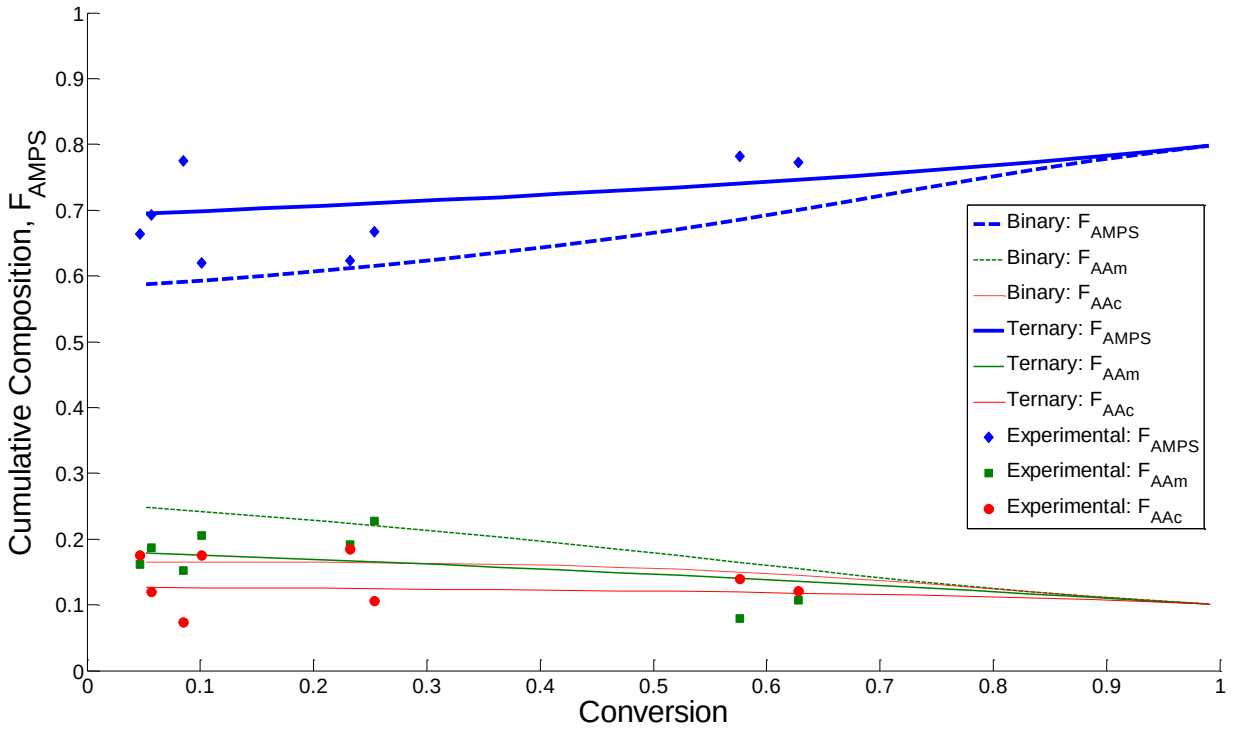

Figure 6.3: Cumulative Terpolymer Composition for AMPS/AAm/AAc ($f_{AMPS,0}/f_{AAm,0}/f_{AAc,0}$ = 0.8/0.1/0.1)

The AAm-rich terpolymer is shown in the second plot of the series, Figure 6.4. Here, we see very little difference between binary and ternary reactivity ratios applied to the recast Alfrey-Goldfinger (A-G) model. In fact, the composition for each of the three components is so consistent throughout conversion that the system may be exhibiting azeotropic behavior. According to the A-G model, for $f_{AMPS,0}/f_{AAm,0}/f_{AAc,0}$ = 0.1/0.8/0.1, $F_{AMPS}/F_{AAm}/F_{AAc}$ = 0.09/0.82/0.09, which is as close as one can be to azeotropic conditions.

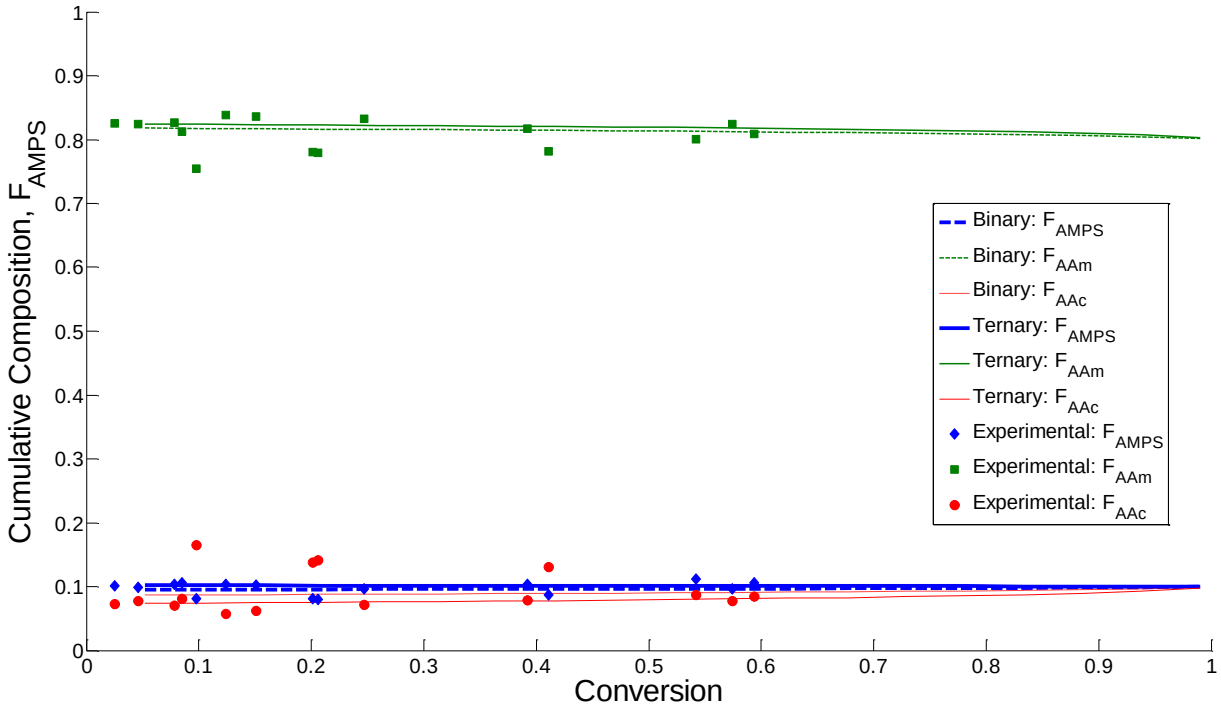

Figure 6.4: Cumulative Terpolymer Composition for AMPS/AAm/AAc ($f_{AMPS,0}/f_{AAm,0}/f_{AAc,0}$ = 0.1/0.8/0.1)

Finally, the AAc-rich terpolymer recipe is presented in Figure 6.5. Again, we see very minimal differences when the binary and ternary reactivity ratio estimates are used in the model, and there is generally good agreement between model predictions and the experimental data.

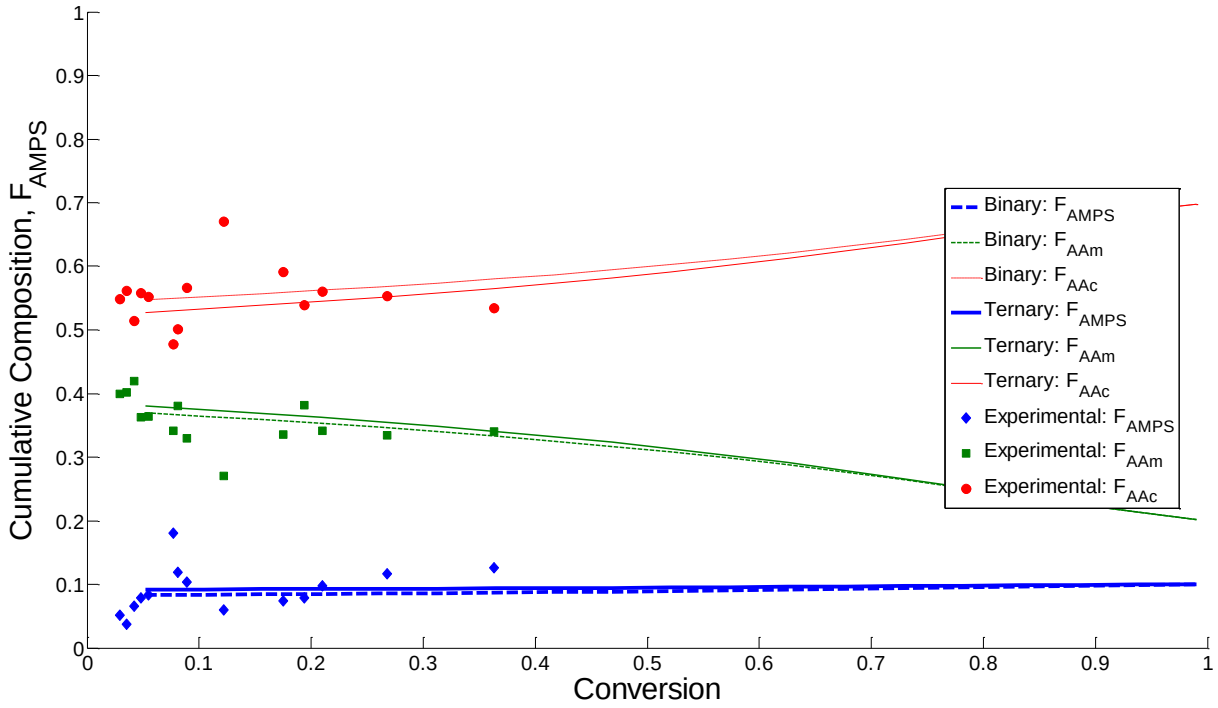

Figure 6.5: Cumulative Terpolymer Composition for AMPS/AAm/AAc ($f_{AMPS,0}/f_{AAm,0}/f_{AAc,0}$ = 0.1/0.2/0.7)

This is a system where using binary and ternary reactivity ratios interchangeably will not drastically affect the overall results. The paired t-test did not show any statistical differences between the binary and ternary reactivity ratio estimates, and the cumulative terpolymer composition analysis showed that the model predictions were only affected when the pre-polymerization recipe was rich in AMPS. However, in other systems studied previously by Kazemi et al. [12], the differences between binary and ternary reactivity ratios were important. Overall, there are clear advantages to using binary data for copolymer studies and ternary data for terpolymerization studies. By doing so, at least one satisfies the statistical admonition that one should use the raw (measured) response data from the system directly for parameter estimation (using the process model that relates system response to system input factors). Using binary copolymer composition data to estimate binary copolymer reactivity ratios as parameters to be employed in a terpolymer model clearly violates that.

CHAPTER 7. CONCLUDING REMARKS, MAIN CONTRIBUTIONS AND RECOMMENDATIONS FOR FUTURE WORK

7.1 Concluding Remarks

Water-soluble polymers of acrylamide (AAm) and acrylic acid (AAc) have significant potential in enhanced oil recovery, as well as in other specialty applications. However, to improve the shear strength of the polymer, it may be beneficial to add a third comonomer to the pre-polymerization mixture. Homopolymerization kinetics of acrylamide and acrylic acid have been studied previously, as have the copolymerization kinetics of these two monomers. Therefore, in the current study, the kinetics of three additional systems were investigated: copolymerization of AMPS/AAm and AMPS/AAc, and terpolymerization of AMPS/AAm/AAc.

Reactivity ratio estimates for all three of the above-mentioned systems were determined, and are summarized in Table 7.1. The binary results for AAm/AAc were taken from previous work by Riahinezhad et al. [10].

Table 7.1: Summary of Reactivity Ratio Estimates for AMPS[1]/AAm[2]/AAc[3]

Experimental Data	r_{12}	r_{21}	r_{13}	r_{31}	r_{23}	r_{32}
Binary Data	0.18	0.85	0.24	0.87	1.33	0.23
Ternary Data	0.46	0.93	0.57	0.92	1.08	0.24

Copolymerization experiments (AMPS/AAm and AMPS/AAc) were designed using two optimal techniques: Tidwell-Mortimer and the error-in-variables-model. The best estimates were assumed to be those obtained from the EVM-designed data, but both techniques gave very

similar results (especially when outlying data points were removed from the AMPS/AAm data set). All optimally-designed experiments led to smaller joint confidence regions (JCRs), which is indicative of greater confidence in the reactivity ratio estimates.

In the same way, terpolymerization experiments for AMPS/AAm/AAc were optimally designed using EVM. The results, shown in Table 7.1, differ from the binary results. The binary and ternary reactivity ratios were not found to be statistically different, and the main effects of the reactivity ratio differences were observed in cumulative composition model predictions.

7.2 Main Contributions

In the current study, accurate reactivity ratio estimates have been determined for copolymers AMPS/AAm and AMPS/AAc, as well as for terpolymer AMPS/AAm/AAc. These binary reactivity ratios can be used with a higher level of confidence (than prior literature sources), and the ternary reactivity ratios for this system have been established for the first time.

In this work, a direct comparison of binary and ternary reactivity ratio estimates has also been completed. Finally, with significant experimental effort and carefully chosen experimental conditions, we can compare binary and ternary data for the same system, with all other variables kept constant. Variables such as pH, ionic strength, monomer concentration, and other polymerization conditions were kept constant; to the extent possible, only the number of comonomers (2 or 3) and the feed composition were varied. Therefore, a direct and more meaningful comparison of binary and ternary reactivity ratios was finally possible.

7.3 Recommendations

7.3.1 Short-Term Recommendations

- Further investigation should be done to confirm the repeatability of the elemental analysis equipment for cumulative copolymer composition. It may also be useful to confirm select copolymer compositions using NMR.

- The effect of residual monomer on cumulative composition data should be considered, as these monomers are difficult to remove. Techniques that would ensure the removal of residual monomer in the samples should be employed, especially at low conversion. This may be more time-consuming, but potential solutions include allowing polymerizations to go to higher conversion levels, introducing a more extensive precipitation/purification process, or keeping the samples under vacuum for longer periods of time.

- The recast Alfrey-Goldfinger model described in Section 2.1.3 is a significant improvement over the original model, as it no longer distorts the error structure. Also, the composition values can be determined individually, and composition ratios are no longer necessary. However, it may be beneficial to re-derive the Alfrey-Goldfinger model by applying the Mayo-Lewis derivation approach/steps to three comonomers, without introducing limiting assumptions or distorting the error structure.

7.3.2 Long-Term Recommendations

- While this project provided us with a better understanding of the reaction kinetics, we still know very little about how polymerization conditions will affect the microstructure of the AMPS/AAm/AAc terpolymer. It may be useful to do some additional characterization experiments (molecular weight determination, sequence length distribution, cumulative triad fractions, etc.) to better understand the terpolymer properties.

- Since the end goal for this terpolymer is as a viscosity modifier for enhanced oil recovery, an in-depth study of desirable characteristics should be completed. Larger AMPS/AAm/AAc samples should be synthesized, so that properties such as shear stability (in high-salinity brines and high-temperature conditions), viscosity, and polymer flooding efficiency can be determined.

- To facilitate the synthesis of larger terpolymer samples, scale-up from vial polymerizations to a larger pilot-plant reactor should be investigated.

REFERENCES

[1] "Water-Soluble Polymers," in *Kirk-Othmer Encyclopedia of Chemical Technology*, John Wiley & Sons, 2000, pp. 1-21.

[2] F. G. Hutchinson, "Medical and Pharmaceutical Applications of Water Soluble Polymers," in *The Chemistry and Technology of Water-Soluble Polymers*, C. A. Finch, Ed., New York and London, Plenum Press, 1983.

[3] Dow Chemical Company, "POLYOX Water-Soluble Resins," 2002.

[4] K. C. Taylor and H. A. Nasr-El-Din, "Water-Soluble Hydrophobically Associating Polymers for Improved Oil Recovery: A Literature Review," *Journal of Petroleum Science and Engineering,* vol. 19, pp. 265-280, 1998.

[5] SNF Inc., "FLOPAAM: World Leader in Polymers for Enhanced Oil Recovery," Riceboro, Georgia, 2004.

[6] A. Zaitoun, P. Makakou, N. Blin, R. Al-Maamari, A. Al-Hashmi, M. Abdel-Goad and H. Al-Sharji, "Shear Stability of EOR Polymers," in *Society of Petroleum Engineers International Symposium*, The Woodlands, Texas, 2011.

[7] P. Singh and H. K. Sawhney, "Studies on Copolymerization of Acrylamide and N-Vinylpyrrolidone," *Journal of Macromolecular Science, Part A: Pure and Applied Chemistry,* vol. 31, pp. 613-627, 1994.

[8] D. Xie, B. M. Culbertson and W. M. Johnston, "Improved Flexural Strength of N-Vinylpyrrolidone Modified Acrylic Acid Copolymers for Glass-Ionomers," *Journal of Macromolecular Science, Part A: Pure and Applied Chemistry,* vol. 35, pp. 1615-1629, 2006.

[9] Q. Li, W. Pu, Y. Wang and T. Zhao, "Synthesis and Assessment of a Novel AM-co-AMPS Polymer for Enhanced Oil Recovery (EOR)," in *International Conference on Computational and Information Sciences*, 2013.

[10] M. Riahinezhad, N. Kazemi, N. McManus and A. Penlidis, "Optimal Estimation of Reactivity Ratios for Acrylamide/Acrylic Acid Copolymerization," *Journal of Polymer Science, Part A: Polymer Chemistry,* vol. 51, pp. 4819-4827, 2013.

[11] A. Sabhapondit, A. Borthakur and I. Haque, "Water Soluble Acrylamidomethyl Propane Sulfonate," *Energy & Fuels,* vol. 17, pp. 683-688, 2003.

[12] N. Kazemi, T. A. Duever and A. Penlidis, "Demystifying the Estimation of Reactivity Ratios for Terpolymerization Systems," *AIChE Journal,* vol. 60, pp. 1752-1766, 2014.

[13] G. Odian, Principles of Polymerization, Hoboken, New Jersey: Wiley-Interscience, 2004.

[14] M. A. Dubé, E. Saldivar-Guerra and I. Zapata-González, "Chapter 6: Copolymerization," in *Handbook of Polymer Synthesis, Characterization, and Processing*, Hoboken, New Jersey, John Wiley & Sons, 2013.

[15] F. R. Mayo and F. M. Lewis, "Copolymerization. I. A Basis for Comparing the Behavior of Monomers in Copolymerization; The Copolymerization of Styrene and Methyl Methacrylate," *Journal of the American Chemical Society,* vol. 66, pp. 1594-1601, 1944.

[16] J. Brandrup, E. H. Immergut and E. A. Grulke, Polymer Handbook, 4th Edition, Wiley-Interscience, 2003.

[17] A. Srivastava, M. Kamal, M. Kaur, S. Pandey, N. Daniel, A. K. Chaurasia and P. Pandey, "Terpolymerization: A Review," *Journal of Polymer Research,* vol. 9, pp. 213-220, 2002.

[18] T. Alfrey and G. Goldfinger, "Copolymerization of Systems of Three and More Components," *Journal of Chemical Physics,* vol. 12, pp. 322-323, 1944.

[19] R. Slocombe, "Multicomponent Polymers. I. Three-Component Systems," *Journal of Polymer Science,* vol. XXVI, pp. 9-22, 1957.

[20] N. Kazemi, T. A. Duever and A. Penlidis, "Reactivity Ratio Estimation from Cumulative Copolymer Composition Data," *Macromolecular Reaction Engineering,* vol. 5, pp. 385-403, 2011.

[21] M. Dube, R. Amin Sanayei, A. Penlidis, K. F. O'Driscoll and P. M. Reilly, "A Microcomputer Program for Estimation of Copolymerization Reactivity Ratios," *Journal of Polymer Science: Part A Polymer Chemistry,* vol. 29, pp. 703-708, 1991.

[22] A. L. Polic, D. T. A and A. Penlidis, "Case Studies and Literature Review on the Estimation of Copolymerization Reactivity Ratios," *Journal of Polymer Science: Part A: Polymer Chemistry,* vol. 36, pp. 813-822, 1998.

[23] N. Kazemi, T. A. Duever and A. Penlidis, "Design of Experiments for Reactivity Ratio Estimation in Multicomponent Polymerizations Using the Error-In-Variables Approach," *Macromolecular Theory and Simulations,* vol. 22, pp. 261-272, 2013.

[24] P. W. Tidwell and G. A. Mortimer, "An Improved Method of Calculating Copolymerization Reactivity Ratios," *Journal of Polymer Science: Part A,* vol. 3, pp. 369-387, 1965.

[25] P. W. Tidwell and G. A. Mortimer, "Science of Determining Copolymerization Reactivity Ratios," *Journal of Macromolecular Science, Part C,* vol. 4, pp. 281-312, 1970.

[26] P. J. Rossignoli and T. A. Duever, "The Estimation of Copolymer Reactivity Ratios: A Review and Case Studies Using the Error-in-Variables Model and Nonlinear Least Squares," *Polymer Reaction Engineering Journal,* vol. 3, pp. 361-395, 1995.

[27] P. M. Reilly and H. Patino-Leal, "A Bayesian Study of the Error-in-Variables Model," *Technometrics,* vol. 23, pp. 221-231, 1981.

[28] N. Kazemi, T. A. Duever and A. Penlidis, "A Powerful Estimation Scheme with the Error-in-Variables Model for Nonlinear Cases: Reactivity Ratio Estimation Examples," *Computers and Chemical Engineering,* vol. 48, pp. 200-208, 2013.

[29] P. M. Reilly, H. V. Reilly and S. E. Keeler, "Parameter Estimation in the Error-in-Variables Model," *Journal of the Royal Statistical Society. Series C (Applied Statistics),* vol. 42, pp. 693-701, 1993.

[30] N. Kazemi, "Reactivity Ratio Estimation Aspects in Multicomponent Polymerizations at Low and High Conversion Levels," MASc Thesis, Department of Chemical Engineering, University of Waterloo, Waterloo, 2010.

[31] V. E. Meyer and G. G. Lowry, "Integral and Differential Binary Copolymerization Equations," *Journal of Polymer Science, Part A,* vol. 3, pp. 2843-2851, 1965.

[32] N. Kazemi, "Reactivity Ratio Estimation in Multicomponent Polymerization Systems Using the Error-in-Variables-Model (EVM) Framework," PhD Thesis, Department of Chemical Engineering, University of Waterloo, Waterloo, Ontario, Canada, 2014.

[33] A. L. Burke, T. A. Duever and A. Penlidis, "Revisiting the Design of Experiments for Copolymer Reactivity Ratio Estimation," *Journal of Polymer Science, Part A: Polymer Chemistry,* vol. 31, pp. 3065-3072, 1993.

[34] S. Durmaz and O. Okay, "Acrylamide/2-Acrylamido-2-methylpropane Sulfonic Acid Sodium Salt-Based Hydrogels: Synthesis and Characterization," *Polymer,* vol. 41, pp. 3693-3704, 2000.

[35] Y. Liu, J.-J. Xie and X.-Y. Zhang, "Synthesis and Properties of the Copolymer of Acrylamide with 2-Acrylamido-2-methylpropanesulfonic Acid," *Journal of Applied Polymer Science,* vol. 90, pp. 3481-3487, 2003.

[36] Y. Liu, J.-J. Xie, M.-F. Zhu and X.-Y. Zhang, "A Study of the Synthesis and Properties of AM/AMPS Copolymer as Superabsorbent," *Macromolecular Materials and Engineering,* vol. 289, pp. 1074-1078, 2004.

[37] A. Pourjavadi, H. Salimi and M. Kurdtabar, "Hydrolyzed Collagen-Based Hydrogel with Salt and pH-Responsiveness Properties," *Journal of Applied Polymer Science,* vol. 106, pp. 2371-2379, 2007.

[38] F. Rosa, J. Bordado and M. Casquilho, "Kinetics of Water Absorbency in AA/AMPS Copolymers: Applications of a Diffusion-Relaxation Model," *Polymer,* vol. 43, pp. 63-70, 2002.

[39] F. Rosa and M. Casquilho, "Effect of Synthesis Parameters and of Temperature of Swelling on Water Absorption by a Superabsorbent Polymer," *Fuel Processing Technology,* vol. 103, pp. 174-177, 2012.

[40] C. Zhang and A. J. Easteal, "Study of Poly(acrylamide-co-2-acrylamido-2-methylpropane sulfonic acid) Hydrogels Made Using Gamma Radiation Initiation," *Journal of Applied Polymer Science,* vol. 89, pp. 1322-1330, 2003.

[41] A. Moradi-Araghi, D. H. Cleveland and I. J. Westerman, "Development and Evaluation of EOR Polymers Suitable for Hostile Environments: II - Copolymers of Acrylamide and Sodium AMPS," in *Society of Petroleum Engineers,* San Antonio, 1987.

[42] A. Sabhapondit, A. Borthakur and I. Haque, "Characterization of Acrylamide Polymers for Enhanced Oil Recovery," *Journal of Applied Polymer Science,* vol. 87, pp. 1869-1878, 2003.

[43] A. Sabhapondit, A. Borthakur and I. Haque, "Water Soluble Acrylamidomethyl Propane Sulfonate (AMPS) Copolymer as an Enhanced Oil Recovery Chemical," *Energy & Fuels,* vol. 17, pp. 683-688, 2003.

[44] Y. A. Aggour, "Thermal Degradation of Copolymers of 2-acrylamido-2-methylpropanesuiphonic Acid with Acrylamide," *Polymer Degradation and Stability,* vol. 44, pp. 71-73, 1994.

[45] F. W. Billmeyer, Textbook of Polymer Science, New York: John Wiley & Sons, Inc., 1971.

[46] Y. V. Bune, A. Barabanova, Y. S. Bogachev and V. Gromov, "Copolymerization of Acrylamide with Various Water-Soluble Monomers," *European Polymer Journal,* vol. 33, pp. 1313-1323, 1996.

[47] C. L. McCormick and G. S. Chen, "Water-Soluble Copolymers. IV. Random Copolymers of Acrylamide with Sulfonated Comonomers," *Journal of Polymer Science: Polymer Chemistry Edition,* vol. 20, pp. 817-838, 1982.

[48] J. Travas-Sejdic and A. Easteal, "Study of Free-Radical Copolymerization of Acrylamide with 2-Acrylamido-2-methyl-1-propane Sulphonic Acid," *Journal of Applied Polymer Science,* vol. 75, pp. 619-628, 2000.

[49] A.-A. A. Abdel-Azim, M. S. Farahat, A. M. Atta and A. A. Abdel-Fattah, "Preparation and Properties of Two-Component Hydrogels Based on 2-Acrylamido-2-methylpropane Sulphonic Acid," *Polymers for Advanced Technologies,* vol. 9, pp. 282-289, 1998.

[50] A. M. Atta, Z. H. Abd El Wahab, Z. A. El Shafey, W. I. Zidan and Z. F. Akl, "Characterization and Evaluation of Acrylic Acid Co-2-acrylamido-2-methylpropane-1-sulfonic Acid Hydrogels for Uranium Recovery," *Journal of Dispersion Science and Technology,* vol. 31, pp. 1415-1422, 2010.

[51] L. Liao, H. Yue and Y. Cui, "Crosslink Polymerization Kinetics and Mechanism of Hydrogels Composed of Acrylic Acid and 2-Acrylamido-2-methylpropane Sulfonic Acid," *Chinese Journal of Chemical Engineering,* vol. 19, pp. 285-291, 2011.

[52] Y. Jie, Y. Pan, Q. Lu, W. Yang, J. Gao and Y. Li, "Synthesis and Swelling Behaviors of P(AMPS-co-AAc) Superabsorbent Hydrogel Produced by Glow-Discharge Electrolysis Plasma," *Plasma Chemistry and Plasma Processing,* vol. 33, pp. 219-235, 2013.

[53] A. Pourjavadi, S. Barzegar and F. Zeidabadi, "Synthesis and Properties of Biodegradable Hydrogels of K-Carrageenan Grafted Acrylic Acid-co-2-Acrylamido-2-Methylpropanesulfonic Acid as Candidates for Drug Delivery Systems," *Reactive and Functional Polymers,* vol. 67, pp. 644-654, 2007.

[54] A. Pourjavadi, F. Seidi, H. Salimi and R. Soleyman, "Grafted CMC/Silica Gel Superabsorbent Composite: Synthesis and Investigation of Swelling Behavior in Various Media," *Journal of Applied Polymer Science*, vol. 108, pp. 3281-3290, 2008.

[55] Y. Wang, X. Shi, W. Wang and A. Wang, "Synthesis, Characterization, and Swelling Behaviors of a pH-Responsive CMC-g-poly(AA-co-AMPS) Superabsorbent Hydrogel," *Turkish Journal of Chemistry*, vol. 37, pp. 149-159, 2013.

[56] R. Ryles and R. Neff, Water-Soluble Polymers for Petroleum Recovery, G. Stahl and D. Schulz, Eds., Anaheim: Springer, 1986.

[57] Y. Bao, J. Ma and N. Li, "Synthesis and swelling behaviors of sodium carboxymethyl cellulose-g-poly(AA-co-AM-co-AMPS)/MMT superabsorbent hydrogel," *Carbohydrate Polymers*, vol. 84, pp. 76-82, 2011.

[58] J. Ma, H. Zheng, M. Tan, L. Liu, W. Chen, Q. Guan and X. Zheng, "Synthesis, Characterization, and Flocculation Performance of Anionic Polyacrylamide P (AM-AA-AMPS)," *Journal of Applied Polymer Science*, vol. 129, pp. 1984-1991, 2013.

[59] T. S. Anirudhan and S. R. Rejeena, "Poly(Acrylic Acid-co-Acrylamide-co-2-Acrylamido-2-Methyl-1-Propanesulfonic Acid)-Grafted Nanocellulose/Poly(Vinyl Alcohol) Composite for the In Vitro Gastrointestinal Release of Amoxicillin," *Journal of Applied Polymer Science*, vol. 131, 2014.

[60] B. Peng, S. Peng, B. Long, Y. Miao and W.-Y. Guo, ""Properties of High-Temperature-Resistant Drilling Fluids Incorporating Arylamide/(Acrylic Acid)/(2-Acrylamido-2-Methyl-1-Propane Sulfonic Acid) Terpolymer and Aluminum Citrate as Filtration Control Agents," *Journal of Vinyl & Additive Technology*, vol. 16, pp. 84-89, 2010.

[61] M. Riahinezhad, N. Kazemi, N. McManus and A. Penlidis, "Effect of Ionic Strength on the Reactivity Ratios of Acrylamide/Acrylic Acid (sodium acrylate) Copolymerization," *Journal of Applied Polymer Science*, vol. 131, 2014.

[62] M. Riahinezhad, N. T. McManus and A. Penlidis, "Effect of Monomer Concentration and pH on Reaction Kinetics and Copolymer Microstructure of Acrylamide/Acrylic Acid Copolymer," *Macromolecular Reaction Engineering*, vol. 9, pp. 100-113, 2015.

[63] N. Kazemi, T. A. Duever and A. Penlidis, "Design of Optimal Experiments for Terpolymerization Reactivity Ratio Estimation," *Macromolecular Reaction Engineering*, vol. 9, pp. 228-244, 2015.

[64] A. Akyüz, A. Paril and A. Giz, "Reactivity Ratios of Acrylamide-Vinyl Pyrrolidone Copolymerization System Obtained by Sequential Sampling," *Journal of Applied Polymer Science*, vol. 100, pp. 3822-3827, 2006.

[65] A. Chatterjee and C. Burns, "Solvent Effects in Free Radical Copolymerization," *Canadian Journal of Chemistry*, vol. 49, pp. 3249-3251, 1971.

[66] G. van Paesschen and G. Smets, "Copolymères Ordinaires et Copolymères Greffés: Structure de Polyampholytes et Interactions Acide-Base," *Bulletin des Sociétés Chimiques Belges*, vol. 64, pp. 173-188, 1955.

[67] A. Chapiro and L. D. Trung, "Copolymerization of Acrylic and Methacrylic Acids with N-Vinylpyrrolidone," *European Polymer Journal*, vol. 10, pp. 1103-1106, 1974.

[68] S. Ponratnam and S. Kapur, "Effect of pH on the Reactivity Ratios in Aqueous Solution Copolymerization of Acrylic Acid and N-Vinylpyrrolidone," *Journal of Polymer Science: Polymer Chemistry Edition*, vol. 14, pp. 1987-1992, 1976.

APPENDIX A – INVESTIGATION OF N-VINYLPYRROLIDONE (NVP) AS POTENTIAL COMONOMER

Since the AAm/AAc copolymer is known to have poor shear stability in EOR applications, the addition of a third comonomer may be beneficial. N-vinylpyrrolidone (NVP) should be considered, as it has been used previously as a comonomer in water-soluble polymers and its presence within polymers has been known to improve shear stability [8]. The addition of bulky monomer groups increases the rigidity of the polymer structure (and hence the glass transition temperature), and ultimately provides greater stability, which is beneficial for the application [6]. However, before investigating the AAm/AAc/NVP terpolymer any further, a detailed review of the literature will provide more information about the potential to synthesize this terpolymer.

A.1 Copolymerization of Acrylamide and N-Vinylpyrrolidone

Over the last 40 years, only a handful of studies have been published on the topic of acrylamide/N-vinylpyrrolidone copolymerization kinetics. Most of these studies included determination of reactivity ratios, r_1 and r_2, but the final results vary significantly from one group to the next. In one of the more recent studies, Akyüz et al. [64] suggest that one of the reasons for the discrepancy may be the data analysis methods used for reactivity ratio determination. Reactivity ratios may be estimated through linear (incorrect) or non-linear (correct) methods; non-linear methods are generally more accurate, but some early efforts used linear methods [46, 65]. Discrepancies are also influenced by the quality of the collected data and by the process type used (solution vs. emulsion or precipitation), initiator type, solvent, reaction temperature, and so on [64]. However, all of the studies are in agreement that r_1 (AAm) > r_2 (NVP) , or that the

copolymer will be richer in acrylamide than the monomer feed. For comparison purposes, some relevant AAm/NVP studies will be discussed briefly.

The first investigation of AAm/NVP copolymerization kinetics was performed in 1971 by Chatterjee and Burns [65]. Their study examined copolymer composition and comonomer reactivity by varying the monomer feed concentration. Copolymer composition was determined using UV absorption spectroscopy, and was compared to the feed composition to determine relative reactivities. A linear "least-squares" technique was used to calculate r_1 (for AAm) and r_2 (for NVP). It was found that $r_1 = 0.66$ and $r_2 = 0.17$ for the aqueous polymerization of AAm/NVP [65]. Since both reactivity ratios are less than 1, we can assume that each monomer prefers to bond with the other monomer type present in the system (that is, AAm radicals prefer NVP monomer, and NVP radicals prefer AAm monomer). It is expected, then, that copolymers with an alternating tendency will be produced under these conditions [65].

Chatterjee and Burns also investigated the effect of solvent type on the reaction system [65]. The experimental conditions included pure water, and glycerol/water mixtures with 5, 67, and 80 weight % glycerol. AAm/NVP copolymerizations were completed in these four different solvents, so that the effects of solvent on copolymer composition and relative reactivities could be better understood. It was found that increased glycerol concentration led to higher acrylamide reactivity (see Figure A.1). In fact, at 80 weight % glycerol, $r_1 = 10.6$ and $r_2 = 0.11$ (compared to $r_1 = 0.66$ and $r_2 = 0.17$ in water) [65]. This is likely due to the hydrogen bonding that is induced between AAm units in the presence of glycerol [65]. Therefore, more acrylamide units were present in the copolymer, and the alternating behaviour of aqueous solution polymerization was

reduced significantly. The relationship between feed monomer composition and copolymer composition in different solvents is presented in Figure A.2.

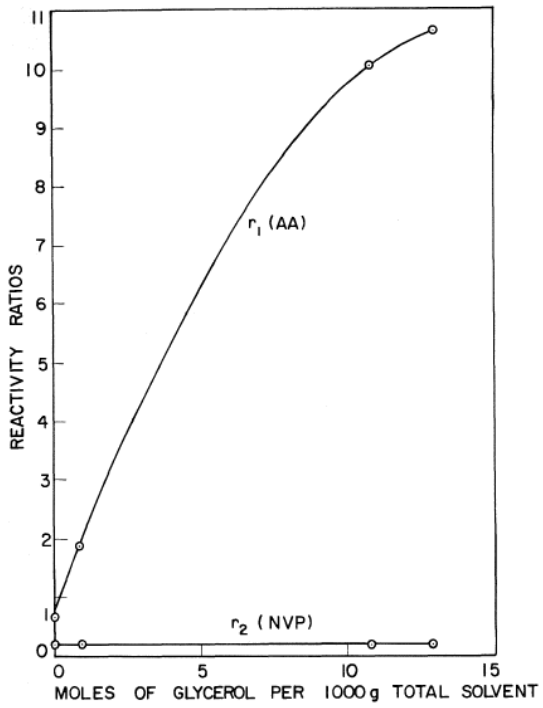

Figure A.1: Effect of Solvent Composition on Reactivity Ratios for AAm/NVP Copolymerization [65]

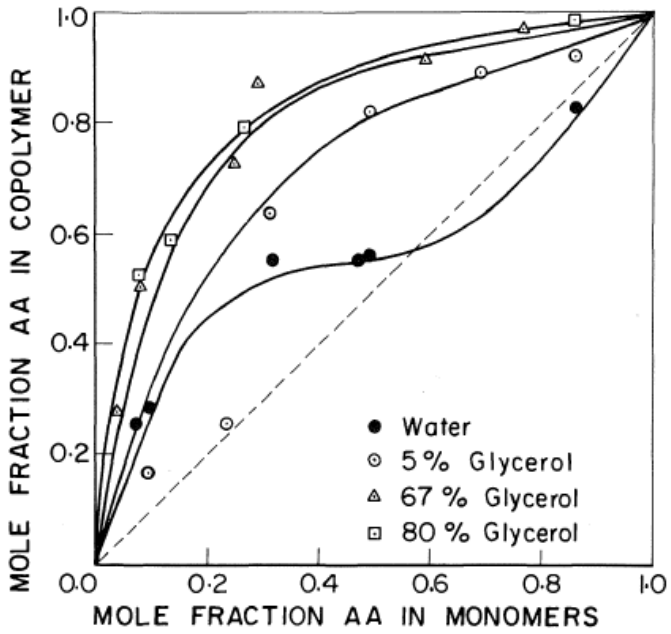

Figure A.2: Effect of Feed Composition on Copolymer Composition with Varying Solvent [65]

Another study focusing on the kinetics of this system was completed by Singh and Sawhney [7]. Their investigation examined different polymerization methods, including solution, precipitation, and inverse emulsion polymerization. Again, different feed compositions were used to determine the reactivity ratios of acrylamide and N-vinylpyrrolidone. For this system, elemental analysis of carbon, hydrogen, and nitrogen was used to determine the copolymer composition. The Fineman-Ross (linear) method was used to calculate r_1 and r_2, based on only 3 data points [7]! The reactivity ratios were found to be fairly similar to those estimated by Chatterjee and Burns: $r_1 = 0.61$ and $r_2 = 0.05$ [7] (compared to $r_1 = 0.66$ and $r_2 = 0.17$ [65]). However, it is important to note that the polymerization systems were entirely different.

In the investigation by Singh and Sawhney [7], most of the work was done using inverse emulsion polymerization in xylene. This method was chosen in an attempt to minimize the drastic increase in viscosity that occurs during solution polymerization, and was found to be stable for 7.5% to 15% monomer [7]. It was found that, in this type of polymerization, both the rate of reaction and the copolymer composition varied with the ratio of AAm to NVP in the monomer feed. The relationship between feed composition and copolymer composition was similar to that observed in previous work (Figure A.2). Experimental results also showed that as the AAm concentration increases, the reaction occurs more quickly and reaches higher levels of conversion (see Figure A.3).

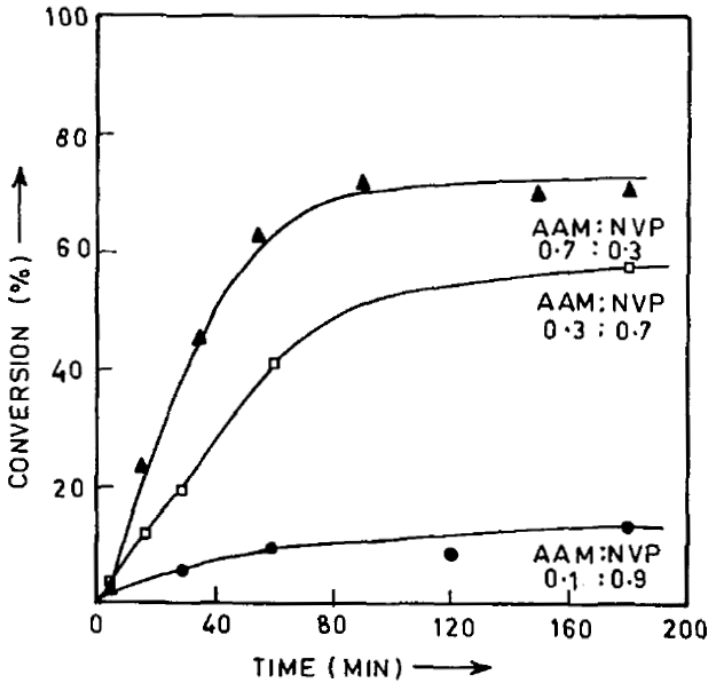

Figure A.3: Conversion vs. Time Profiles for AAm/NVP Copolymers with Varying Monomer Feed Composition [7]

The effect of pH was also briefly studied by Singh and Sawhney [7]. The copolymer system was studied with and without buffer (for pH control), and much more consistent results were obtained in the presence of buffer. When no buffer was used, the system was acidic (pH < 5), and only 65% conversion was obtained. On the other hand, when the addition of buffer kept the pH at around 7, 100% conversion was achieved. In both cases, though, pH stayed approximately constant throughout the reaction, with the exception of a drop in pH during initiator addition [7].

In 1996, Bune et al. [46] brought forward an interesting question: if the reaction mixture composition changes with conversion, can we assume that the reactivity ratios remain constant throughout the reaction? For the first time, the copolymerization of AAm and NVP was allowed to react to high levels of conversion; most studies completed previously only looked at low conversions, since kinetic analyses often rely on the assumption of constant monomer

concentration. Rather than removing samples from the solution for analysis, the entire polymerization system was analyzed using nuclear magnetic resonance (NMR) spectroscopy. By measuring the concentration of each comonomer left in the feed mixture, it was possible to estimate the amount of each comonomer that had been consumed in the polymerization [46].

Bune et al. [46] hypothesized that the reactivity ratios (and the copolymer composition) would change with conversion. However, they found that the values remained constant up to 50% to 70% conversion. This may have been due to the interaction between water-soluble monomers and water itself during solution polymerization. Although the composition of the solution changes, concentrations are believed to remain approximately constant within active polymerization regions (zones that are likely isolated by polymer coils forming at higher conversions) [46]. Therefore, the assumption that reactivity ratios remain constant throughout the reaction is valid. The reactivity ratios for the system were again calculated using the Fineman-Ross method, and were found to be as follows for the aqueous system: $r_1 = 1.2 \pm 0.2$ and $r_2 = 0.8 \pm 0.2$ [46]. The copolymerization was also investigated with dimethyl sulfoxide (DMSO) as the solvent, and the Fineman-Ross method indicated that $r_1 = r_2 = 1$ [46]. This study also examined the relationship between monomer feed concentration and reaction rate. The results agreed with the trends that Singh et al. [7] had observed: higher AAm concentration led to a faster polymerization.

Despite the varied methods used throughout these analyses for copolymer composition measurements, Akyüz et al. returned to UV spectroscopy [64] (used by Chatterjee and Burns in the original AAm/NVP analysis [65]). A sequential sampling technique was used to obtain more information (and higher levels of conversion) in fewer experimental runs. In this recent study,

the solution copolymerization of acrylamide and NVP was examined with varying monomer feed composition. Additionally, one experimental run (50 wt% AAm, 50 wt% NVP) was repeated three times, so that error analysis could be included in the investigation [64].

A non-linear parameter estimation technique was used to estimate reactivity ratios. It was found that $r_1 = 2.03 \pm 0.14$ and $r_2 = 0.09 \pm 0.02$ [64]. These results were confirmed using the Extended Kelen Tüdös (EKT) method, which gave similar results: $r_1 = 2.08 \pm 0.04$ and $r_2 = 0.12 \pm 0.04$ [64].

To summarize, studies of copolymerization kinetics of acrylamide and N-vinylpyrrolidone have provided the information of Table A.1.

Table A.1: Summary of Kinetic Studies for AAm/NVP Copolymerization

Reaction Conditions	Solvent	Composition Determination	Estimation Technique	r_1	r_2	Ref.
Solution; T = 60°C	Water	UV absorption	Linear least squares	0.66	0.17	[65]
Solution; T = 60°C	20% water; 80% glycerol	UV absorption	Linear least squares	10.6	0.11	[65]
Inverse emulsion; T = 50°C	Xylene	Elemental analysis	Fineman-Ross	0.61	0.05	[7]
Solution; T = 35 & 55°C	Water	NMR	Fineman-Ross	1.2	0.8	[46]
Solution; T = 45 - 55°C	DMSO	NMR	Fineman-Ross	1.0	1.0	[46]
Solution (sequential sampling); T = 60°C	Water	UV absorption	Non-linear regression	2.03	0.09	[64]
Solution (sequential sampling); T = 60°C	Water	UV absorption	Extended Kelen Tüdös	2.08	0.12	[64]

A.2 Copolymerization of Acrylic Acid and N-Vinylpyrrolidone

The copolymerization kinetics of acrylic acid (AAc) and N-vinylpyrrolidone (NVP) have also been studied, but not nearly to the same extent as for the AAm/NVP copolymer system. Some of the main difficulties associated with this system are the low reactivity ratios and the more significant dependence on pH.

One of the first studies in AAc/NVP copolymerization to determine reactivity ratios was completed by van Paesschen and Smets [66]. Their goal was to investigate whether different polymerization methods would affect the overall structure of the polymer. They studied a variety of AAc/NVP copolymer synthesis methods, including typical bulk polymerization of acrylic acid and N-vinylpyrrolidone. The copolymerization was studied with three different feed compositions, and the copolymer composition was analyzed using conductometric titration. For bulk polymerization at 75°C, it was found that r_1 (AAc) = 1.3 ± 0.2 and r_2 (NVP) = 0.15 ± 0.1 [66]. With $r_1 > r_2$, the AAc/NVP copolymer will be rich in acrylic acid. These early results are in agreement with later studies [67, 68].

One of the challenges in the copolymerization of acrylic acid and NVP is the acidity of AAc combined with the basic nature of NVP. Therefore, Chapiro and Trung [67] chose to investigate interactions between the two comonomers, and between the monomers and various solvents. Not only did they find strong interactions between AAc and NVP in the stock monomer solution, but also that NVP may spontaneously polymerize in the presence of AAc. Therefore, the

comonomers were not combined until the very last minute, and temperatures were kept fairly low (~30°C) during polymerization [67].

In the study by Chapiro and Trung [67], the AAc/NVP copolymer was synthesized in bulk as studied by van Paesschen and Smets [66], as well as in solution with ethanol, toluene and DMF as solvents. Again, several different feed compositions were used to determine reactivity ratios for the system. It was found that the polymerization rate increased with acrylic acid concentration, which was analogous to the AAm/NVP copolymerization studies; in both copolymer systems (and in the homopolymerization), higher NVP concentration resulted in lower reactivity [67].

To determine the copolymer composition, elemental analysis based on nitrogen was used in parallel with potentiometric titration. Good agreement between the analysis methods (within 5%) significantly increased confidence in the results [67]. The composition of the copolymer synthesized in bulk was almost identical to the composition of those solution copolymers synthesized in ethanol and in toluene. For these three systems, $r_1 = 0.48 \pm 0.04$ and $r_2 = 0.05 \pm 0.01$ [67]. Solution polymerization in DMF yielded a copolymer that was slightly richer in AAc, which means that r_1 was slightly higher than for the other systems. Some minor solvent effects were present here, as $r_1 = 0.67 \pm 0.05$ and $r_2 = 0.03 \pm 0.01$ [67]. Additional tests indicated that composition (and therefore reactivity ratios) seemed independent of temperature and feed monomer concentration. However, r_2 was quite low in all cases, which confirmed the trends observed by van Paesschen and Smets [66].

In 1976, Ponratnam and Kapur [68] identified a significant factor in the copolymerization kinetics of acrylic acid and N-vinylpyrrolidone: pH. Aqueous solution polymerization was completed at 30°C with varying feed concentrations and acidities (pH = 4 to 9). The monomer reactivities were determined using two different linear techniques [68]. Both methods gave similar results, so only the values obtained from the first technique (Mayo-Lewis method) are presented for the sake of brevity. The values of r_1 and r_2 as a function of pH are presented in Figure A.4, and are summarized later in Table A.2.

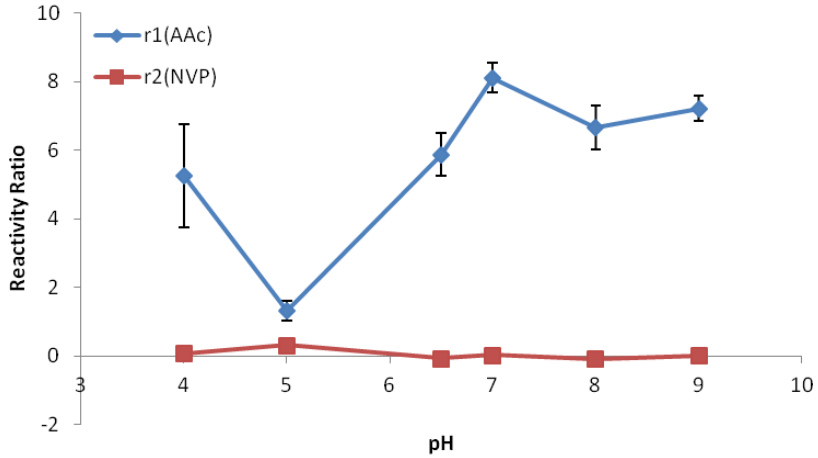

Figure A.4: Effect of pH on Reactivity Ratios for AAc/NVP Copolymerization [68]

It is important to note that r_1 varied significantly with pH. The low reactivity observed at pH = 5 was likely due to the electrostatic repulsion between monomer and polymer molecules with different charges. However, reactivity increased again at higher pH, since the system exhibited behaviour characteristic of acrylic acid homopolymerization [68]. This homopolymerization behaviour was likely due to the extremely low values of r_2 and high values of r_1. It is unlikely that NVP will be incorporated to a great extent in the polymer formed, except perhaps at pH = 5 (where r_1 is lowest and r_2 is highest). Ultimately, at any pH, the copolymer will likely have high levels of acrylic acid.

Table A.2: Summary of Kinetic Studies for AAc/NVP Copolymerization

Reaction Type	Solvent	Temperature	pH	r_1	r_2	Ref.
Bulk	--	75°C	--	1.30	0.15	[66]
Bulk	--	0 & 20°C	--	0.48	0.05	[67]
Solution	Toluene, ethanol	0 & 20°C	--	0.48	0.05	[67]
Solution	DMF	20°C	--	0.67	0.03	[67]
Solution	Water	30°C	4	5.26	0.078	[68]
Solution	Water	30°C	5	1.32	0.31	[68]
Solution	Water	30°C	6.5	5.87	-0.077	[68]
Solution	Water	30°C	7	8.12	0.019	[68]
Solution	Water	30°C	8	6.66	-0.084	[68]
Solution	Water	30°C	9	7.22	0.010	[68]

APPENDIX B – SAFETY CONSIDERATIONS FOR EXPERIMENTAL WORK

This is an excerpt from the author's departmental safety report. More details can be found in that document, which was submitted to the Chemical Engineering Department in October 2013.

B.1 General Safety Awareness and Practices

B.1.1 Emergency Telephone Numbers

Fire and Ambulance	911
Waterloo Regional Police	911
UW Police and Security	22222
Plant Operations	33793
Health Services	84096
Poison Information Center	6-1-800-268-9017
Chemical Spills	22222
Director of Safety (Kevin Stewart)	35814
Environmental Health Co-ordinator (Ian Fraser)	36268
Department Chair (Eric Croiset)	32296
Departmental Health & Safety (Ralph Dickhout)	33311
Labs	E6-5113 Ext. 33927
	E6-5119 Ext. 31669
Office	E6-5114 Ext. 31666

B.1.2 Chemical Spills

Before working with hazardous materials:

- Determine spill procedures from Material Safety Data Sheets (MSDS) for all chemicals
- Obtain proper spill kits and clean up equipment (from ESC 109)

In case of a small spill that poses no immediate threat to health:

- Notify occupants in the immediate area of the spill
- Use spill kits to absorb and contain chemical, according to spill procedure
- Place material in a secure and ventilated area
- Contact supervisor, departmental safety officer, and/or the University of Waterloo Safety Office (ext. 36268) for disposal instructions

In case of a large spill or a spill that poses an immediate threat to health:

- Remove sources of ignition, if possible
- Evacuate immediate area
- Call UW Police at extension 22222

Additional precautions for flammable liquids:

- Immediately remove all sources of ignition from the area
- Identify the location of the nearest fire extinguisher
- Use non-sparking tools (like bronze) during clean up

B.2 Safety Assessment for Research Project

B.2.1 Personal Protective Equipment

Eyes: Safety glasses and/or safety goggles (face shield, if necessary)
Hands: Gloves (appropriate gloves should be selected according to the substance being handled)
Body: Lab coat and pants
Feet: Closed-toe shoes (sandals, open-toed shoes, and similar footwear should not be worn in a laboratory, especially if there is potential for chemical spills)

B.2.2 Fire and/or Explosion Hazards

- Compressed gas cylinders
- Flammable or combustible chemicals either in use or in storage
- Ampoules and vials
- Waste drums

B.2.3 Pressure and Temperature Hazards

- Ampoules and vials are at high temperature and pressure during reactions
- Ampoules are under vacuum during distillation and degasification
- Gas cylinders are at high pressures
- Liquid nitrogen is a cryogenic gas
- Oil bath, burners, and ovens are at high temperatures

B.2.4 High Voltage Electrical Hazards

- The circuit breaker panel should only be used by qualified technicians

B.2.5 Falling Objects

- Compressed gas cylinders
- Storage containers like vials, beakers and bottles
- Glassware on shelves or lab bench

B.2.6 Leaks and Spills

- Compressed gas cylinders
- Chemical containers like beakers and bottles
- Reactors, pumps, piping, valves

B.3 List of Chemicals (Selective)

The chemicals that will be used in the laboratory are listed in Table B.1. The Material Safety Data Sheets (MSDS) for these chemicals can be found in E6-5113 and E6-5119. If any additional materials are used in the future, they will be added to this table. In the case of common monomers, initiators or chain transfer agents, the appropriate MSDS will be consulted before first use.

Table B.1: List of Laboratory Chemicals

Chemical Name	**Carcinogen, Toxic, etc.**	**Properties**	**Safety Precautions**
AMPS (2-acrylamido-2-methylpropane sulfonic acid; monomer)	• Toxic • Corrosive	• Solid white powder • Soluble in water • MP = 195°C • AIT > 400°C • S.G. = 1.36 g/cm^3	• Wear safety glasses and gloves • Handle under a fume hood (toxic upon inhalation) • Keep container tightly sealed, in a dry and well-ventilated place • Eye Contact: Severe eye irritant. Remove any contact lenses and flush eyes with water. • Skin Contact: Immediately flush skin with soap and plenty of water, while removing contaminated clothing and shoes. • Inhalation: Remove to fresh air. If not breathing, give artificial respiration. • Ingestion: Rinse mouth with water (never give anything by mouth to an unconscious person!); consult a physician.
ACVA (4,4'-azo-bis-(4-cyano valeric acid); initiator)	• Unstable reactive material • Heating may cause fire, but generally not flammable	• Solid white powder • Odourless • Insoluble in water • MP = 118˚C – 125°C	• Wear safety glasses and gloves • Handle under a fume hood • Keep container tightly sealed, in a dry and well-ventilated place (avoid heat, flames, sparks and oxidizing agents; best stored between 2°C – 8°C) • In case of fire, use water spray, alcohol-resistant foam, CO_2 or dry chemical extinguisher • Eye Contact: Remove any contact lenses. Flush eyes with water as a precaution. • Skin Contact: Immediately flush skin with soap and plenty of water for at least 15 min., while removing contaminated clothing and shoes. • Inhalation: Remove to fresh air. If not breathing, give artificial respiration. If breathing is difficult, give oxygen. • Ingestion: Rinse mouth with water (never give anything by mouth to an unconscious person!); consult a physician.

Chemical Name	Carcinogen, Toxic, etc.	Properties	Safety Precautions
Acrylamide (monomer)	• Toxic; carcinogen; neurotoxin • Harmful if swallowed or inhaled • Thermally unstable	• Colorless crystals • Odorless • B. Point = 125˚C • M. Point = 84.5˚C • F. Point = 138˚C • MW = 71.08 g/mol • SG = 1.122	• Keep in closed container; store in cool, dry ventilated area, away from heat and sources of ignition • Isolate from oxidizing agents • Wear nitrile gloves, goggles, and lab coat • Eye Contact: Remove any contact lenses. Immediately flush eyes with plenty of water for at least 15 min. • Skin Contact: Immediately flush skin with plenty of water for at least 15 minutes while removing contaminated clothing and shoes. • Inhalation: Remove to fresh air. If not breathing, give artificial respiration. If breathing is difficult, give oxygen. • Ingestion: Do not induce vomiting unless directed to do so by medical personnel. Loosen tight clothing.
Acrylic Acid (monomer)	• Very hazardous in case of skin & eye contact • Harmful if swallowed or inhaled; causes burns • Flammable • Extremely reactive or incompatible with oxidizing agents, acids, alkalis. • Reactive with moisture.	• Clear colorless liquid with acrid odor. • BP = 141˚C • MP = 14˚C • AIT = 438˚C • FP = 50˚C • MW = 72.06 g/mol • SG = 1.05	• Store in cool, dry & well ventilated area, separate from oxidizing agent • Handle only in fume hood • Wear nitrile gloves, goggles, and lab coat • Eye Contact: Remove contact lenses. Immediately flush eyes with plenty of water for at least 15 min. • Skin Contact: Immediately flush skin with plenty of water for at least 15 min., while removing contaminated clothing & shoes. • Inhalation: Remove to fresh air. If not breathing, give artificial respiration. If breathing is difficult, give oxygen. • Ingestion: Do NOT induce vomiting unless directed to do so by medical personnel. Never give anything by mouth to an unconscious person. Loosen tight clothing.
Hydroquinone (inhibitor)	• Very toxic by ingestion • Carcinogen/ mutagen • Moderate skin & eye irritant	• Solid white crystals • Soluble in water and methanol • MP: 172°C – 175°C • AIT = 516°C	• Handle only in fume hood • Wear nitrile gloves, goggles, and lab coat • Eye Contact: Remove contact lenses. Immediately flush eyes with plenty of water. • Skin Contact: Immediately flush skin with soap and water, while removing contaminated clothing & shoes. • Inhalation: Remove to fresh air. If not breathing, give artificial respiration. If breathing is difficult, give oxygen. • Ingestion: Do NOT induce vomiting unless directed to do so by medical personnel. Never give anything by mouth to an unconscious person. Loosen tight clothing.

Chemical Name	Carcinogen, Toxic, etc.	Properties	Safety Precautions
Methanol (solvent)	• Mutagen • Toxic • Flammable	• Colourless liquid • B. Point = 64.7°C • F. Point = -11°C • M. Point = -98°C • Very volatile	• Wear safety glasses and gloves • Handle under a fume hood, away from flame • Incompatible and reactive with strong oxidizers • Exposure through inhalation, ingestion, eye or skin contact • Symptoms: irritated skin, eyes, and respiratory tract, coughing dizziness, headache, nausea • Eye Contact: Rinse in eye-washing station for at least 15 minutes. • Skin contact: Wash off thoroughly with soap and water. Take victim to hospital immediately and remove any contaminated clothing. • Inhalation: Move to fresh air and administer artificial respiration if not breathing. • Ingestion: Rinse mouth with water. Do not induce vomiting.
Nitrogen (gas)		• Colourless • Odourless	• Wear safety glasses • Can cause rapid suffocation
Nitrogen (liquid; freezing agent & oxidation inhibitor)	• May cause burn or frostbite during skin contact • May cause tissue freezing during eye contact	• Colourless liquid • Odourless • BP = -196°C • SG = 1.25	• Wear safety glasses and insulated gloves • Transfer slowly • Use porous stopper • Can cause freezing on contact
Oxygen (gas)	• Flammable in the presence of reducing, combustible, and organic materials	• Colourless • Odourless • Slightly soluble in water • BP = -183˚C • SG = 1.309	• Wear safety glasses • Keep away from open flames • Accelerates combustion • Do not mix with other organic or combustible substances • Store cylinder in ventilated area
Sodium hydroxide (base)	• Corrosive • Irritant • Highly reactive with metals. • Reactive with oxidizing and reducing agents, acids, alkalis, and moisture	• White pellets, flakes or beads • Highly soluble in water • Odourless • BP = 1388˚C • MP = 318˚C • SG = 2.13 • MW = 40 g/mol	• Wear safety glasses and gloves • Add water slowly (exothermic mixing) • Reacts violently with strong acid, aluminum, and many organic chemicals • Causes burns when in contact with skin • May be fatal if swallowed • Keep in tight and closed container, • Store in cool, dry and ventilated area, • Do not touch vessels or beaker with freshly prepared caustic solution • Eye Contact: Rinse in eye-washing station for at least 15 minutes. Continue rinsing during transport to hospital. • Skin contact: Remove contaminated clothing. Wash thoroughly with soap and water. • Inhalation: Move to fresh air and administer artificial respiration if not breathing. • Ingestion: Rinse mouth with water. Do not induce vomiting

B.4 List of Equipment (Selective)

A list of the laboratory equipment and the associated hazards is presented in Table B.2.

Table B.2: Laboratory Equipment

Equipment	Hazards	Recommendations
Glassware	• Shattering	• Wear safety glasses and proper footwear • Handle with care
Thermostat bath	• Scalding • Ampoules breaking • Use of high temperatures and/or flammable materials could result in fire	• Wear safety glasses, proper footwear, and insulated gloves • Heating bath containers should be durable, and set up with a firm support • Do not place heating baths near flammable or combustible materials • Move heating baths only when the liquid is cool • Set the thermostat well below the flash point of the heating liquid in use
Vacuum pump	• Implosion of glass and ampoules • Chemical vapours	• Wear safety glasses • Vent vapours to fume hood • Protect pumps with cold traps • Assemble vacuum apparatus in a manner that avoids strain, particularly to the neck of the flask • Avoid putting excessive pressure on a vacuum line to prevent stopcocks from popping out or glass apparatus from exploding • When possible, avoid using mechanical vacuum pumps for distillation or concentration operations using large quantities of volatile materials
GPC/LALLS/VISC, IR, NMR, SEC, DSC	• Chemical splashes during sample preparation • High temperatures • Leaking of flammable solvents and/or buffer	• Wear safety glasses, lab coat and gloves • Use caution during operation

Equipment	Hazards	Recommendations
Distillation setup	• Chemical splashes • Spills or leaks • Shattering glassware • Compressed oxygen • High temperature	• Wear safety glasses, lab coat and gloves • Glassware and fittings should be checked before use
N_2 cylinder	• Unusual Explosion Hazards and general cylinder hazard	• Use in an upright position, and secure firmly with chains or clamps • Wear safety goggles • Reduce the pressure through a manufacturer's specified regulator attached to the cylinder valve
Needles	• Puncture skin • Risk of infection and/or chemical contact from contaminated needle	• Use best practices for safe collection and removal of needles • Provide proper sharps containers (not garbage bags) • Use gloves and tongs or pliers to pick up needles.

APPENDIX C – PRELIMINARY EXPERIMENTAL DATA

C.1 Preliminary Copolymerization of AMPS/AAm (see Chapter 4)

Table C.1: Experimental Data for AMPS/AAm Copolymerization; Preliminary Experiments

Run #	X	$f_{AMPS,0}$	$f_{AAm,0}$	$\overline{F}_{AMPS}$	$\overline{F}_{AAm}$
1	0.1634	0.15	0.85	0.1478	0.8522
	0.2353	0.15	0.85	0.1524	0.8476
	0.2223	0.15	0.85	0.1534	0.8466
	0.3583	0.15	0.85	0.1567	0.8433
2	0.2019	0.80	0.20	0.4639	0.5361
	0.3074	0.80	0.20	0.5807	0.4193
	0.5240	0.80	0.20	0.8500	0.1500
	0.6139	0.80	0.20	0.8371	0.1629
	0.7233	0.80	0.20	0.6404	0.3596
3	0.1808	0.15	0.85	0.1119	0.8881
	0.2606	0.15	0.85	0.2141	0.7859
	0.3694	0.15	0.85	0.1636	0.8364
	0.4421	0.15	0.85	0.1454	0.8546
	0.5072	0.15	0.85	0.1290	0.8710
4	0.3480	0.80	0.20	0.4995	0.5005
	0.3337	0.80	0.20	0.7489	0.2511
	0.5950	0.80	0.20	0.7425	0.2575
	0.6444	0.80	0.20	0.7230	0.2770

C.2 Preliminary Copolymerization of AMPS/AAc (see Chapter 5)

Table C.2: Experimental Data for AMPS/AAc Copolymerization; Preliminary Experiments

Run #	X	$f_{AMPS,0}$	$f_{AAc,0}$	$\overline{F}_{AMPS}$	$\overline{F}_{AAc}$
1	0.1210	0.15	0.85	0.2362	0.7638
	0.4324	0.15	0.85	0.0857	0.9143
	0.3384	0.15	0.85	0.1085	0.8915
2	0.0959	0.80	0.20	0.6870	0.3130
	0.0953	0.80	0.20	0.7793	0.2207
	0.5501	0.80	0.20	0.7093	0.2907
	0.7212	0.80	0.20	0.6797	0.3203
3	0.4382	0.15	0.85	0.1420	0.8580
	0.4522	0.15	0.85	0.1699	0.8301
	0.4571	0.15	0.85	0.1604	0.8396
4	0.8469	0.80	0.20	0.6889	0.3111

APPENDIX D – SAMPLE CALCULATIONS

D.1 Conversion Calculations

As an example, conversion vs. time results for a preliminary analysis of the AMPS/AAm copolymer ($f_{AMPS,0}$ = 0.15) are presented in Table D.1:

Table D.1: Gravimetry Calculations for Conversion vs. Time

#	Time (min)	Empty Vial (g)	Vial + Solution (g)	Solution (g)	Monomer (g)	Empty Filter (g)	Filter + Polymer (g)	Polymer (g)	Conversion (%)
1	10	21.7740	39.7740	18.0000	1.6471	1.0353	1.3410	0.3057	18.56
2	15	21.7066	42.5454	20.8388	1.9068	1.0411	1.5638	0.5227	27.41
3	20	21.6603	39.7913	18.1310	1.6591	1.0380	1.6748	0.6368	38.38
4	25	21.5985	40.5731	18.9746	1.7362	1.0296	1.8237	0.7941	45.74
5	35	21.6748	40.2675	18.5927	1.7013	1.0322	1.9214	0.8892	52.27

Where time values are pre-selected according to process knowledge, and the masses of the empty vial, the vial filled with (pre-polymer) solution, the filter and the filter containing polymer are measured directly. The other values are calculated as follows:

$$\text{Solution} = (\text{Vial} + \text{Solution}) - \text{Empty Vial} = 39.7740\ \text{g} - 21.7740\ \text{g} = 18.0000\ \text{g} \qquad \text{(D.1)}$$

$$\text{Monomer} = \frac{(\sum(\text{g monomer}))\left(\frac{\text{ml stock soln in pre-polymer soln}}{\text{total ml stock soln}}\right)}{\text{total ml pre-polymer soln}} \times \text{ml pre} - \text{polymer soln} \qquad \text{(D.2)}$$

$$= \frac{(15.5417\ \text{g AMPS} + 30.2101\ \text{g AAm})\left(\frac{50\ \text{ml}}{250\ \text{ml}}\right)}{100\ \text{ml}} \times 18.0000\ \text{g}\ \left(\frac{\text{ml}}{1\ \text{g}}\right) = 1.6471\ \text{g}$$

*Note: there is an assumption here that the pre-polymer solution has a density of 1 g/ml, since it is essentially water.

$$\text{Polymer} = (\text{Filter} + \text{Polymer}) - \text{Empty Filter} = 1.3410\ \text{g} - 1.0353\ \text{g} = 0.3057\ \text{g} \qquad \text{(D.3)}$$

$$\text{Conversion} = \frac{\text{Polymer}}{\text{Monomer}} \times 100 = \frac{0.3057\ \text{g}}{1.6471\ \text{g}} \times 100 = 18.56\% \qquad \text{(D.4)}$$

Sodium ions are added to the pre-polymerization recipe, both during titration with NaOH and during ionic strength regulation with NaCl. Therefore, the conversion calculations must be modified slightly, as per Riahinezhad et al. [61]. The same experimental data from Table D.1 is presented in Table D.2, but these final results include this additional modification. Only the AMPS/AAm conversion needed to be recalculated, as the ionic strength remained constant for all AMPS/AAc copolymerizations.

Table D.2: Corrected Conversion Calculations, with Na Consideration

#	Time (min)	Conversion (%)	mole AMPS	mole AAm	Na (g)	Monomer (g)	Polymer (g)	Corrected Conversion (%)
1	10	18.56	0.1119	0.8881	2.5721	1.6471	0.3057	18.08
2	15	27.41	0.2141	0.7859	4.9213	1.9068	0.5227	26.06
3	20	38.38	0.1636	0.8364	3.7608	1.6591	0.6368	36.94
4	25	45.74	0.1454	0.8546	3.3431	1.7362	0.7941	44.21
5	35	52.27	0.1290	0.8710	2.9666	1.7013	0.8892	50.72

The number of moles of each comonomer in the resulting copolymer was determined using elemental analysis, and sample calculations will be presented in Section D.2. The mass of Na in the system is directly related to the number of moles of AMPS, since the molar ratio of Na:AMPS is 1:1. Calculations for Na mass and corrected conversion are shown below:

$$\text{g Na} = 0.1119 \text{ mol AMPS} \times \frac{1 \text{ mol Na}}{1 \text{ mol AMPS}} \times \frac{22.989 \text{ g Na}}{\text{mol Na}} = 2.5721 \text{ g} \quad \text{(D.5)}$$

$$\text{Corrected Conversion} = \frac{\text{g polymer} - (\text{g polymer})(0.01)(\text{g Na})}{\text{g monomer}} \times 100 \quad \text{(D.6)}$$

$$= \frac{0.3057 \text{ g} - (0.3057 \text{ g})\left(\frac{2.5721 \text{ g}}{100 \text{ ml}}\right)\left(\frac{1 \text{ ml}}{1 \text{ g}}\right)}{1.6471 \text{ g}} \times 100 = 18.08\%$$

D.2 Cumulative Composition Calculations

Cumulative composition was measured using elemental analysis, and the content of elemental carbon, nitrogen and sulfur were used in the calculations. Hydrogen was not included, as the data would be too easily influenced by moisture in the atmosphere. A sample calculation is shown below for sample #1 in Tables D.1 and D.2.

Table D.3: Cumulative Composition Calculations for AMPS/AAm Copolymer

Elements	wt %	# moles	mole ratio	m	F_{AMPS}	F_{AAm}
N	13.15	0.9388	8.9380	7.9380	0.1119	0.8881
C	42.59	3.5460	33.7600			
H	6.18	6.1280	58.3413			
S	3.37	0.1050	1.000			

The weight percent values are obtained directly from the elemental analysis readout and the number of moles is found by dividing wt% values by elemental molecular weights (see Equation D.7). Then, we select sulfur (S) as a basis for calculations, as it is only present in AMPS; molar ratios represent the number of moles for a particular element divided by the number of moles of sulfur (see Equation D.8).

$$\#\ \text{moles N} = \ 13.15\ \text{wt\% N}\ \times \frac{1\ \text{mol N}}{14.007\ \text{g N}} = 0.9388\ \text{mol N} \tag{D.7}$$

$$\text{N mole ratio} = \ \frac{0.9388\ \text{mol N}}{0.1050\ \text{mol S}} = 8.9380 \tag{D.8}$$

Now, if we assume that we have z moles of AMPS ($C_7H_{13}NO_4S$) and m moles of AAm (C_3H_5NO), we can use the relative amount of each element (C, N and S) to calculate how many moles of each comonomer are present in the product copolymer.

Given:
$C = 3m + 7z$ (D.9)
$N = m + z$
$S = z$

$$m\ = \ (\text{N mole ratio}) - z = 8.9380 - 1 = 7.9380 \tag{D.10}$$
and $\overline{F}_{AMPS} = \frac{z}{m+z} = \frac{1}{7.9380+1} = 0.1119$ for this copolymer.

Similar techniques are used (with slightly modified expressions) for both the AMPS/AAc copolymer and the AMPS/AAm/AAc terpolymer. For the AMPS/AAc copolymer, either sulfur or nitrogen can be used as a basis. The process for determining composition using a sulfur basis is described in what follows.

Table D.4: Cumulative Composition Calculations for AMPS/AAc Copolymer

Elements	wt %	# moles	mole ratio	m	F_{AMPS}	F_{AAc}
N	3.3170	0.2368	1.4292	3.4276	0.2258	0.7742
C	34.3953	2.8637	17.2829			
H	4.5727	4.5364	27.3775			
S	5.3131	0.1657	1.0000			

Again, the weight percent values are obtained directly from the elemental analysis readout. By selecting sulfur (S) as a basis for calculations, molar ratios are calculated by dividing the number of moles of a particular element by the number of moles of sulfur.

As before, we assume that we have z moles of AMPS ($C_7H_{13}NO_4S$) and m moles of AAc ($C_3H_4O_2$), we can use the relative amount of each element (C and S, in this case) to calculate how many moles of each comonomer are present in the product copolymer.

Given:
$C = 3m + 7z$ (D.11)
$S = z = 1$

$$m\ = \ \frac{(\text{C mole ratio}) - 7(z)}{3} = \frac{17.2829 - 7(1)}{3} = 3.4276 \tag{D.12}$$
and $\overline{F}_{AMPS} = \frac{z}{m+z} = \frac{1}{3.4276+1} = 0.2258$ for this copolymer.

D.3 Determination of Experimental Conditions

D.3.1 Ionic Strength Calculations

To ensure that all systems were analyzed at the same ionic strength (IS), calculations for all feed compositions were performed prior to experimentation. The recipe with the highest ionic strength ($f_{AMPS,0}$ = 0.91) was used as a reference, and NaCl was added to all other recipes to achieve that same IS. The IS calculations for optimally designed experiments (AMPS/AAm copolymerization) are shown below for reference.

$f_{AMPS,0}$ = 0.91:

$$\frac{94.2987\ \text{g AMPS}}{250\ \text{ml stock soln}} = \frac{37.7195\ \text{g AMPS}}{50\ \text{ml stocksoln}} \times \frac{\text{mol AMPS}}{207.25\ \text{g AMPS}} = \frac{0.1820\ \text{mol AMPS}}{50\ \text{ml stock soln}} = \frac{0.1820\ \text{mol AMPS}}{100\ \text{ml pre-polymer soln}}\ (\text{after dilution}) \quad \text{(D.13)}$$

$\alpha = 0.9996,$

$$\therefore \text{I} = (0.1820\ \text{mol AMPS})(0.9996) = 0.18193\ \text{mol (in 100 ml pre} - \text{polymer soln)} \quad \text{(D.14)}$$

*Reference: no NaCl addition required.

$f_{AMPS,0}$ = 0.84:

$$\frac{87.0448\ \text{g AMPS}}{250\ \text{ml stock soln}} = \frac{34.8179\ \text{g AMPS}}{50\ \text{ml stocksoln}} \times \frac{\text{mol AMPS}}{207.25\ \text{g AMPS}} = \frac{0.1680\ \text{mol AMPS}}{100\ \text{ml pre-polymer soln}} \quad \text{(D.15)}$$

$$\therefore \text{I} = (0.1680\ \text{mol AMPS})(0.9996) = 0.16793\ \text{mol (in 100 ml pre} - \text{polymer soln)} \quad \text{(D.16)}$$

$$\text{*NaCl addition: } (0.18193\ \text{mol} - 0.16793\ \text{mol})\left(\frac{58.44\ \text{g NaCl}}{\text{mol}}\right) = 0.8182\ \text{g NaCl} \quad \text{(D.17)}$$

$f_{AMPS,0}$ = 0.30:

$$\frac{31.0881\ \text{g AMPS}}{250\ \text{ml stock soln}} = \frac{12.4352\ \text{g AMPS}}{50\ \text{ml stocksoln}} \times \frac{\text{mol AMPS}}{207.25\ \text{g AMPS}} = \frac{0.06\ \text{mol AMPS}}{100\ \text{ml pre-polymer soln}} \quad \text{(D.18)}$$

$$\therefore \text{I} = (0.06\ \text{mol AMPS})(0.9996) = 0.05998\ \text{mol (in 100 ml pre} - \text{polymer soln)} \quad \text{(D.19)}$$

$$\text{*NaCl addition: } (0.18193\ \text{mol} - 0.05998\ \text{mol})\left(\frac{58.44\ \text{g NaCl}}{\text{mol}}\right) = 7.1268\ \text{g NaCl} \quad \text{(D.20)}$$

$f_{AMPS,0}$ = 0.10:

$$\frac{10.3617\ \text{g AMPS}}{250\ \text{ml stock soln}} = \frac{4.1447\ \text{g AMPS}}{50\ \text{ml stocksoln}} \times \frac{\text{mol AMPS}}{207.25\ \text{g AMPS}} = = \frac{0.02\ \text{mol AMPS}}{100\ \text{ml pre-polymer soln}} \quad \text{(D.21)}$$

$$\therefore \text{I} = (0.02\ \text{mol AMPS})(0.9996) = 0.01999\ \text{mol (in 100 ml pre} - \text{polymer soln)} \quad \text{(D.22)}$$

$$\text{*NaCl addition: } (0.18193\ \text{mol} - 0.01999\ \text{mol})\left(\frac{58.44\ \text{g NaCl}}{\text{mol}}\right) = 9.4636\ \text{g NaCl} \quad \text{(D.23)}$$

D.4 Investigation of Experimental Error

D.4.1 Determination of Pooled Standard Deviation

During some early elemental analysis runs, the equipment was poorly calibrated and the resulting composition measurements were clearly incorrect. Therefore, the instrument was recalibrated and all samples were analyzed a second (and sometimes a third) time. This setback was somewhat inconvenient, but it also provided an estimate of the error associated with the elemental analysis equipment when it is not properly maintained. Therefore, the initial (incorrect) composition estimates and the more accurate data were combined to calculate the pooled variance for both feed compositions associated with the EVM-designed analysis ($f_{AMPS,0}$ = 0.10 and $f_{AMPS,0}$ = 0.84); calculations are shown below.

Table D.4: Replicated EA Results for $f_{AMPS,0}$ = 0.10

#	F_{AMPS} (with replicates)			Average	STDEV
1	0.5103	0.5162	0.2336	0.4200	0.1614
2	0.2687	0.2125	0.1878	0.2230	0.0414
3	0.1089	0.1141		0.1115	0.0037
4	0.1001	0.0937		0.0969	0.0045
5	0.0950	0.0801		0.0875	0.0106
1R	0.1683	0.1681		0.1682	0.0001
2R	0.1051	0.0911		0.0981	0.0099
3R	0.1096	0.2525	0.2431	0.2017	0.0799
4R	0.1021	0.0898		0.0959	0.0087
5R	0.1103	0.0922		0.1013	0.0128

S_p^2 = 0.0053

S_p = 0.0728

Table D.5: Replicated EA Results for $f_{AMPS,0}$ = 0.84

#	F_{AMPS} (with replicates)			Average	STDEV
1	0.6293	0.4965	0.7033	0.6097	0.1048
2	0.6746	0.5977		0.6362	0.0544
3	0.5504	0.6332		0.5918	0.0585
4		0.7141		0.7141	0.0000
5	0.7430	0.6555		0.6993	0.0619
1R	0.6274	0.6741		0.6507	0.0330
2R	0.7049			0.7049	0.0000
3R	0.6127			0.6127	0.0000
4R	0.9229	0.7030	0.6322	0.7527	0.1516
5R	0.8659	0.6917		0.7788	0.1231

S_p^2 = 0.0105

S_p = 0.1024

D.4.2 Data Sets for Sensitivity Analysis

With s_p values for both $f_{AMPS,0}$ = 0.10 and $f_{AMPS,0}$ = 0.84, the data sets are modified for the sensitivity analysis in Section 4.4.2. The data associated with the controlled variability study (Figure 4.12) is presented in Table D.7, while that associated with the randomized study (Figure 4.13) is presented in Table D.8.

The colour-coding in Table D.7 indicates the outlying data that was removed in Section 4.4.1; the red (bold) text shows the 2 outliers that were removed at low conversion ($f_{AMPS,0}$ =0.84) and the green (italicized) text shows the 3 outliers that were removed at mid-conversion ($f_{AMPS,0}$ =0.10). Essentially, removing the red data results in Figure 4.9, removing the green data leads to Figure 4.10, and Figure 4.11 is the product of all red and green data being removed from the data set.

Table D.7: Effect of Additional (Controlled) Variability (Data for Figure 4.12)

Conversion	**$f_{AMPS,0}$**	**F_{AMPS}**	**$F_{AMPS} + S_p$**	**$F_{AMPS} - S_p$**	**$F_{AMPS} \pm S_p$**
0.2202	*0.10*	*0.2336*	*0.3064*	*0.1609*	*0.3064*
0.2065	*0.10*	*0.1878*	*0.2605*	*0.1150*	*0.1150*
0.3408	0.10	0.1141	0.1869	0.0413	0.1869
0.3425	0.10	0.0937	0.1664	0.0209	0.0209
0.7073	0.10	0.0801	0.1528	0.0073	0.1528
0.1064	0.10	0.1681	0.2409	0.0954	0.0954
0.1473	0.10	0.0911	0.1638	0.0183	0.1638
0.2373	*0.10*	*0.2431*	*0.3158*	*0.1703*	*0.1703*
0.3556	0.10	0.0898	0.1625	0.0170	0.1625
0.6174	0.10	0.0922	0.1650	0.0194	0.0194
0.0267	**0.84**	**0.7033**	**0.8057**	**0.6306**	**0.8057**
0.0731	0.84	0.5977	0.7001	0.5249	0.5249
0.1412	0.84	0.6332	0.7356	0.5604	0.7356
0.1923	0.84	0.7141	0.8165	0.6413	0.6413
0.3348	0.84	0.6555	0.7579	0.5828	0.7579
0.0261	**0.84**	**0.6741**	**0.7765**	**0.6013**	**0.6013**
0.2862	0.84	0.7030	0.8054	0.6302	0.8054
0.3589	0.84	0.6938	0.7962	0.6210	0.6210

Table D.8: Effect of Additional (Random) Variability (Data for Figure 4.13)

Conversion	$f_{AMPS,0}$	F_{AMPS}	$F_{AMPS} \pm S_p$ (Random 1)	$F_{AMPS} \pm S_p$ (Random 2)	$F_{AMPS} \pm S_p$ (Random 3)
0.2202	0.10	0.2336	0.3064	0.1609	0.1609
0.2065	0.10	0.1878	0.1150	0.2605	0.2605
0.3408	0.10	0.1141	0.1869	0.0413	0.0413
0.3425	0.10	0.0937	0.0209	0.0209	0.0209
0.7073	0.10	0.0801	0.0073	0.1528	0.0073
0.1064	0.10	0.1681	0.2409	0.0954	0.0954
0.1473	0.10	0.0911	0.0183	0.1638	0.1638
0.2373	0.10	0.2431	0.1703	0.1703	0.3158
0.3556	0.10	0.0898	0.1625	0.0170	0.1625
0.6174	0.10	0.0922	0.0194	0.0194	0.0194
0.0267	0.84	0.7033	0.6306	0.6306	0.8057
0.0731	0.84	0.5977	0.5249	0.7001	0.5249
0.1412	0.84	0.6332	0.5604	0.7356	0.5604
0.1923	0.84	0.7141	0.6413	0.6413	0.8165
0.3348	0.84	0.6555	0.5828	0.7579	0.7579
0.0261	0.84	0.6741	0.6013	0.6013	0.7765
0.2862	0.84	0.7030	0.8054	0.6302	0.6302
0.3589	0.84	0.6938	0.6210	0.6210	0.6210

D.5 Paired t-test for Reactivity Ratio Comparison

The statistical difference between binary and ternary reactivity ratios can be determined using a paired t-test, and is shown below:

Table D.9: Comparison of Reactivity Ratio Estimates

Reactivity Ratio	Binary	Ternary	d
$r_{AMPS/AAm}$	0.18	0.46	-0.28
$r_{AAm/AMPS}$	0.85	0.93	-0.08
$r_{AMPS/AAc}$	0.24	0.57	-0.33
$r_{AAc/AMPS}$	0.87	0.92	-0.05
$r_{AAm/AAc}$	1.33	1.08	0.25
$r_{AAc/AAm}$	0.23	0.24	-0.01
		$\overline{d} =$	-0.0833
		$s_d =$	0.2084

Hypothesis test: $H_0: \mu_D = 0$ $H_1: \mu_D \neq 0$

$$t_{obs} = \frac{\overline{d} - 0}{s_d/\sqrt{n}} = \frac{-0.0833}{0.2084/\sqrt{6}} = -0.9795$$

$$t_{crit} = t_{5,0.05} = 2.02$$

Since $|t_{obs}| < t_{crit}$ ($0.9795 < 2.02$), we fail to reject H_0. Therefore, the difference in reactivity ratio estimates for the binary and ternary data is not statistically significant.